Geochemistry of Forest Rings in Northern Ontario:

Identification of Ring Edge Processes in Peat and Soil

Kerstin M. Brauneder, B.Sc.

Under the supervision of:
Dr. Keiko Hattori[1] and Dr. Stewart Hamilton[2]

[1] Department of Earth Sciences, University of Ottawa, Ottawa, Ontario
[2] Ontario Geological Survey, Sudbury, Ontario

A thesis submitted to the Faculty of Graduate and Postdoctoral Studies
in partial fulfillment of the requirements for the degree of
M.Sc. in Earth Sciences, University of Ottawa

Abstract

Forest rings are large features common in Ontario's boreal forests that comprise circular topographic depressions in carbonate mineral soil that are filled with peat. This thesis documents differences in peat and soil chemistry along transects across the "Bean" and "Thorn North" rings, which are centered on accumulations of CH_4 and H_2S, respectively. Within the mineral soil, ring edges are characterized by strong negative anomalies in pH, ORP and carbonate, as well as positive anomalies of Al, Fe and Mn in the results of aqua regia and hydroxylamine-hydrochloride digestions. Within the peat, positive carbonate and pH anomalies are recorded. This antithetic relationship suggests vertical migration of carbonate species from clay to peat. An inverse relationship exists between ORP, versus redox inferred from aqua regia. Strong ORP lows occur where oxidized products show highest concentrations. This is interpreted to reflect the proliferation of autotrophic organisms occupying the strong redox gradient at the ring edge.

Keywords: forest ring, reduced chimney, H_2S, CH_4, oxidation-reduction potential (ORP).

Résumé

Les anneaux forestiers de la forêt boréale d'Ontario sont des formations circulaires causées par une dépression topographique du sol carbonaté remplie de tourbe. Cette thèse décrit les changements chimiques de la tourbe et des sols sous les anneaux "*Bean*" et "*Thorn North*", respectivement centrés sur des accumulations de CH_4 et H_2S. Le sol minéral au bord des anneaux présente des anomalies négatives de pH, potentiel d'oxydo-réduction et carbonates, et des anomalies positives de Al, Fe et Mn obtenus par digestion sous eau régale et chlorhydrate d'hydroxylamine. La tourbe affiche des anomalies positives de carbonate et pH. Cette relation antithétique suggère une migration verticale d'espèces carbonatées entre argile et tourbe. Une relation inverse existe entre le POR et les conditions redox déduites des mesures d'eau régale. De fortes anomalies négatives de POR surviennent où les produits d'oxidation sont enrichis. Ceci pourrait indiquer la prolifération d'organismes autotrophiques occupant le fort gradient redox de l'anneau.

Mots-clés: anneau forestier, cheminée réduite, H_2S, CH_4, potentiel d'oxydo-réduction (POR).

Table of Contents

List of figures

List of tables

List of appendices

List of acronyms

ORP	Oxidation-reduction potential
TN-WE	West-East (WE) sampling transect across the Thorn North (TN) ring
TN-NS	North-South (NS) sampling transect across the Thorn North (TN) ring
BE-SWNE	Southwest-Northeast (SWNE) sampling transect across the Bean (BE) ring
BE-SENW	Southeast-Northwest (SENW) sampling transect across the Bean (BE) ring
PCA	Principal Component Analysis
PC	Principal Component

Introduction

1. Preamble

Forest rings are light-coloured circular imprints on the boreal forest of northern Ontario and northwestern Québec, ranging in diameter from 50 m to 1.6 km. They are visible on air photos, satellite images and from aircraft (Figure 1). Over 2000 forest rings have been identified in northern Ontario and Québec in mapping efforts by the Ontario Geological Survey and the Geological Survey of Canada since 1999. Previous work on individual forest rings in Canada has established that:

1) Forest rings in northern Ontario are abundant above glaciomarine and marine sediments of Quaternary age and commonly occur over Phanerozoic bedrock (Veillette and Giroux, 1999; Hamilton et al., 2004a);

2) Forest rings are visible because of poor tree growth or high tree mortality, spatially coinciding with a topographic depression in carbonate-rich soils that is commonly filled with peat (Giroux et al. 2001);

3) Accumulations of reduced gases such as H_2S (Hamilton and Hattori, 2008) and CH_4 (Hamilton et al. 2004a) occur in the overburden beneath a number of forest rings, and are released into the groundwater and the overlying atmosphere.

4) Forest rings are likely the surficial expression of reduced chimneys within carbonate terrain developing over sources of reduced material (Hamilton and Hattori, 2008). In at least one case, a reduced chimney was detected over an H_2S accumulation, but other reduced material may produce forest rings as well.

The last conclusion was drawn from the case-study of the Thorn North ring. Groundwaters at this ring were found to be characterized by an accumulation of H_2S at the ring center, as well as negative inward oxidation-reduction potential (ORP) anomalies coupled with the generation of trace amounts of CH_4 at the ring edge. As a consequence, Hamilton and Hattori (2008) suggested that

forest rings develop in a process similar to reduced chimneys over mineral deposits. The model of formation of reduced chimneys, explained in the literature review, involves electrochemical processes resulting in a negative redox anomaly that influences pH and carbonate speciation. No detailed studies have been completed to date documenting such changes in the shallow subsurface of a forest ring.

2. Thesis objectives and structure

The objective of this thesis was to study geochemical data from two forest rings with an emphasis on changes occurring in the shallow subsurface at the ring edges. To this end, soil and peat samples were collected across a forest ring known to be centered on a CH_4 accumulation in overburden (the *Bean*, Hamilton et al., 2004a) and a second over an accumulation of H_2S in groundwater (*Thorn North*; Hamilton and Hattori, 2008). First, the thesis provides analytical data documenting changes in redox and pH conditions, carbonate contents, as well as redox- and pH-sensitive species in aqua regia and weak acid leach solutions. Secondly, a principal component analysis was conducted along one of the transects at the Bean ring, in order to evaluate geochemical trends related to the presence of the ring. The thesis discusses the data in light of the reduced chimney model, which was previously proposed to account for the formation of forest rings. A sequence of chemical reactions occurring at the ring edge is proposed in order to explain the observed geochemical responses in pH, ORP and carbonate contents.

FIGURE 1: Aerial photographs of forest rings in northern Ontario. The annulus is visible due to stunted tree growth, as well as growth of moisture-tolerant tree species, such as tamarack (coloured in orange on Figure 1B). A) Location is near 565800E, 5482600N, UTM zone 17N and the rings are approximately 150 m in diameter. B) Location is 292400E, 5551000N, UTM zone 17N and the ring is approximately 550 m in diameter.

A.

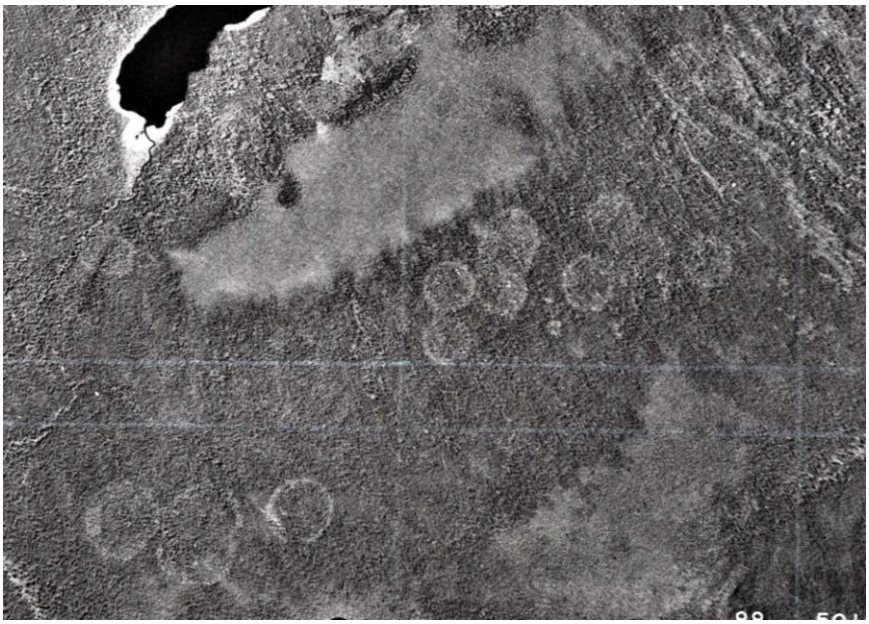

B.

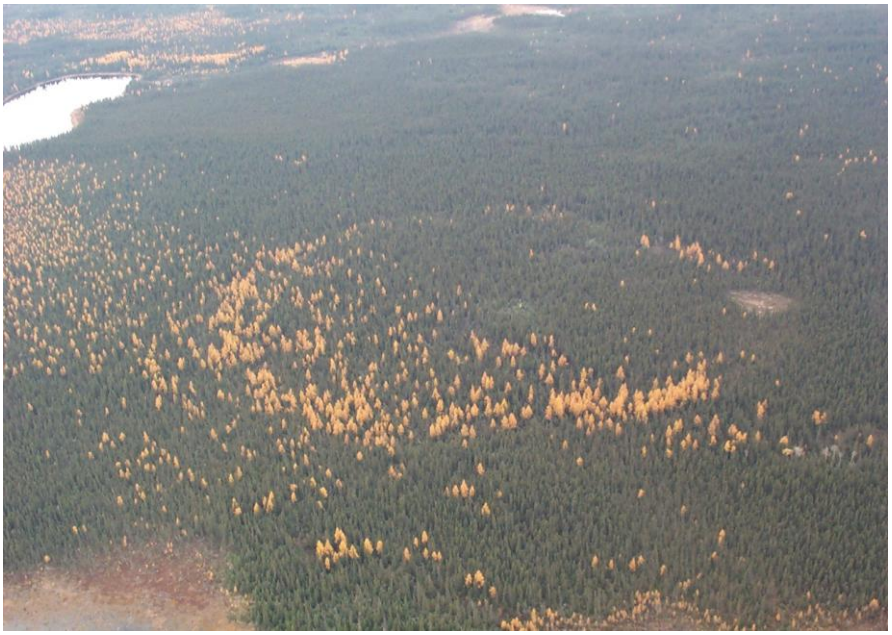

Literature review

1. Vegetation and distribution of Forest Rings

Forest rings are visible due to circular zones of low tree density, forming in stands of black spruce (*Picea mariana*). The ring edge (annulus) is visible as a light-coloured zone of forest that is primarily an expression of stunted tree growth that is particularly visible in winter when the snow-covered understory contrasts with the darker surrounding forest. In addition, the edge is commonly highlighted by an increase in Tamarack (*Larix laricina*) abundance, changing the colour of the forest canopy (Figure 1B). During the fall, the orange colour of the Tamarack contrasts sharply with the unchanged green colour of the surrounding black spruce. The core and the areas surrounding the forest rings are dominated by black spruce, which thrive under moderately to well-drained conditions. The ring annulus is a poorly-vegetated bog with low relief. Although the thickness of the annulus can vary, it is typically 10 m for the majority of rings.

Forest rings were first reported in the 1950s (Dean, 1956) with the advent of aerial photography as a surveying tool. The term *forest ring* was first applied by the Ontario Geological Survey, in order to differentiate the features from “fairy rings”, smaller rings caused by fungus growing in a radial pattern, and to establish a unique name for them. Previous designations included “circular ring features” (Pinson, 1979), “giant circular patterns” and “whitish rings” (Giroux et al., 2001). To date, the overall published literature regarding forest rings is sparse: 7 forest rings were studied in Québec by Giroux et al. (2001) and 14 forest rings were examined by the Ontario Geological Survey (Hamilton, 1999 ; Hamilton et al., 2004a ; Hamilton and Hattori, 2008). In addition to Ontario and northwestern Quebec, 200 rings have been identified on Anticosti island in Canada (Dubois, 1993), and anecdotally in Russia, Minnesota (USA), and Australia (Hamilton, personal communication). Their abundance in northern Ontario is however unmatched with over 2000 forest rings inventoried to date within a study area of 150 000 km², stretching westwards from Timmins to Geraldton, and northwards from Timmins to the western edge of the James Bay Lowlands (Hamilton et al., 2004a; Veillette and Giroux, 1999). Within this area, the spatial and size distribution of forest rings appears correlated to both the regional bedrock, and the overburden geology. Rings are larger and twice as abundant above Phanerozoic than Precambrian bedrocks. Rings are also six times more likely to

occur over glaciomarine and marine deposits, rather than organic, glaciolacustrine and till deposits. Rings are least likely to occur over fluvial, glaciofluvial and bedrock deposits, although they sometimes do.

2. Forest ring formation

Early studies of the formation of rings

Early studies suggested a biological origin, where forest rings are caused by radial growth of giant fungi within the Black Spruce root system (e.g. Mollard, 1980). These conclusions were speculative, based on the circular morphology of forest rings, without providing field evidence. Usik (1966) was the first to favour a geological origin, interpreting forest rings as the surface expression of dispersion halos, caused by the localized diffusion of elements above zones of mineralization. Prospectors in Ontario have repeatedly observed these features and believed them to be the surface expression of buried kimberlites or other circular features of economic interest (e.g. Millar, 1973; Reed, 1980; Adams, 1998; Diatreme Explorations, 1999). The results of repeated drilling in several forest rings have so far not supported this possibility. Other possible origins of forest rings include relict permafrost features, thermokarst and periglacial features (Mollard, 1980).

Veillette and Giroux (1999) and Giroux et al. (2001) discredited the biological origin of radial spruce mortality by disproving the underlying assumption that the average tree ages near the ring edge are graded, being low within the edge and increasing inward to a point of stabilization. Stabilization would have occurred at the distance covered by the fungi over the average lifespan of a black spruce (250 years). For *Armillaria* spp., one of the species with the slowest known rate of radial expansion (0.2m/yr), this would have amounted to a minimal zone of graded tree growth of 50m inward of the ring edge. The dendrochonological work by Giroux et al. (2001) found no gradient in the age of spruce across seven forest rings. Thus forest rings were demonstrated to be static features, unless expanding at a rate much slower than 0.2 m/yr. Giroux et al. (2001) also noted a decrease in elevation of the mineral substrate at the ring edge up to 3 m, coinciding with changes in forest productivity variables. These are a lower total basal area of spruce, a higher relative mortality of spruce and a decreased height growth. The visible ring edge is therefore a poorly forested zone with stunted tree growth. Discontinuous forest rings, where tree growth is not stunted over portions of the ring edge, display either no change in topography or a slight rise in topography (~ 0.5

m). The depressions at the ring edge are filled with peat and have high soil moisture. Poor drainage, known to inhibit nutrient uptake and photosynthesis of black spruce, was therefore identified as the cause for low productivity. Based on the spatial correlation between rings and calcareous substrate, Veillette and Giroux (1999) hypothesized the depression at the ring edge to be caused by geologic processes at depth, rather than geomorphologic processes at the surface. The significant depth of the depression and the occurrence of a thick infill of peat suggest that forest rings have been stationary for long periods of time (Hamilton et al., 2004a).

The reduced chimney theory

A possible origin for forest rings was discussed by Hamilton and Hattori (2008), who proposed that at least one forest ring (the Thorn North ring) is the surface expression of a reduced chimney. Reduced chimneys form over a buried source of negative charge and maintain redox-sensitive species in a reduced state in the overlying overburden (Figure 2). Groundwaters within the Thorn North ring were indeed characterized by low ORP values inside the ring. Negative redox conditions also occurred within the shallow subsurface, where positive spontaneous potential anomalies were detected. Hamilton and Hattori (2008) proposed the concept of redox-induced spontaneous polarization to account for this correlation. This would result in low electrical fields at the margins of the ring and transport of ionic species within the electrical field. Reduced species would migrate upwards and outwards to the edge of the reduced chimney through electrochemical dispersion along the electrochemical gradient (Cameron et al. 2004). At the top and edges of the chimney, oxidation of the reduced species, notably Fe^{2+}, above the water table is expected to result in the precipitation of Fe-oxyhydroxydes, production of H^{+} and dissolution of carbonates. This model explains the development of geochemical dispersion halo above mineral deposits buried under thick glacial sediments (Hamilton et al. 2004b, 2004c). Tracing a redox/pH sensitive geochemical parameter across a reduced chimney and beneath the water table produces a positive (or negative) response symmetrical with respect to the center of the reduced chimney, commonly referred to as “rabbit-ear anomaly” due to the resulting symmetrical shape.

FIGURE 2: Reduced chimney model (Cameron et al. 2004). The 14 forest rings investigated to date were centered over reduced sources within overburden, although reduced sources in bedrock are possible.

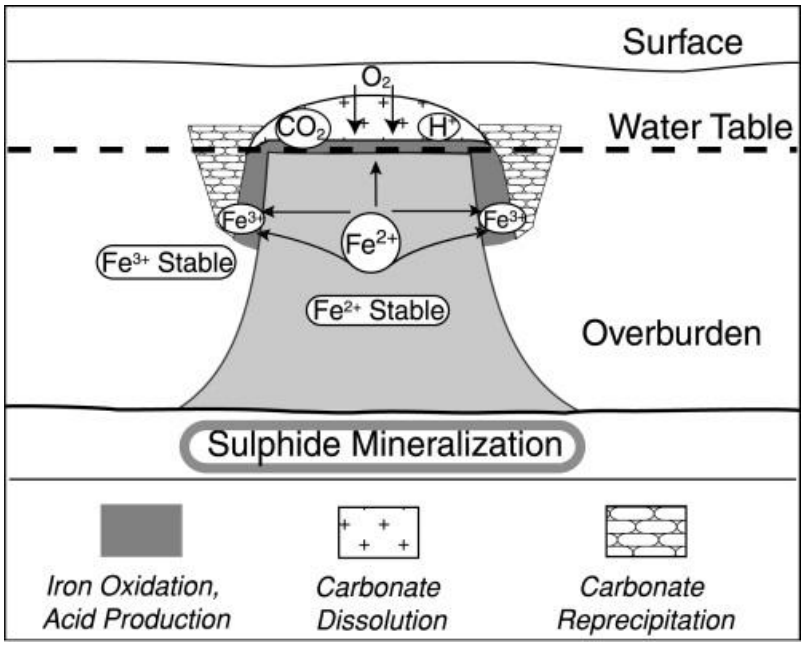

The work by Hamilton et al. (2004a) suggests that methane accumulations act as a reduced source for the majority of forest rings in northern Ontario. The study measured CH_4 levels in shallow soil and peat, and in the near-ground air across 11 forest rings near Hearst in order to assess the prevalence of methane-sourced rings. The selected rings occurred over different types of overburden (till, glaciolaculstrine clay and organic terrain) and bedrock (Precambrian and Paleozoic limestone). In 9 out of 11 examined rings, average methane concentrations in air were higher within the ring, than the values outside of the ring unless dominant winds were blowing outwards. Values outside of the ring ranged between 1.80 and 1.91 ppm, while values inside of the rings ranged between 1.85 and 1.95 ppm. These results were confirmed by measuring the methane in the mineral soil at a depth of 0.5 m. Rings displaying high atmospheric methane concentrations displayed increases in concentrations from 10,000 to 40,000 ppm from the background value less than 4000 ppm. Concentrations across known or suspected non-methane sourced rings, displayed less variability and also reached maximal concentrations of 4,000 ppm.

3. Biogeochemistry of Al, Fe and Mn within soils

The edges of a reduced chimney are expected to show high redox gradients from reducing conditions inside of the chimney, to oxidizing conditions outside. A high redox gradient environment reflects the occurrence of electron-transfer reactions which influence the distribution and mobility of redox and acid-base elements. Both inorganic (abiotic) and microbial (biotic) reactions are competing in the soil environment. Bacterial metabolism relies on the availability of a carbon source, an energy source, nutrients and an oxidized compound as electron acceptor. In the absence of sunlight, biotic reactions in the subsurface gain energy chemotrophically. Chemo-organoheterotrophic organisms oxidize organic carbon, and chemo-lithoautotrophic organisms oxidize inorganic species. This is coupled to the reduction of an inorganic species, acting as terminal electron acceptor. Abiotic secondary reactions and mineral precipitation-dissolution reactions occur simultaneously, influencing the distribution of adsorbed metals.

In this study, Al, Fe and Mn were chosen to describe the chemical dynamics in peat and soil at the ring edge. The biogeochemical cycles of Fe and Mn are driven by redox processes, while the solubility of Al in soil is pH dependent. The description of soil biogeochemical processes is based on Paul (2007) and Konhauser (2007), and the relationship between Al and soil acidity is based on Tan (2010).

Soil redox and Fe-Mn species

Iron is present in the ferric Fe(III) form under oxidized conditions. Fe(III) is stable under near-neutral pH, where it precipitates as Fe(III) (hydr)oxides. Abiotic oxidation mechanisms of ferrous iron (Fe^{2+}) are very rapid in aerobic environments at pH > 5. Under anoxic conditions, abiotic Fe oxidation may be coupled with the activity of nitrate-reducers and photo-autotrophic bacteria. Biotic Fe oxidation may take place even when chemical oxidation is unfavourable, such as at low pH when the reaction is catalyzed by acidophilic Fe-oxidizers. Low levels of O_2 are required for aerobic bacteria, so they can out-compete the rapid chemical oxygenation of Fe which is common at the oxic-anoxic interface.

Iron is soluble as Fe (II) in the form of Fe^{2+} under reduced and acidic conditions, or as Fe^{3+} under oxidizing conditions. Biotic reduction of Fe^{3+} occurs under anaerobic conditions if insufficient sulfate

and nitrate are present to allow sulfate and nitrate respiration. Iron is then used as an electron acceptor during anaerobic respiration by Fe-reducing bacteria. Biotic reduction uses dominantly dissimilatory pathways, where the electron used during the metabolic process is transferred to an extracellular electron acceptor. Biotic Fe-reduction is coupled to the oxidation of organic matter and a wide range of organic compounds. Both biotic and abiotic reductive dissolution are accompanied by the release of passively adsorbed elements, such as Co, Ni, V, Ba, REE and Al.

Reduced manganese, Mn (II), is soluble as Mn^{2+} under neutral to acidic pH conditions. Its oxidation forms Mn (III, IV) and precipitate as oxides (MnO_2, Mn_2O_3, $MnO.Mn_2O_3$), and oxyhydroxide species ($Mn(OH)_3$). Precipitation due to chemical (abiotic) oxidation only occurs at pH > 8, and if sulfide or carbonate species are present favouring the formation of $Mn^{II}S$ and $Mn^{II}CO_3$. Biotic Mn-oxidation dominates in acidic and neutral pH and is dominantly dissimilatory. The biotic formation of Mn-oxides can trigger secondary reactions, such as the coupling of Mn-reduction with the oxidation of As (III), N (III) and Cr (III) (Post, 1999). These reactions produce poorly crystalline layered Mn (IV) minerals, which occur as coatings or fine-grained aggregates. The resulting high surface area strongly influences the distribution of passively sorbed elements, such as heavy metals.

Soil acidity and Al

Aluminum is abundant in aluminosilicates and aluminum oxides of clay fractions. The solubility of Al depends on soil acidity, rather than redox conditions. The release of Al from clay to pore waters occurs with decreasing pH. Biotic oxidative activity, as previously described, can be one of the main sources of active acid production within soil. A drop in pH causes the formation of H-Al-clay complexes as the Al present within the octahedral layer of clay minerals is replaced by H^+. Aluminum ions are released from the H-Al-Clay complex through cation-exchange. Al^{3+} does however not stay in solution by itself, but tends to form complexes with six H_2O molecules into aluminum hexahydronium. The continued hydrolysis of this compound involves the formation of several Al-hydroxy compounds and release of protons (H^+). Thus the overall change in pH in soil is dependent on the ability to replace and release Al via exchange with H^+ at the clay interface. Soil pH remains stable despite the release of H^+, as long as exchangeable Al is present on the clay surface. This buffering effect occurs at pH < 5.1, therefore acid soils are rich in soluble Al and Al-hydroxy compounds. At more neutral and basic pH, the H^+ is not readsorbed on the clay but neutralized and precipitated as $Al(OH)_3$.

Study area

1. Climate and vegetation

Northern Ontario is located within the Abitibi plains eco-region, part of the boreal-shield climate zone and the boreal forest biome. The vegetation cover is dominated by black spruce, balsam fir and tamarack growing on a thick horizon of well decomposed organic matter (peat). The region has a continental climate, characterized by long cold winters, short warm summers and abundant precipitation year-long. Climatic records in Timmins (Ontario) from 1971 to 2000 yield a mean annual temperature of 1.3 ^{o}C and total annual precipitation of 831.3 mm (http://www.climate.weatheroffice.ec.gc.ca/climate_normals/index_e.html). The mean summer (June-August) temperature and precipitation values over the 1971-2000 period range at 14.5 ^{o}C/month and 87.8 mm/month. Sampling was carried out in Timmins and Hearst (located 210 km south-east of Timmins) in August 1999 and July 2000. August 1999 had an average temperature of 15 ^{o}C and total precipitation of 81.4 mm. July 2000 was a dry year with an average temperature of 16 ^{o}C and total precipitation of 45.4 mm. The area is located south of the permafrost and sporadic permafrost boundary (Smith and Burgess, 2002). During sampling, ice was however noted in peat on two sites at the center of the Bean ring.

2. Location and general geology

The Thorn North ring is located 40 km northwest of Timmins, Ontario, in a black-spruce dominated forest (Figure 3). The bedrock geology is mapped as Archean mafic metavolcanic rocks of the Superior Province. A drilling initiative by the Ontario Geological Survey in 2000 encountered quartz-feldspar porphyry with minor (~1 vol.%) pyrite and chalcopyrite near the center of the ring, and an intensely sheared component of the same lithology in a neighbouring hole. The orientation of the shear zone is presumed to be north-south trending based on the regional structure (Hamilton and Hattori, 2008). The Quaternary geology in this area has been mapped and interpreted in detail by Paulen and McClenaghan (1998). The ring is located in an area with approximately 30 m of glacial drift cover. Most of the deposits were laid down during a period of deglaciation that began

approximately 9.4 kA. A thick varved clay unit was deposited in the region following the development of the proglacial lakes Barlow and Ojibway starting at 9.6 kA. Lake Ojibway is the northward succession of lake Barlow and started forming at 9 kA. A brief 450 year long re-advance of glaciers began around 8.4 kA (Dyke, 2004). During this time the Cochrane till was formed during over-riding of the glaciolacustrine deposits. Esker deposits are also likely relicts from the glacial re-advance. The near-shore sands on the Thorn-North site formed in a brief period when lake Barlow-Ojibway prograded northward as the ice started receding again. The lake started draining at 7.6 kA following the opening of an outlet, likely northward into the Tyrell sea. Peat deposits have been forming in the area since that period.

FIGURE 3: Location of the Bean and Thorn-North forest rings in northeastern Ontario (from Brauneder et al. 2008).

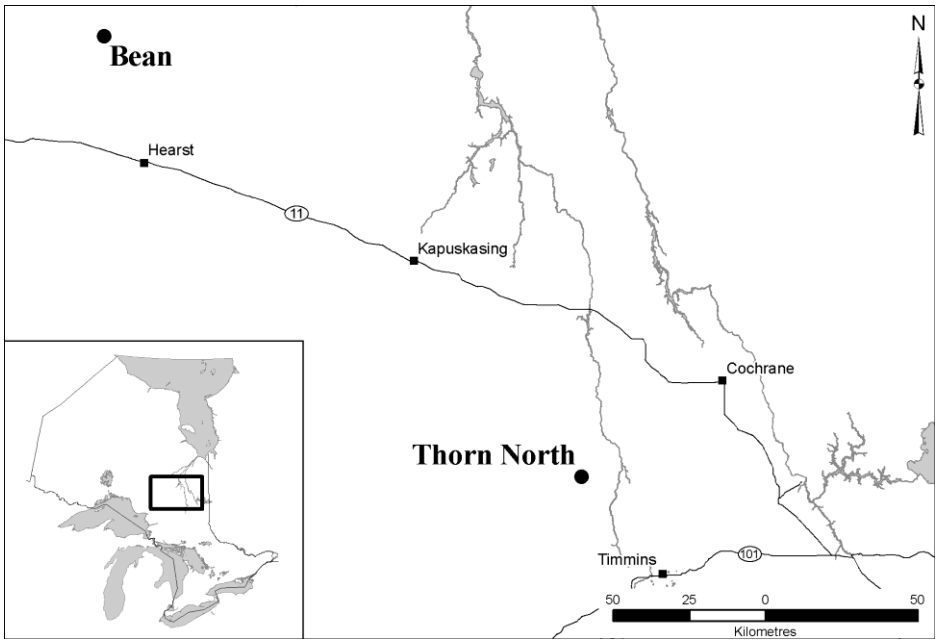

The Bean Ring is located within the James Bay Lowlands where the bedrock geology is mapped as Devonian carbonate. Drilling by the Ontario Geological Survey in 1999 confirmed the presence of thickly bedded non-fossiliferous micritic limestone as bedrock, but the age could not determined. The quaternary geology has not been mapped in detail but the drilling initiative showed that the

sediments consist largely of stony clay, carbonate-rich (~35 vol.%) till of the Cochrane Formation, intercalated with numerous sand lenses. The overburden is less than 30 m in thickness. The till likely originated as glacially-overridden glaciolacustrine clays. The Bean Ring is located outside and within several kilometres of the southern limit of the Tyrell Sea incursion. Glacial sediments in this part of the James Bay lowlands are thought to be 8.5 kA in age (Dyke, 2004).

3. Description of studied rings

The Bean and Thorn North forest rings were selected because of their accessibility and previously installed infrastructure, such as deep and shallow monitoring wells. The monitoring wells provided insight into the local hydrogeology and subsurface redox conditions, and the drill holes allowed investigation of the stratigraphy.

The Bean ring

The Bean ring has a diameter of 430 m and is situated on a black spruce dominated terrain. Two orthogonal transects were established across the ring and named after their orientation: southwest-northeast (BE-SWNE) and southeast-northwest (BE-SENW) (Figure 4). The ring is gently sloping downward to the northwest, with an overall relief of 5 m across the 1 km long BE-SENW transect. An unusual black spruce aureole occurs beyond the light coloured rim of the ring. Aureoles beyond the edge of rings are rare and have only been noted in a few other rings.

The occurrence of a CH_4 accumulation in Quaternary sediments beneath the ring was determined in a drilling program carried out by the Ontario Geological Survey in 1999 (Hamilton and Cranston, 2000 ; Hamilton et al., 2004a). 23 shallow monitoring wells were installed at 9 m depth within the shallow overburden (Figure 5). CH_4 gas was escaping groundwater from the shallow overburden but not the bedrock at concentrations high enough to be flammable (Hamilton et al. 2004a). Carbon isotopic compositions indicate the CH_4 gas is biogenic and was formed at low temperature (Hamilton et al., 2004a). This same study suggested the CH_4 resides in sand lenses in the till because no gas was noted in groundwater from bedrock. Several rounds of water level measurement show that the hydraulic head in the monitoring wells within the shallow overburden is up to 2 m above ground surface, indicating flowing artesian conditions across the ring. Artesian conditions in the

Quarternary sediments are more pronounced with increasing depth. Peat and soil are saturated across the whole ring for at least part of the year.

FIGURE 4: Site map of the southeast-northwest (BE-SENW) and southwest-northeast (BE-SWNE) of the Bean ring. Coordinates (m) are in UTM Zone 17N, NAD83. The ring is 430 m in diameter. Note the wide black-spruce aureole surrounding the ring. The road to the right is an overgrown logging road that intersects the Fushimi Lake Road located beyond the southeast corner of the air photo. The site is approximately 40 km north of Highway 11. The photo is clipped from an Ontario Ministry of Natural Resources air photo number 86-5003-09-62. The traces of the sample lines were added later as a differentially corrected GPS track.

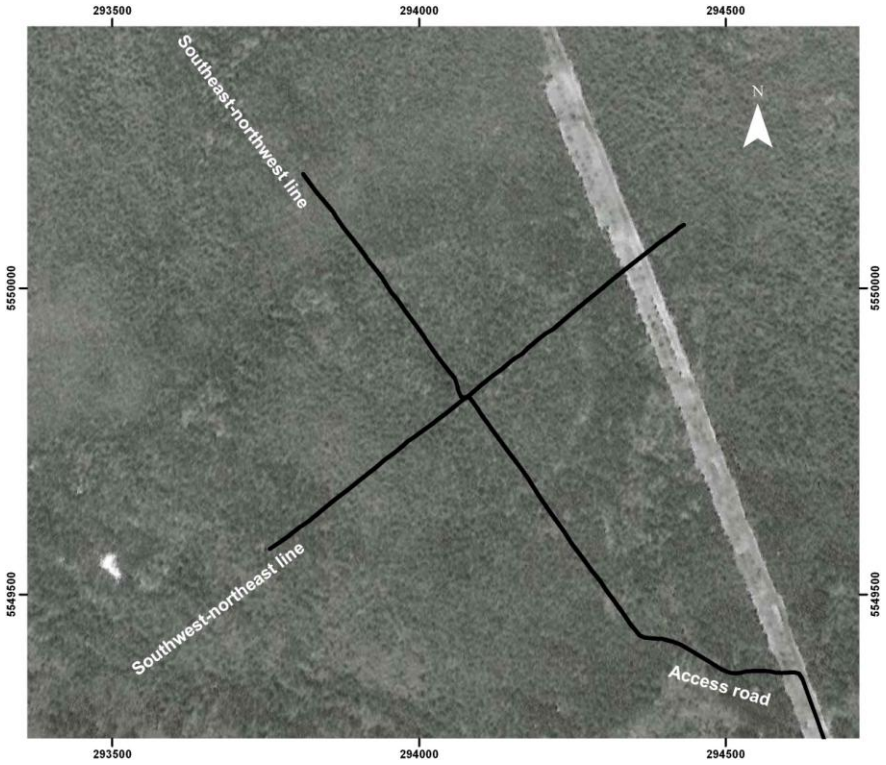

FIGURE 5: Shallow and deep stratigraphy on the Southwest to Northeast (BE-SWNE) and Southeast to Northwest (BE-SENW) sampling transects at the Bean ring. The thick vertical bars indicate the position of the ring edges. The sudden topographic low just inside the SE ring edge is thought to be an iceberg grounding. The piezometric surface was determined during the installation of 23 shallow monitoring wells and a deep borehole drilled to bedrock at the site. Methane is present in vapour phase at flammable concentrations in the 5 central wells, but not in the deep borehole.

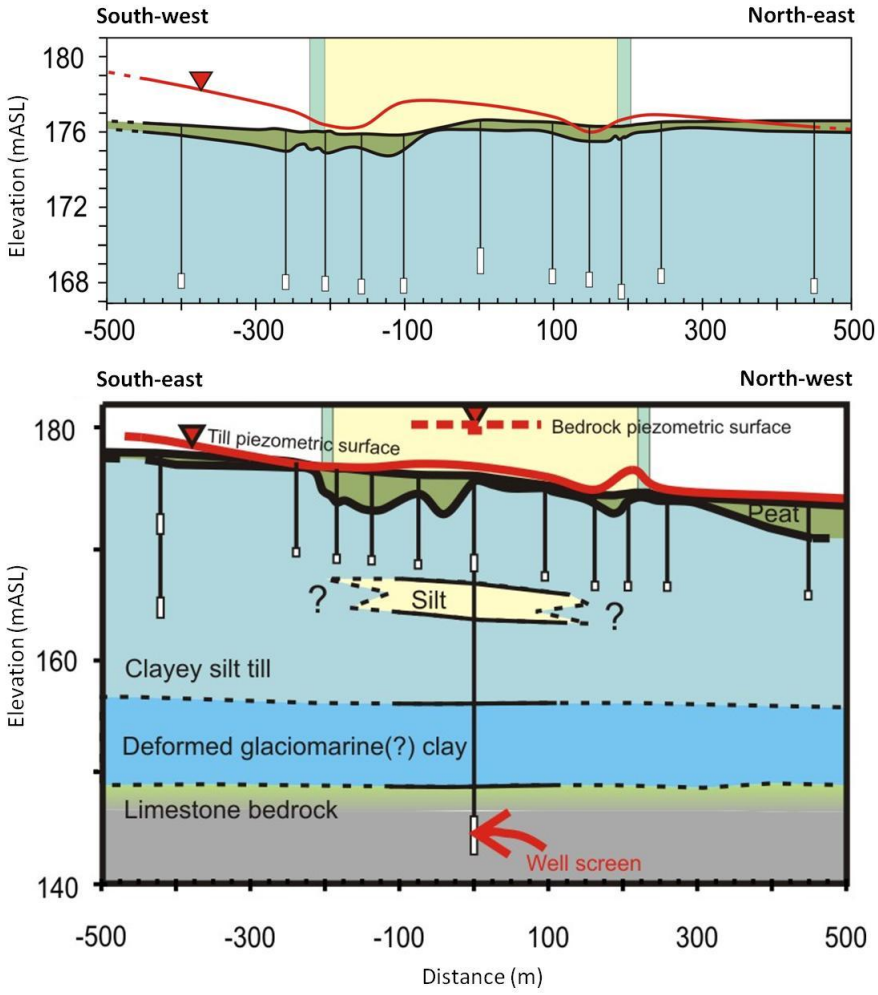

Thorn north

Thorn North (Figure 6) has a diameter of 560 m and is one of the best studied rings due to its road-accessibility. The glacial sedimentary stratigraphy (Figure 7) has been previously described by Hamilton and Hattori (2008). The description is based on an extensive drilling program carried out by the Ontario Geological Survey in 2000, during which 54 shallow wells were installed in Quaternary aged sediments and three boreholes were drilled to bedrock; one outside and two inside of the ring. The shallow monitoring wells were installed to a depth of 8 m using hollow-stem augers.

H_2S was noted in almost all of the shallow wells inside the ring. Drastically lower concentrations occur in water from wells outside of the ring (Hamilton and Hattori, 2008). The Thorn-North ring is therefore centered on an accumulation of H_2S in groundwater. Unlike CH_4 at the Bean ring, the source of H_2S at Thorn North is likely in bedrock. Water from two boreholes that penetrate the sheared quartz-feldspar porphyry zone identified in bedrock, had concentrations of H_2S up to 2.25 and 11 mg/L, which are higher than in groundwater from gabbroic rocks intersected in a borehole located outside of the ring (Hamilton and Hattori, 2008).

The overburden at Thorn North is 30 m thick and is composed of glaciolacustrine clay and clay till in the west half of the ring, and fine to medium sand in the eastern half of the ring. This change is due to a 30 km long south-southeast trending esker underlying the eastern half of the ring. Three transects have been cleared in the forest across the Thorn North ring and were named after their orientation: north-south (TN-NS), west-east (TN-WE) and southwest-northeast (TN-SWNE). Sampling took place along the TN-NS and TN-WE transects. The TN-NS transect is dominated by glaciolacustrine clay and pebbly clay till. A thin oxidized lacustrine sand unit occurs at the center of the line, but was not sampled. The unit is thicker on the TN-WE transect, and accounts for the first five samples on the west end. The lacustrine sand unit thins out towards the east and is replaced by a unit of glaciolacustrine clay. The apparent degree of oxidation of the clay unit varies from low oxidation inside of the ring to high oxidation at the eastern end of the transect. A unit of fine esker sand underlies the clay on its eastern half and unsaturated conditions in the sand result in a perched water table in the overlying clay.

TN-SN is a wet sampling line, with a shallow water table lying between 0.02 m and 0.2 m beneath the ground surface. Moisture conditions along TN-WE are more variable, with the depth of the water table ranging between 0.02 m and 1 m. The water table is deepest, ranging between 0.5 m to 1 m in depth, at the center and the western end of TN-WE. At these locations the uppermost layer of peat and lacustrine sand are unsaturated and oxidized.

FIGURE 6: Site map of the north-south (TN-NS) and west-east (TN-WE) transects of the Thorn North ring. Coordinates (m) are in UTM Zone 17N, NAD83. The ring is 560 m in diameter. The road to the right is the Kamiskotia Lake Road, 21 km north of Kamiskotia Lake, northwest of Timmins, Ontario. The center of the ring can be reached via the SWNE line intersecting with Kamiskotia road. The photo is clipped from an Ontario Ministry of Natural Resources air photo number 91-4826-64-86. The sample lines were added graphically along the trace of surveyed sample locations.

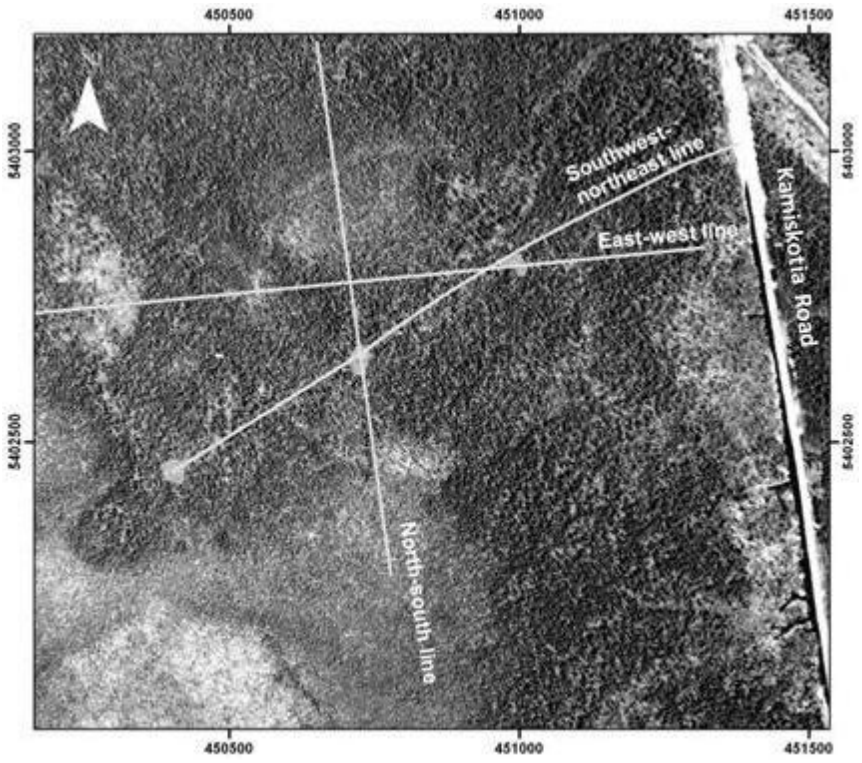

FIGURE 7: Shallow stratigraphy on the south-north (TN-SN) and west-east (TN-WE) sampling lines at the Thorn-North forest ring. The stratigraphy and piezometric surface was determined from 54 monitoring wells installed across the site screened between 8 and 9 m depth. The water table was determined during the sampling program based on the position of standing water in the auger-holes (figure modified after Hamilton and Hattori, 2008).

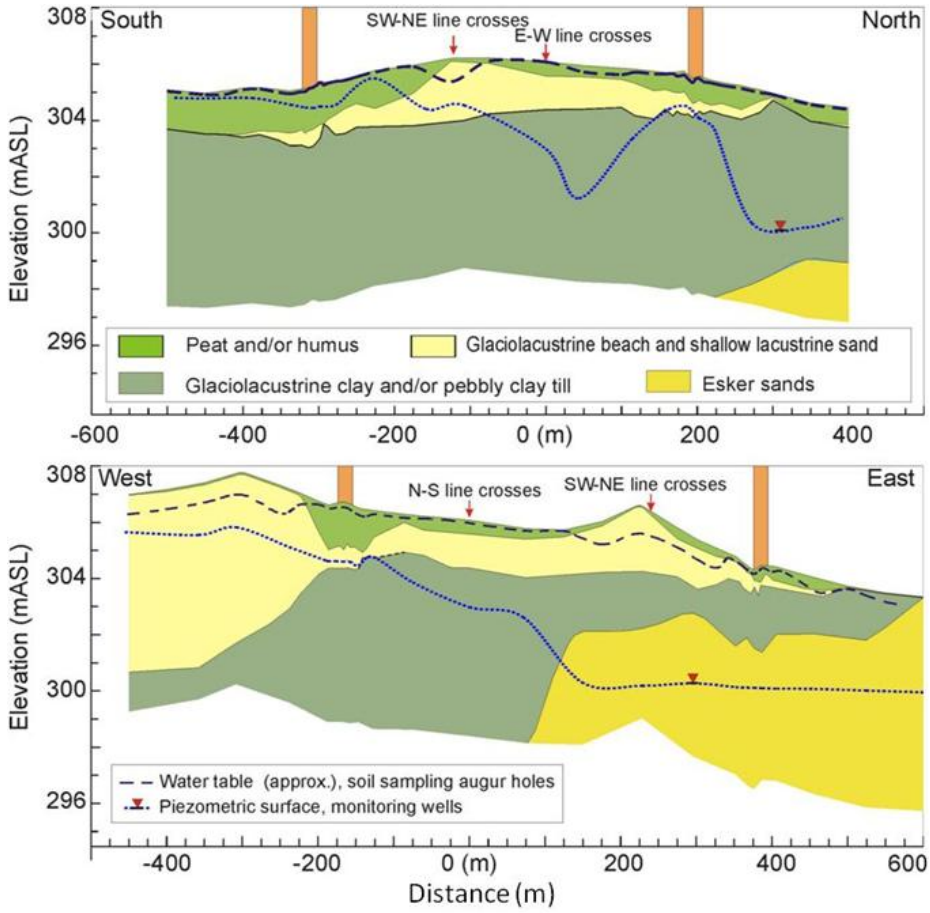

Methodology

1. Sampling

The author visited the Bean and Thorn North in July 2008 and July 2009 in order to examine environmental conditions at the forest rings, soil profiles at the ring edges and to replicate the sampling methodology for soil and peat. However, the data included in this thesis were acquired by soil and peat sampling carried out by the Ontario Geological Survey in August 1999 and July 2000 at the Bean and in July 2000 at the Thorn North ring. The same sampling methodology was used during both years. Two orthogonal sampling lines were established along transects across each ring (Figures 8 and 9). The sample spacing was reduced from 50-100 m in 1999 to 25-50 m in 2000. During both years, sample density across the presumed ring edge was increased to 5 m. The peat thickness was first assessed by measuring the depth to clay with a standard split soil spoon. One soil spoon length (30 cm) of mineral soil was collected beneath the peat-soil interface. Peat samples were collected within 30 cm of the clay sampling site, at the standard depth of 0.5 m using hand-held Dutch augers (Figures 10 and 11).

The top organic horizon is entirely composed of peat. Samples were classified based on visual examination and range from poorly humified to well humified. Poorly humified samples are partially decomposed, fibrous light to medium brown with well distinguishable stems and roots. Well humified samples are extensively decomposed, soft, and homogeneous dark-brown in colour. The interface between organic and mineral horizon, was commonly marked by a noticeable discoloration of the sampling unit, indicative of oxidation. Clay from the Bean site showed mottling or an orange/reddish colour. Mottling is a common occurrence in regularly water-logged soils and did therefore not occur under thick peat deposits. It is caused by a very localized alternation between oxidized (brown) and reduced (grey) environments reflecting iron cycling by iron-oxidizing bacteria (Chorover, 2005).These units, referred to as “mottled clay” on the Bean and “interface unit” on Thorn North on figures 10 and 11, were distinguished from the deeper uniform-grey clay unit and sampled as a different horizon. Only data from samples in the underlying uniform-grey unoxidized clay are used in the thesis.

Field data for the collected peat and soil samples are reported in Appendix 1 for Bean and Appendix 2 for Thorn North. These include sampling depth, location along the transect, water depth at the sampling site, the surveyed topography and a short sample description.

FIGURE 8: Sample locations for the southeast-Northwest (BE-SENW) and southwest-Northeast (BE-SWNE) transects across the Bean ring. Geo-positioning of the air photo is estimated to be accurate to ±10 m but was rubber-sheeted to a Landsat image of unknown accuracy. Actual ring-edge locations (Table 1) were determined with the help of oblique air photos taken from a helicopter orthogonally to the sample lines. Geo-positioning of the sample points is ±1 m, although their accuracy relative to one another is better than this. Photo and location are as per Figure 4.

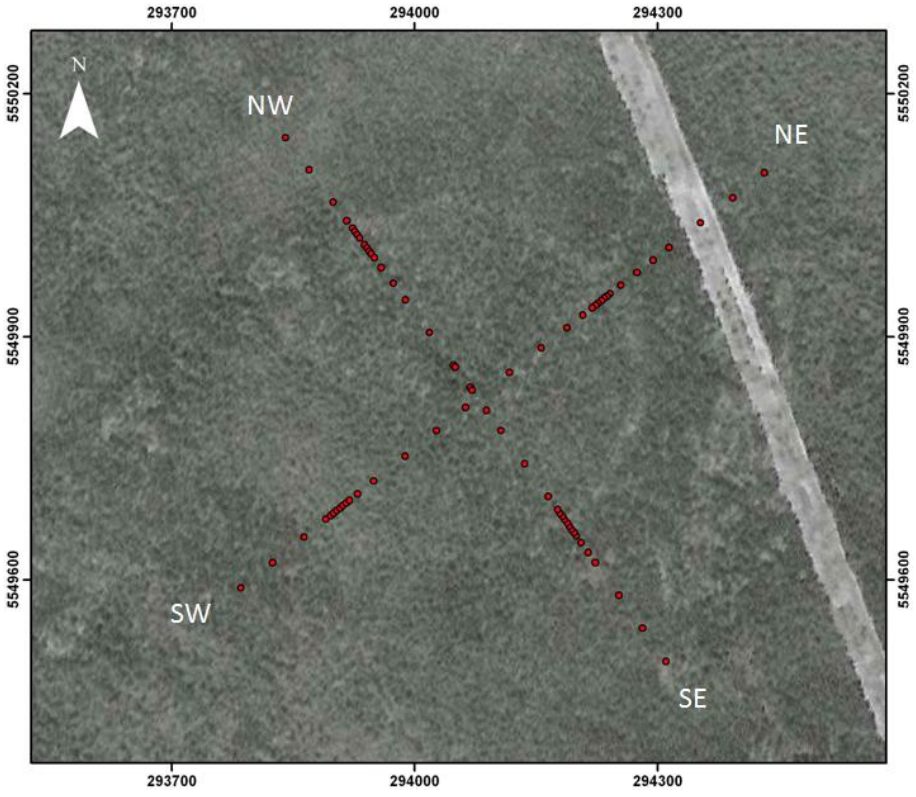

Figure 9: Sample locations for the north-south (TN-NS) and east-west (TN-EW) transects across the Thorn-North ring. Geo-positioning of the air photo is estimated to be accurate to ±5 m. Geo-positioning of the sample points is ±1 m, although their accuracy relative to one another is better than this. Photo and location are as per Figure 5.

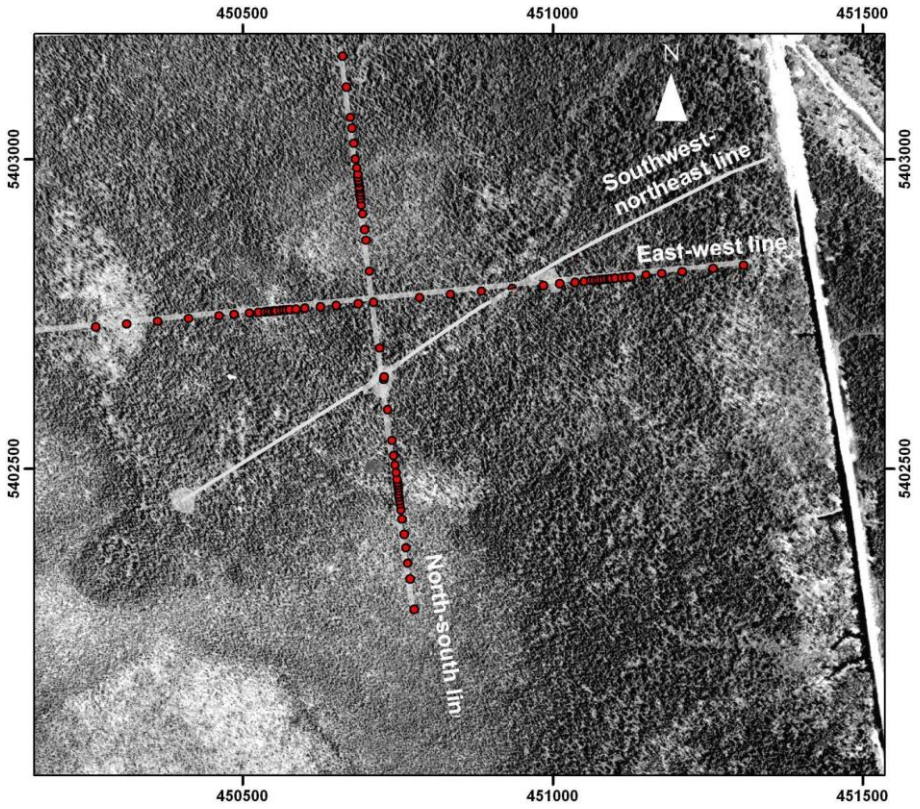

FIGURE 10: Peat and soil sample locations in the stratigraphy of the Bean Ring. The size of the bubbles is proportional to the oxidation degree observed in the field, with larger bubbles indicating higher oxidation (brown discoloration of the sample). 3 horizons were differentiated during the 2000 sampling program: peat, mottled clay directly underlying the peat, and uniform clay. Data from the mottled horizon between peat and clay are not presented in this thesis. Note the increased degree of oxidation at the NW ring edge, as well as the increase in thickness of the mottled horizon. Samples in 1999 (i.e. weak leach samples) were collected directly at the interface of peat and clay without distinguishing the different horizons.

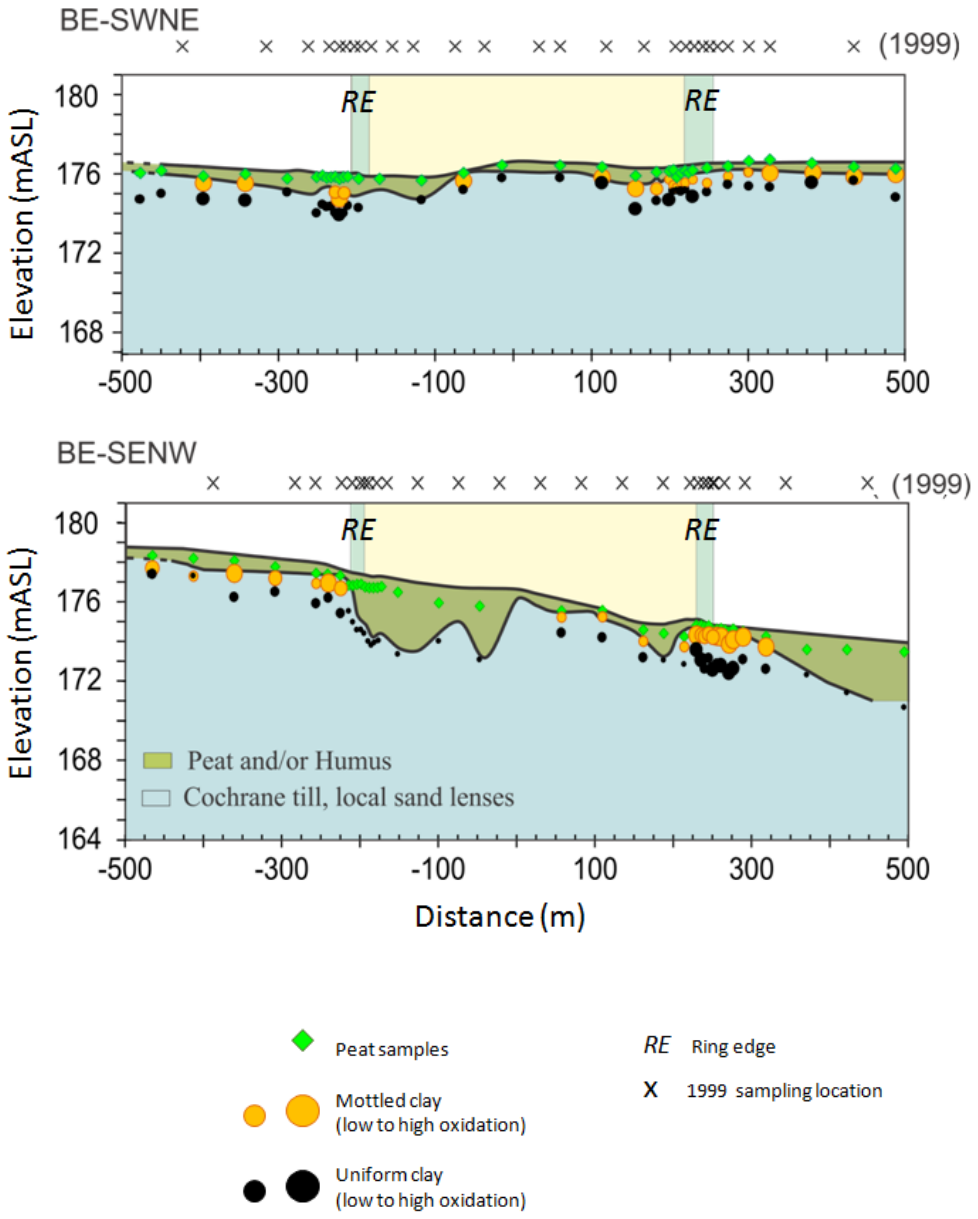

FIGURE 11: Peat and soil sample locations within the stratigraphy of Thorn North. Consistent sampling within a unit of continuously unoxidized glaciolacustrine clay unit was possible along TN-SN, where the glaciolacustrine sand unit was thin. Sampling of the mineral horizon along the TN-WE transect occurred within glaciolacustrine sand on the West end, and glaciolacustrine clay on the East end. The dramatic changes in lithology and oxidation degree along TN-WE diminish the utility of this transect for the study of ring processes (figure modified after Hamilton and Hattori, 2008).

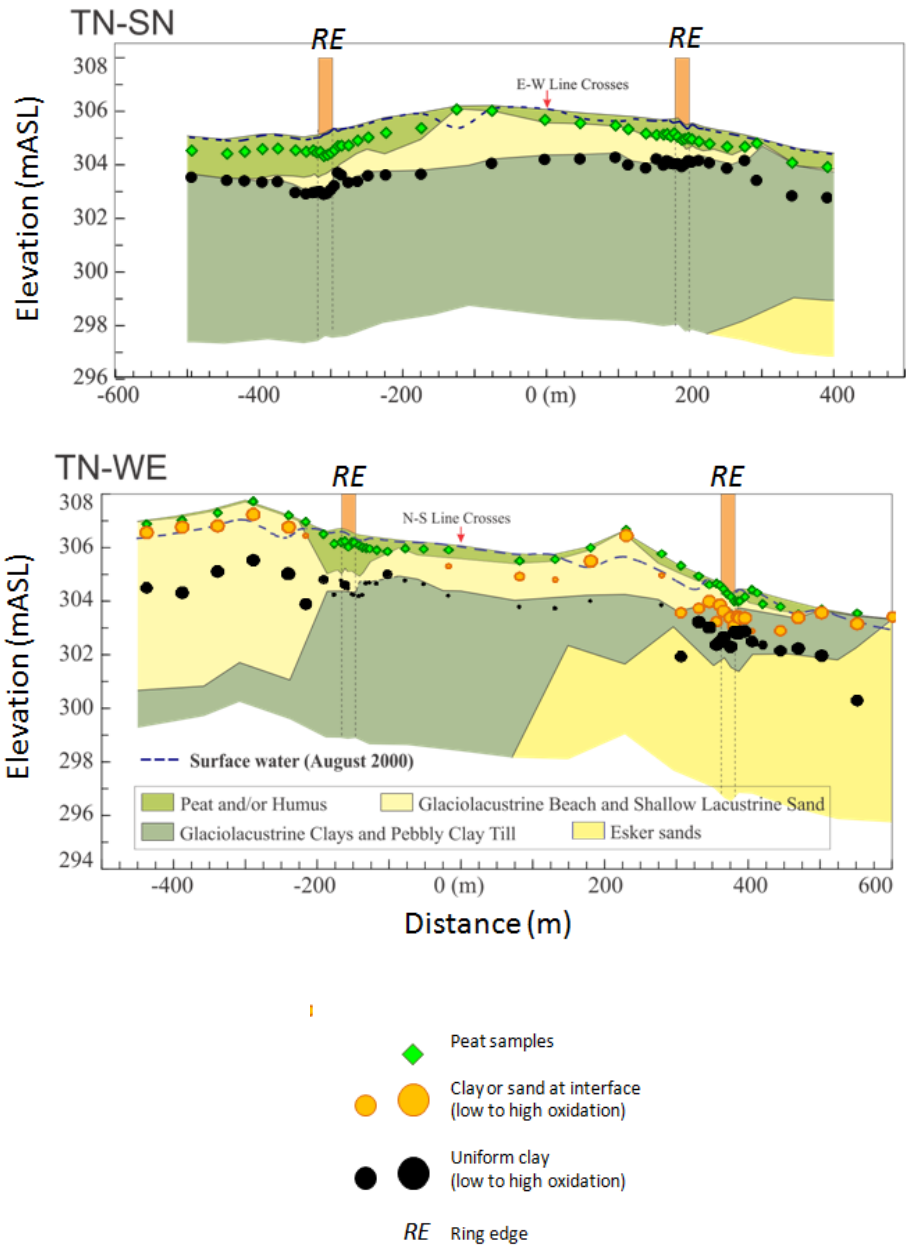

2. Positioning of ring edges

Minimal error on the location of the ring edge on each sampling transect is crucial, in order to precisely locate the relative position of geochemical changes. The position of the ring edges (Table 1) was determined using aerial photography and the location of the inner and outer edges were separately determined. At the Bean ring, the outer and inner ring edges were found to be between 18 and 28 m apart on the southeast, northeast and northwest ring edges. The southwest edge is located in a tamarack and cedar swamp in contrast to the other three which are in black-spruce dominated forest and this makes a consistent estimate of the outer and inner edges difficult. The inner edge is the most clear and therefore the outer edge was estimated by assuming it is located 17 m farther out from the center. The error on the location of the center of the ring edges is estimated to be ±5 m except on the southwest line, where it is likely 50 % poorer (±7.5 m).

At Thorn North, the outer edges of the rings were assessed using aerial photography and ground surveying. The inner edges were clear and a consistent distance from the outer edge. On the north, south, west, and southwest edges, the position is estimated to be accurate to ± 5 m; and on the east and northeast edges to ± 10 m. The large uncertainty on the eastern side is due to a change in vegetation over the north-south trending esker on the eastern third of the ring. Where the inner edge is visible, it is between 15 and 20 m from the outer edge and therefore, for plotting purposes it was assumed to be 20 m inside the position of the outer edge.

TABLE 1: Location of ring edges with respect to the center of each forest ring as determined by air photo interpretation.

	Axis	Inner rim	Outer rim	Thickness of ring edge
BEAN	**SE**	-185	-203	18
	NW	224	252	28
	SW	-201	-221	20
	NE	198	217	19
Thorn	**S**	-322	-300	22
North	**N**	202	182	20
	W	-174	-154	20
	E	394	374	20

3. Field analyses

pH and ORP analysis for both peat and clay were carried out on site, immediately following sampling after the method of Hamilton et al. (2004b). Measurements for peat were obtained by placing the wet peat in a cup, inserting the individual probes into it and compressing the peat around the probe to exclude air. Clay samples were mixed with de-ionized water (1:1 mix in volume) to make a slurry prior to measurements. Prior to usage the deionized water was stripped of dissolved oxygen by continuously bubbling N_2 gas through the squirt bottle for a period of at least 5 min. This method is known to remove dissolved oxygen from water (Barnhart, 1995).

The pH probe was three-point calibrated at pH 4, 7 and 10 at the beginning of each day, cleaned with distilled water after each measurement and stored between samples in a pH 7 buffer solution. The ORP probe was a commercial Ag-Ag/Cl combination (Corning model 476516) and, as per standard protocol, was not calibrated. The ORP reading indicated by the probe is the voltage difference between the half cell and Pt in contact with the sample as measured with a very high impedance voltmeter. Under ideal conditions, the voltage reading is proportional to the difference between the half-cell and the solution in contact with the Pt electrode. To minimize the effects of polarization, the probe was put in a reducing pre-treatment solution (acidic ferrous-sulfate; Hanna Catalogue No. 1230) prior to each new measurement. To allow for further depolarization, ORP values were recorded after 1, 2 and 5 minutes of emersion in the solution. Although ORP readings would follow a continuous trend (decrease or increase) during this period of time, attempting to reach complete stabilization would have led to unreasonably long measurement times. In all cases, the reading at t=5 min was used as the representative value. Between samples the probe was cleaned with distilled water and kept in KCl storage solution to minimize contact with air. When resuming measurements after a storage period longer than 2 hours, the first sample slurry was repeated: first to depolarize, and second to obtain a lower, depolarized and more accurate reading for that sample.

4. Laboratory analyses

Prior to analysis, peat and clay samples were oven dried at temperatures below 60°C, gently disaggregated using a ceramic mortar and pestle and sieved to -230 mesh (<0.066 mm). All analyses were performed by the Ontario Geological Survey Geoscience Laboratories (Sudbury, Ontario,

Canada). The sediment and peat samples were subjected to a near-total digestion by aqua regia, and analyzed using inductively coupled plasma mass spectrometry (ICP-MS) and inductively coupled optical emission spectrometry (ICP-OES). Sediment samples from the 1999 sampling program were subjected to hydroxalymine-HCl leach at room temperatures to selectively dissolve Fe oxy-hydroxides. Carbonate contents (total carbonate, calcite, dolomite) were determined using the Chittick method. A Chittick apparatus measures the volume of CO_2 released from a finely ground rock during the reactionwith hydrochloric acid, and calculates the carbonate content based on the known differing rates of dissolution between calcite and dolomite (Dreimanis, 1962).

5. Statistical data processing (PCA)

Description of method

Although clear to the eye, and justified by their spatial correlation with the ring edges, a major challenge was to validate geochemical signals by demonstrating they are statistically significant. Principal Component Analysis (PCA) is a reductive statistical method used to find common variability amongst multiple variables. It can provide objective insights into the variability of multivariant data. In the case of forest rings, PCA was used on the assumption that the amount of total variance increases drastically at the ring edge and that geochemical processes can be recognized by analyzing the variables contributing to the principal components.

The freeware OpenStat was used to complete the PCA. The program extracts the components through the principal axis method followed by a varimax (orthogonal) rotation. This is a simple rotation of the data in multidimensional space that maximizes the sum of the variances of the squared loadings without actually changing the relative (multidimensional) spatial relationships between samples. The mathematical foundations of PCA are described in many textbooks on the subject.

Terminology

Principal component loadings (abbreviated as *PC load*) are a measure of the influence or weight each variable (element) has within a principal component (PC). A positive loading means the element contributes positively to the PC – and inversely for the negative loading. The percent of variance in an observed variable that is accounted for by the retained components is known as

communality. A large communality indicates that the variable loads heavily on at least one of the PC`s. The principal component score (abbreviated as *PC score*) is the original data (original standardized concentration) weighted by the PC loading. Ultimately, the PC score for each sampling site is calculated as the sum of the concentration of all elements weighted by their respective loadings. These PC scores can be seen as the new geochemical coordinates of the sampling sites following projection onto the 6 major principal components, i.e. into a space of reduced variables. Load plots show the relationship between the variables analyzed, grouping those which have a similar geochemical behaviour. The aim of score plots is to help identify sample sites that display a similar geochemical signature. In the output, PCs with an eigenvalue greater than one are considered significant. An eigenvalue is a matrix algebraic function that tests the significance of the components.

Selection of variables and analyses

Prior to input, the data were tested for normality and standardized automatically within OpenStat. The PCA test was performed on the aqua regia data of mineral soil samples on along BE-SENW and BE-SWNE at the Bean ring. This ring was selected because it is not affected by changes in media and the analysis of geochemical changes along the BE-SENW transect revealed well-defined rabbit-ear anomalies.

22 Variables were included in the PCA: calcite content (Cal), dolomite content (Dol), ORP, pH, and concentrations of Al, Mg, Mn, Na, P, S, Ag, Be, Ca, Cd, Hf, Mo, Nb, Sb, Sn, U, W, and Zr. Appendix 3 presents the correlation values between these variables. The raw geochemical data for these elements is included in Appendix 4 and 9. Elements that were not included despite being available through analytical results were: Fe, K, Ti, V, Ba, Zn, Co, Cr, Cs, Cu, Ga, Li, Lu, Pb, Rb, Th, Tl, Y, REE. These elements displayed a correlation > 0.99 with each other and were excluded to reduce the amount of variance redundancy within the dataset. Al was kept as a proxy for these elements, as it displayed a correlation >0.99 with all of the elements removed. Note that Zr was also highly correlated with Al, and therefore most of the excluded elements. However it was kept because it differs from other elements in its correlation with Hf (>0.99), and its lack of correlation with Al, Fe and V (<0.99).

The data from both sampling lines in the Bean ring were combined and input as one population, resulting in a sample size of p=73 (39 sites along SENW, and 34 sites along SWNE). The distinction between SENW and SWNE is not expected to skew the PCA because the sampling media on both lines are similar, as indicated by similar siliciclastic and carbonate contents.

For statistically reliable results, the minimal number of samples should be greater than 5 times the variables analyzed (SAS, 2012). For this analysis, n/p = 22/73. This convention is neglected, as the validity of the observed trends is justified by their close geographical location next to the ring edge as well as the meaningfulness of the assemblage of elements. The PCA yielded six components with an eigenvalue greater than 1 (Table 2). Combined, these account for 78% of the total variance. The entire output of the PCA, including variable loadings and communalities, is presented in appendix 5.

TABLE 2: Distribution of variance within the principal components

	Factor 1	Factor 2	Factor 3	Factor 4	Factor 5	Factor 6	Total
% variation in factor	34.917	11.379	8.574	8.692	7.08	7.138	77.78

Results

1. Geochemical trends along transect lines

pH

The pH and redox chemistry of peat and soil samples across the Bean and Thorn North rings are displayed in Figures 12 and 13, respectively. The raw geochemical data is listed in Appendix 6 and 7 for Thorn North, and 8 and 9 for the Bean. In addition to the exact values for the field measurements, these appendices also include the numerical results of the Chittick and elemental analyses which are described in subsequent sections.

The pH of clay slurries range between 7.5 and 9.2, whereas peat samples range between 5.3 and 7.0. The peat along TN-WE differ from this trend with low pH values of 2.5 to 4.5 recorded on the westernmost 5 samples and a block of 4 in the center of the ring. This coincides with field observations recording a change in moisture content at these sites and a change from poorly saturated humus samples (low pH, high ORP) to well humified moist peat (high pH, low ORP). This is likely caused by the occurrence of oxidized sand in the mineral soil at the first 5 sites along the line and partially oxidized clay in the 4 samples near the center, caused in both cases by a drop in the water table.

The ring edges of the BE-SENW, BE-SWNE and TN-SN lines are characterized by distinct drops in pH. The observation could not be made on the TN-WE line because of different media on that line. At all 6 ring edges, and most clearly on the BE-SENW and TN-SN lines, the drops in pH are framed by anomalously high values in pH. Towards the center of each ring edge, the total amplitude in pH variations is between 0.5 and 2 pH units. The lows at the ring edges are flanked by even more pronounced pH highs except on the outer edge of BE-NE, where the sample density is low. These show a pH range between 0.8 and 1.5 units below the tops of the adjacent peaks. At TN-SN, a difference of 1.5 pH units and a difference of almost 1 pH-unit occurrs on both lines at the Bean over a distance of only 100 m at the ring edges.

The pH in peat is more variable than the values for clay slurries. Responses at the ring edge are characterized by peaks rather than dips and these occur above or almost above the pH lows in clay. Positive anomalies in peat pH are most evident at BE-SENW, BE-NE and TN-SN with an amplitude of 0.3 to 0.5 pH-units. It is unclear whether the response at BE-SW is missing, or is wider and less sharp. The antithetic peat/carbonate pH relationship is offset by one sample station at both edges on the TN-NS line. This may be a result of a slight misalignment of the peat and clay samples since the samples were spaced very close together and samplers could never collect peat from exactly the same location as the clay sample. This was done in order to avoid siliciclastic contamination from the sampling of the clay, which was always sampled first.

FIGURE 12: pH of peat and mineral soil slurries along transects across Bean and Thorn North.

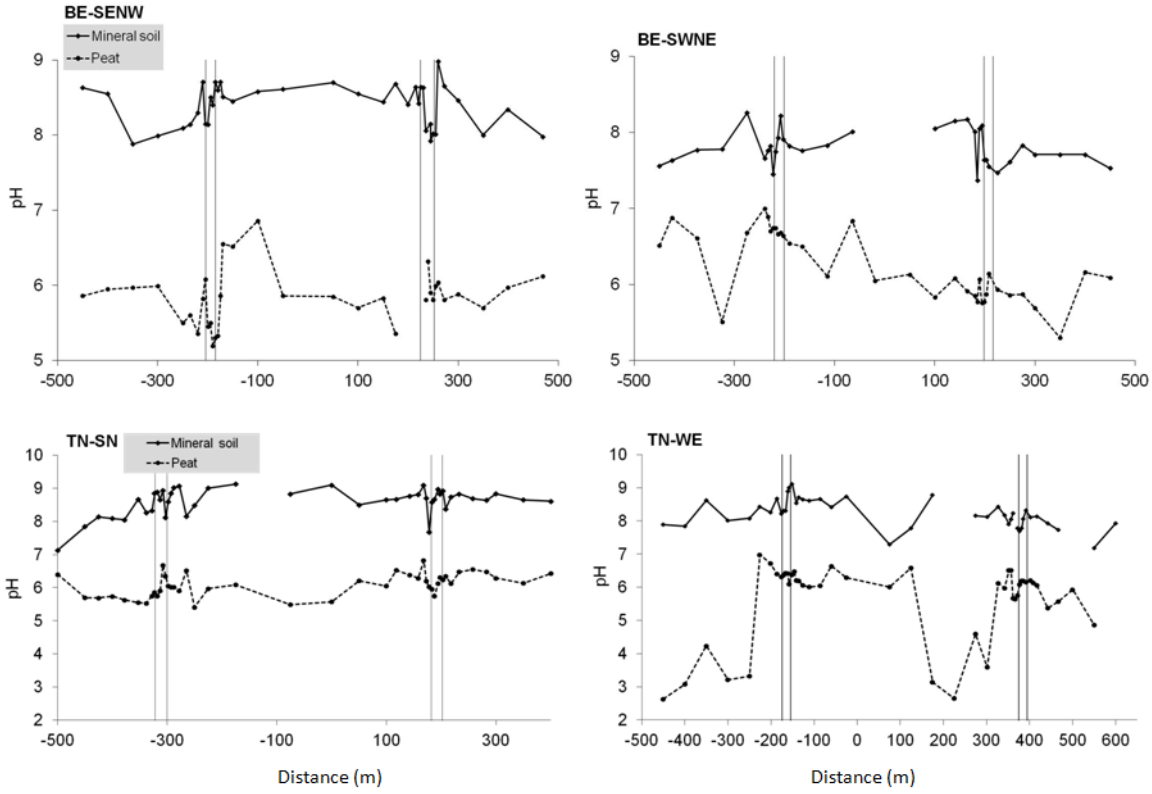

Oxidation-reduction Potential (ORP)

Shallow organic samples were more oxidized than deeper clay samples. The variability was narrower within peat than in clay. The redox state of the peat varied with moisture content; water-logged peat being more reduced because it was more anoxic. The alternation between oxidized, dry and sandy samples and reduced, wet and clay-rich samples along TN-WE clearly appears within the ORP signal of the organic and mineral soil (Figure 13). These obscure responses at the TN-WE sampling line, therefore the discussion of ORP trends on that line is excluded.

Clear responses in both peat and mineral soil occur on all the ring edges with consistent media (BE-SENW, BE-SWNE and TN-SN). ORP displays more variability than pH, and ORP changes of large amplitude coincide with the ring edge and particularly with the location of negative pH responses in clay. This is evident at BE-SENW, where large negative anomalies occur on the outer side of the ring edges, with amplitudes of 150-200 mV in the peat and 50-150 mV in the clay. Responses on BE-SWNE also show large amplitude changes but since the sample density was not perfectly optimized for the ring edges, the signal is not as clear. The responses on TN-NS are less evident. Responses in peat and mineral soil are offset by several sites, but ring edges in wet conditions (BE-NE) appear to correlate a low in the pH/ORP of clay with a low in the ORP of peat, whereas dry ring edges (BE-NW and BE-NE) correlate a high in the ORP of peat with a low in the pH/ORP of clay.

More generally across the Bean ring, the ORP responses in clay are low inside the ring on BE-SWNE and mostly low on the BE-SENW. The exceptions are three samples inside the ring on the northwest side. These are in an area of particularly shallow peat where the clay is partially oxidized.

An oxidized zone occurs inside of the ring edges at TN-SN in mineral soil, but not within peat. It is unlikely that this anomaly is caused by a change in medium similar to TN-WE because the trend is not apparent in any other parameters, such as pH, Ca, Total carbonate and bulk concentrations of major elements; nor was it noted in the field notes. This may be related to a drastic drop in the piezometric surface in the underlying clays in this area (Figure 7), perhaps due to under-drainage into the esker. This could allow periodically unsaturated and oxidizing conditions to develop in the clay and overlying sand. Hamilton and Hattori (2008) did not note a decrease in redox in the groundwater underlying this area, suggesting it is likely a shallow phenomenon.

FIGURE 13: ORP of peat and clay slurries along transects across Bean and Thorn North. Wet/dry annotations indicate the state of surface moisture.

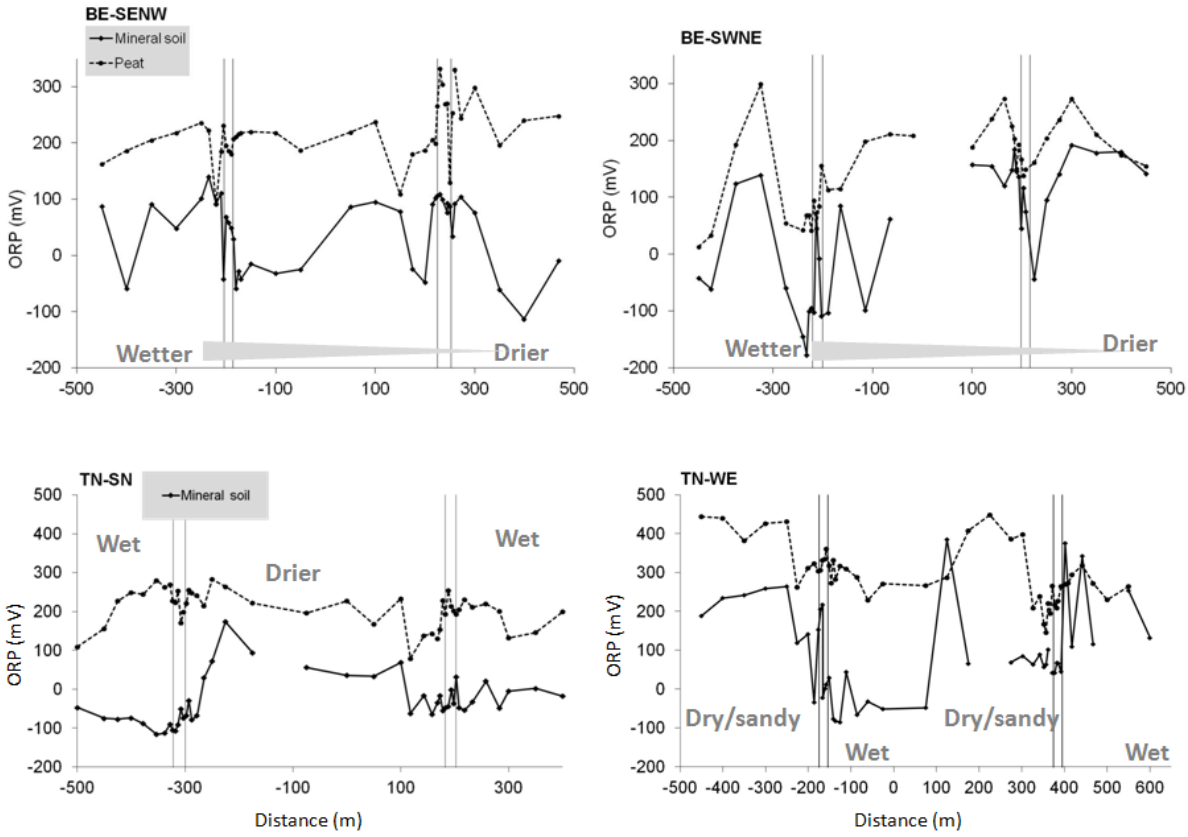

Carbonates

Carbonate contents were measured by the Chittick method, yielding the amounts of calcite, dolomite and total carbonate (=%Calcite+%Dolomite). The values were verified using the Ca concentrations of samples after aqua regia-digestion (Figures 14 and 15).

Well-defined rabbit-ear responses centered over the forest ring occur along the BE-SWNE and BE-SENW transects of the Bean ring. They are characterized by negative responses in calcium and total carbonate of mineral soil. Positive responses in total carbonate characterize the peat, but these are not apparent in the calcium plots probably because the highest of responses has lower equivalent Ca concentrations than typical concentrations of non-carbonate Ca in the peat. The BE-SWNE edges are characterized by a drop of 50% total carbonate at the outer ring edge in mineral soil, coinciding

with a greater than 4 fold increase in peat. Results from the Chittick method are not traditionally considered reliable below values of 5 wt.%, nor is the method typically used on organic soils. However the >5 wt.% responses at the ring edge and their symmetry suggest that upward carbonate mobility into the peat is occurring. The 1999 weak leach data available for the Bean edges (Figure 14) show an increase in concentration of Ca around the ring edges, which suggests an increase in mobility of Ca in these areas. The values in aqua regia digestion in 2000 are elevated inside and outside all 4 of the ring edges. Although different sampling stations are used for the collection of samples in 1999 and 2000, it appears that the drop in the contents of Ca and total carbonate inside the ring edge, relative to the outside, coincides with a similar drop in mobility of Ca in approximately the same locations.

Distinct positive ratios of calcite to dolomite occur within the peat samples at the edges of BE-SE, BE-NW and TN-N edges. Notably, TN-N is the only site where a distinction between inner and outer ring edge processes is suggested within peat samples. This appears as distinct peaks in calcite/dolomite ratios on the inner and outer ring edge that amount to a doubling of total carbonate values just outside of the ring edges. An increase in the calcite/dolomite ratio is likely due to a relative increase in calcite rather than a decrease in dolomite since dolomite concentrations were low to begin with. A distinct double-dip anomaly is also observed in the pH data for underlying clay on the same line but the emplacement of the two sites occurs 5 and 10 m apart with the calcite/dolomite anomaly in peat occurring 1 to 2 stations inward of the clay pH anomaly. These anomalies within the peat do not correlate with changes in the mineral soil, as TN-SN is the only transect where the overall Ca concentrations and total carbonate values in the clay remain stable. Significant drops in the concentrations of Ca and total carbonate also occur at TN-W but it is unclear whether the drop is a characteristic of the ring edge, or if the trend of low Ca contents on the ring interior is a result of the inconsistent sample medium at the western end of TN-WE.

FIGURE 14: Proxies for carbonate content in peat and mineral soil at Bean. Fe-leach concentrations for Ca (ppm) are available only for the Bean ring, for which a preliminary survey was completed in 1999. Note that sampling sites and sample depths vary slightly between 1999 and 2000 (as described in Figure 10).

.

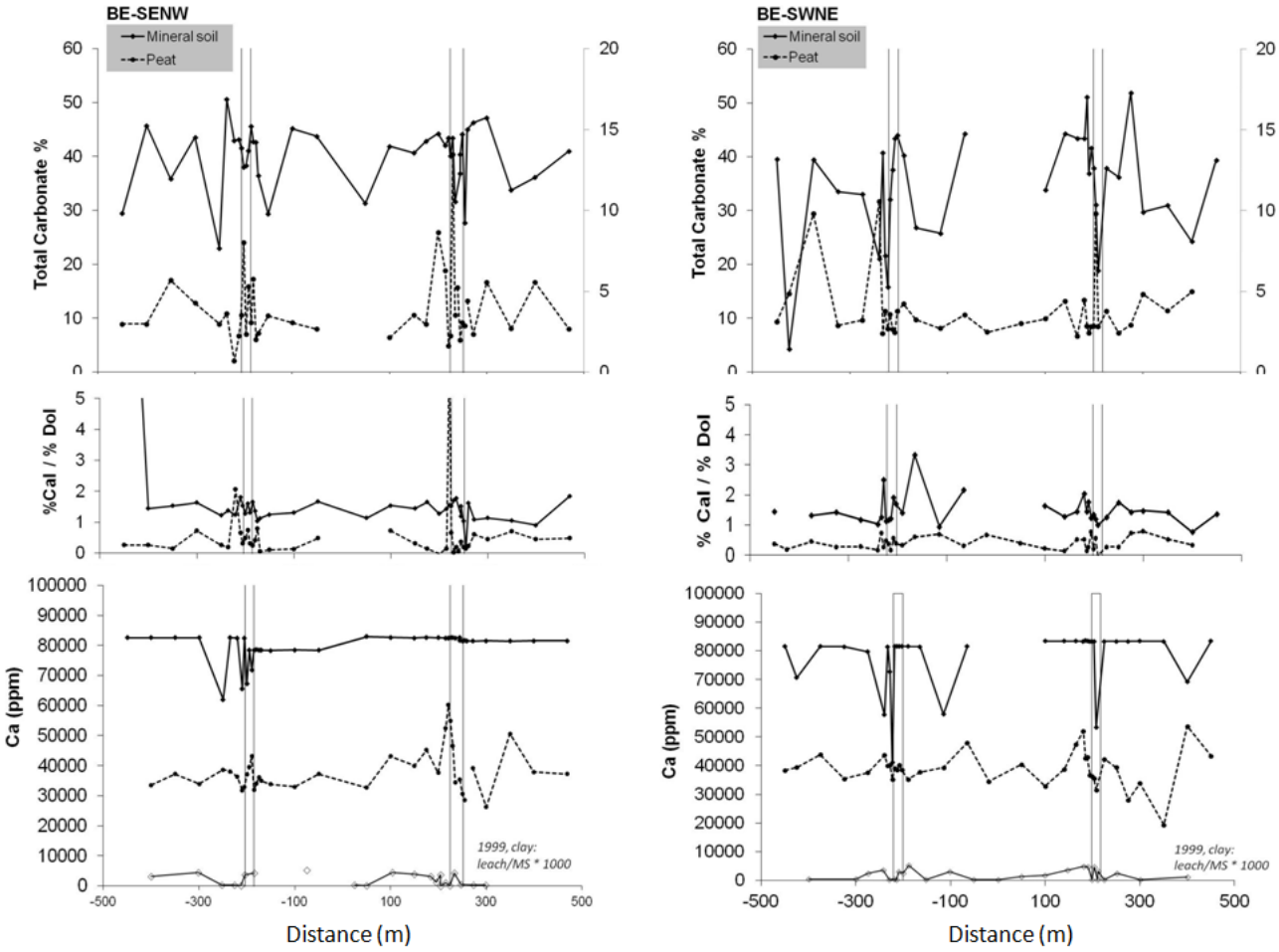

FIGURE 15: Proxies for carbonate content in the organic and mineral horizons at Thorn North. On the TN-WE line, Ca (ppm) concentrations exhibit strong variability due to changes in the sampling medium. As with the Bean ring, a carbonate response in the ring edge is apparent only in the peat samples and in particular on the north edge.

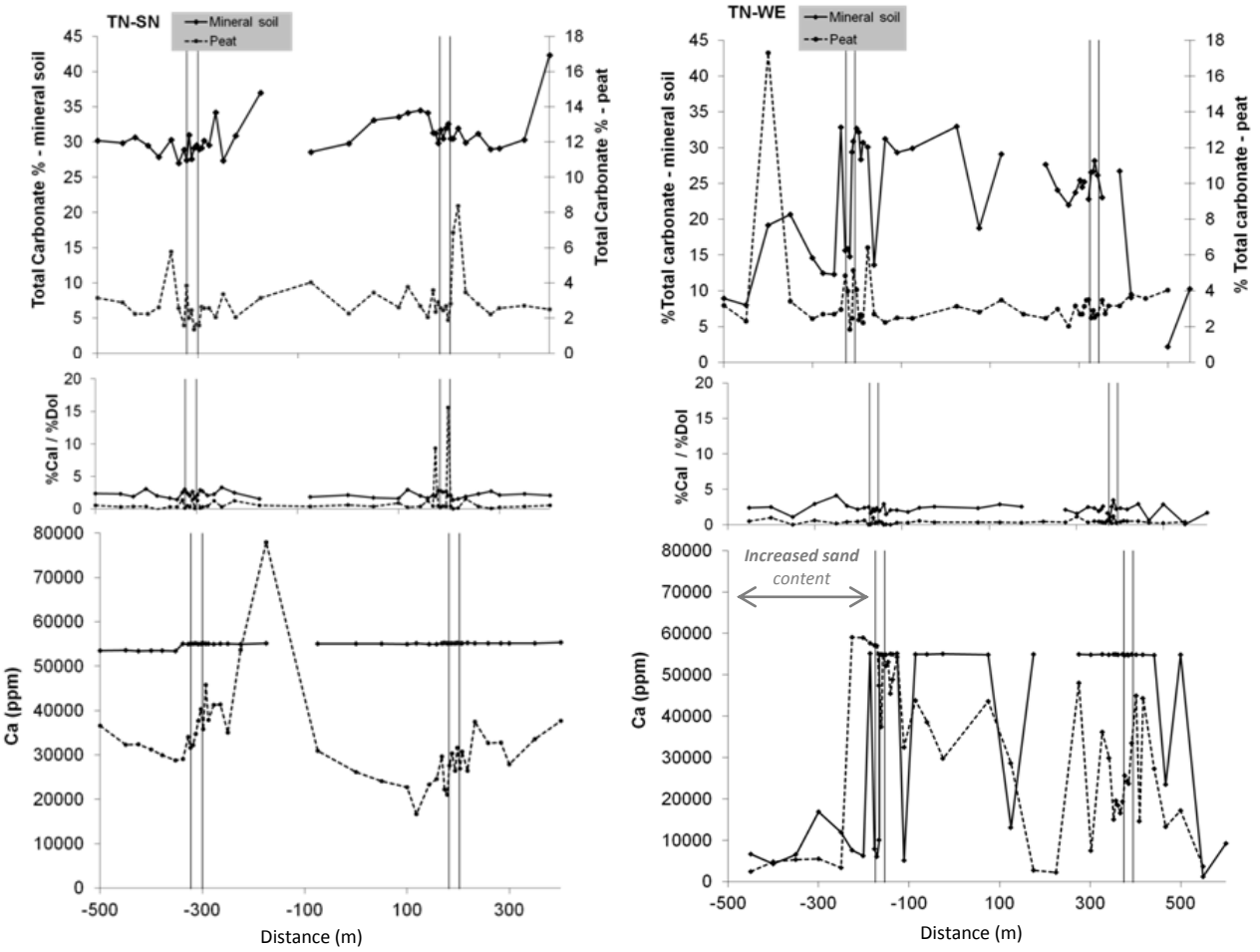

Elements (full digestion and leach data)

Fe and Mn are redox-sensitive elements known to dominate redox processes within soils (Brady and Weil, 2002). Al plays a major role in the production of soil acidity (Tan, 2010). Figures 16, 17 and 18 display results of the full-digestion (aqua regia) of peat and soil samples, as well as the weak Fe-leach data for clay soils (only available for the mineral soil above the Bean). The aqua regia data were normalized with Ti in order to remove the effect of variable carbonate/siliciclastic ratios related to ring-edge processes. Data along the TN-WE transect are not presented, as the change in medium documented in carbonate, pH and ORP values overrides the metals geochemistry.

Ti-normalized aqua regia in clay. Strong positive and negative metal responses are recorded in Ti-normalized oxide responses by aqua regia in clay. At Bean, responses in clay are positive on the northern ring edges but lower or negative on the southern ring edges, i.e. they are positive on the drier end of each line and weaker or negative on the wetter ends. At TN-NS, both ring edges occupy wet parts of the line and both similarly show negative oxide responses. The occurrence of peaks or lows in clay coincides with the locations of the pH anomalies and carbonate depletions. Thus they also correspond with the sudden ORP lows at the ring edges.

Ti-normalized aqua regia in peat. Positive responses dominate in Ti-normalized aqua regia in peat regardless of the moisture conditions. However, opposite to the clay response, the metals responses in peat are greater in the wetter areas than the drier areas. The most significant iron response is arguably on TN-SN where peat along almost the whole line was fully saturated at the time of sampling. The strongest ring-edge peaks for metals in peat occur above the pH low/carbonate depletion area that occurs in the underlying carbonate. Responses within peat and clay are antithetic at BE-SW and TN-N suggesting that clay is the likely source for species in the peat. This is supported by upwards hydraulic gradients. In peat, positive anomalies at the ring edge are surrounded by broad enrichments stretching across the ring edge over a distance of up to 200 m. Correlation of trends is more prevalent between Fe and Mn, which are more soluble than Al. These responses could either be due to an enrichment at the ring edge, or active depletion within the ring edge.

Fe-hydroxide leach (Hydroxylamine-HCl) in clay. The Fe-hydroxide leach is considered to selectively digest amorphous iron oxides and as such, it removes much more weakly bound metals than a

strong acid digestion would (Hall et al. 1996). Figures 17 and 18 show the weak leach response directly and normalized against aqua regia. The latter parameter reduces the signal resulting from changing total concentrations of metals in the samples. The results generally show lower concentrations across the ring relative to the outside, presumably because there are fewer amorphous iron oxides to be leached in the reducing environment within the ring. There are also significant anomalies at most ring edges, even on the wet edges where aqua regia extractable metals show low concentrations. This suggests that kinetic processes are occurring at the ring edges that maintain a signal in weakly bound metals. Presumably on the dry edges these metals later go on to mineralize, whereas on the wet edges they are removed before converting into more permanent phases.

FIGURE 16: Concentrations of Al, Fe and Mn to Ti across the SN line at Thorn North. Concentrations are for aqua regia digestion of peat and soil samples.

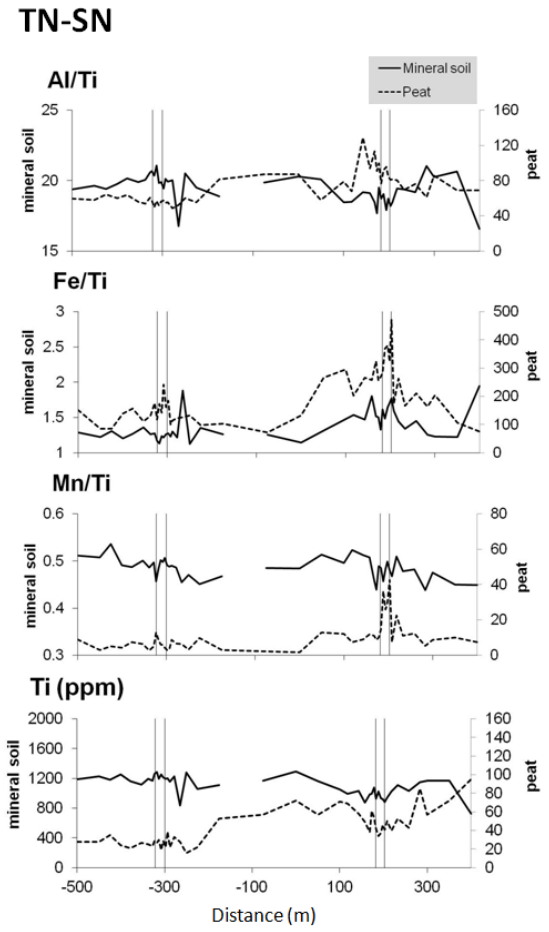

FIGURE 17: Ratios of Al, Fe and Mn over Ti across the Bean SWNE line. Full digestion concentrations (aqua regia) were determined from peat and soil collected during the 2000 sampling program. Fe-leach concentrations are only available for soils sampled during the 1999 sampling program. Note that sampling sites and sample depths varied slightly between 1999 and 2000 (as described on Figure 10).

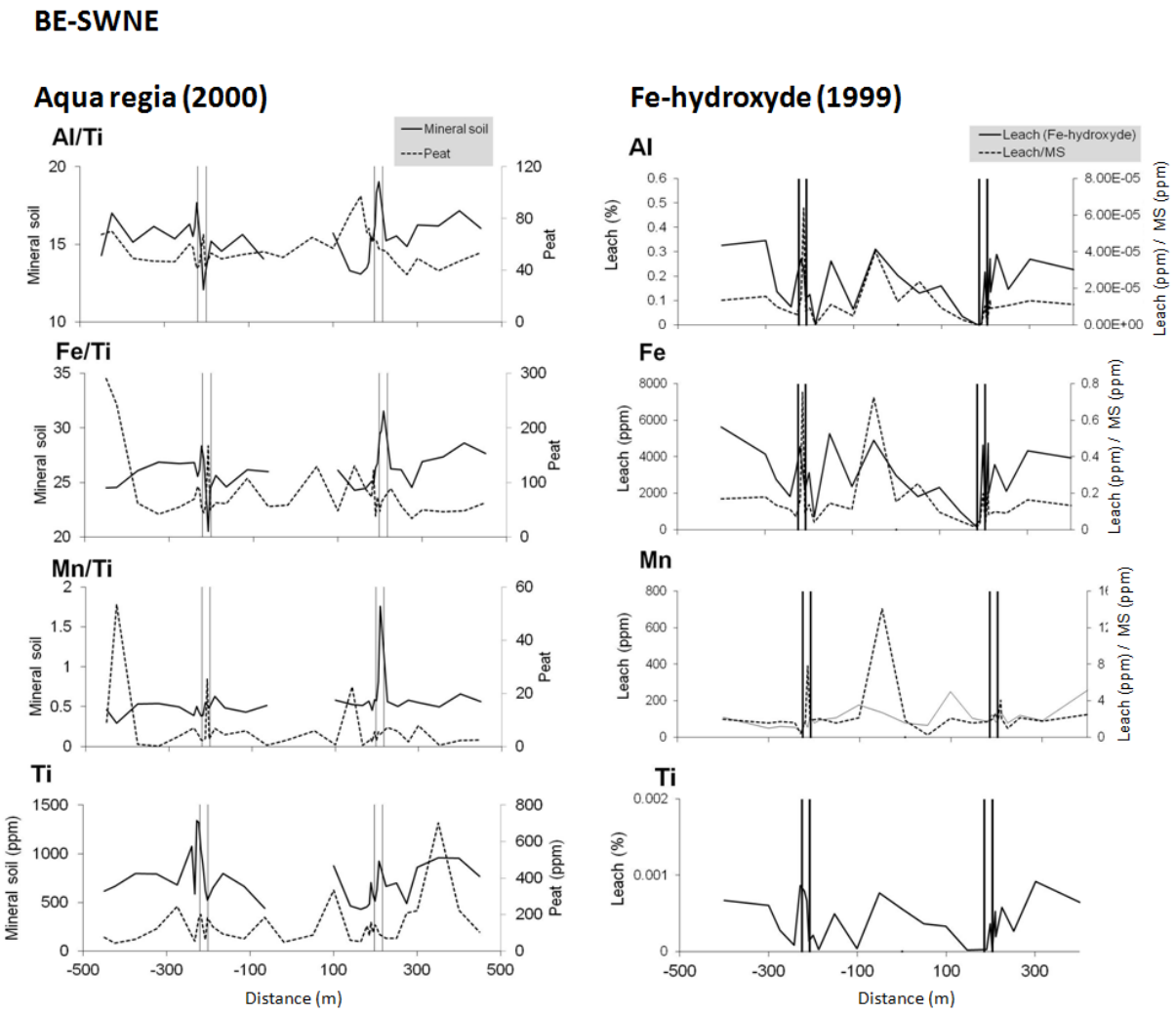

FIGURE 18: Ratios of Al, Fe and Mn over Ti across the Bean SENW line for full digestion concentrations in peat and soil, and Fe-leach concentrations in soil. Note that sampling sites and sample depths vary slightly between 1999 and 2000 (as described on Figure 10).

.

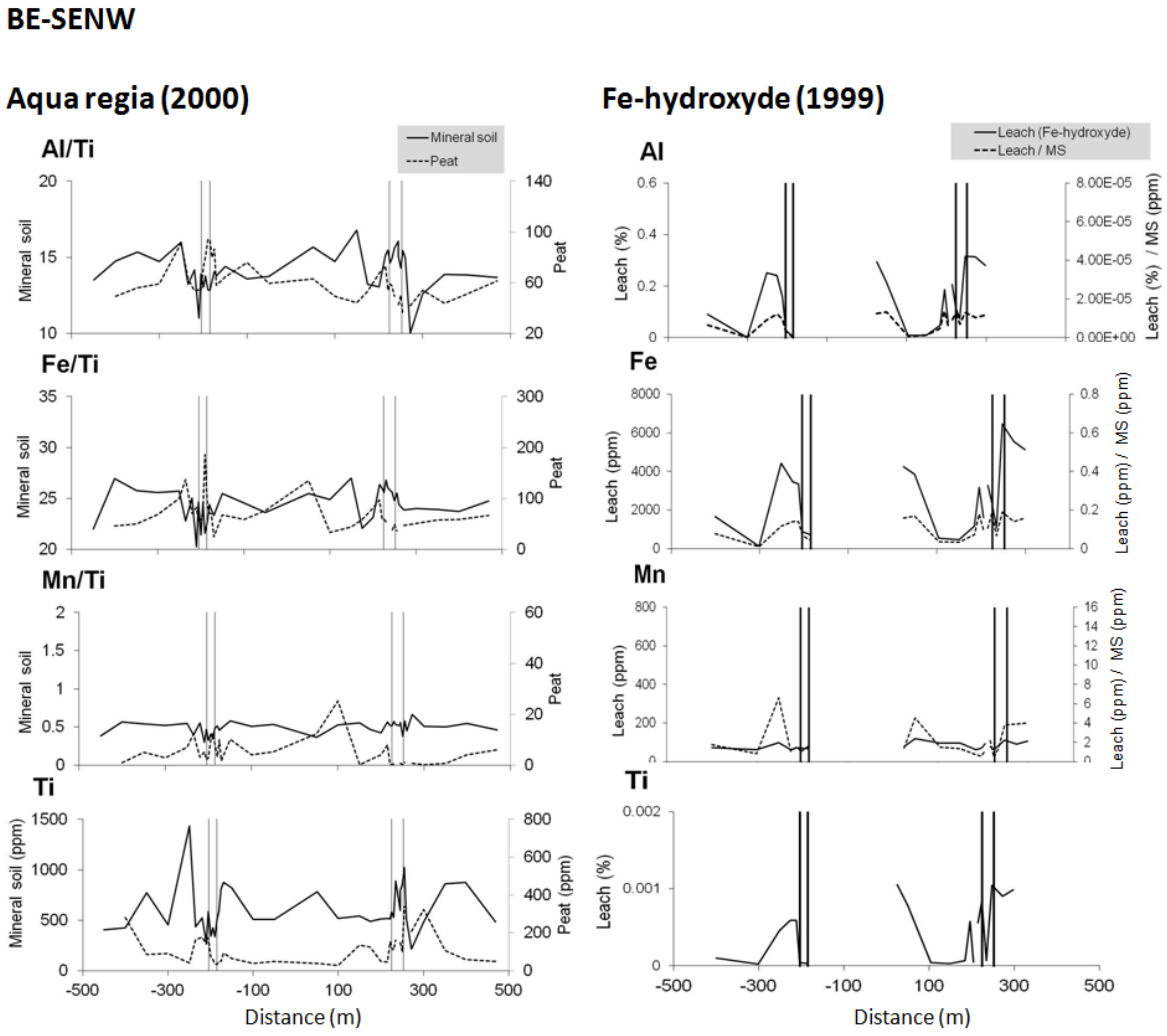

2. Principal Component Analysis of the Bean ring

Principal component loadings and interpretation

The aqua regia digestion data for the mineral soil samples along BE-SENW and BE-SWNE was subjected to a PCA. The PC loading of variables is presented in Figure 19, with the corresponding values and communalities included in Appendix 5. A variable was considered to significantly load on a given component if the absolute value of its loading was >0.30. This threshold value was chosen because major breaks within the loadings of the variables occurred at $\left|0.3\right|$. The components were labelled based on the element assemblage: residual-PC1; carbonate-PC2; ORPDol-PC3; ORPCal-PC4; NbSn-PC5 and pH-PC6.

Together, residual-PC1 and carbonate-PC2 accounted for 46 % of the total variability within the dataset. PC1 contains Zr, Al, Hf, P, Cd, Sb, Na, Be, U, and Mn. This component is believed to represent a residual component, unaffected by changes in carbonate. It is therefore likely to be mainly influenced by the proportion of primary siliciclastics in the soil. Al and Mn positively load PC1, as well as negatively load PC2. PC2 is the second most important component, dominated by carbonate compounds (Mg, Ca, Cal, Dol) and S. A positively correlation between Al and Mn to high carbonate content is indicated by the concurrence of peaks in carbonate and Al, Mn at the ring edges. S is known to be redox-sensitive and displays a cross-loading trend between carbonate-PC2 and PC6, dominated by pH.

ORP and transition metals are grouped into PC3 and PC4. ORP is associated with a negative Dol loading within PC3 and negative Ca and Cal within PC4. This indicates that part of the variability in carbonate species is caused by changes in ORP, rather than changes in pH. Transition metals are mobilized by increases in ORP, as indicated by the positive loadings of Mo, Nb, Sn on PC3 and Ag, W on PC4. PC5 is dominated by Nb (positive) and Sn (negative) and is unrelated to other elements with correlation values $<\left|0.2\right|$. ORP has one the lowest communalities, indicating that it correlates least with all other elements despite being expected to be a controlling variable within the ring edge system. This might be method-induced as the ORP probe requires a long time to re-equilibrate with the test-slurry and changing samples before complete re-equilibration is achieved, could have added artificial variability to the measurements.

FIGURE 19: Distribution of PC loadings among 6 retained components resulting from a PCA on aqua regia digestion data of mineral soils at the Bean ring. Dark columns indicate elements where PC loadings are greater than $|0.3|$. These elements account for most of the variability within the component.

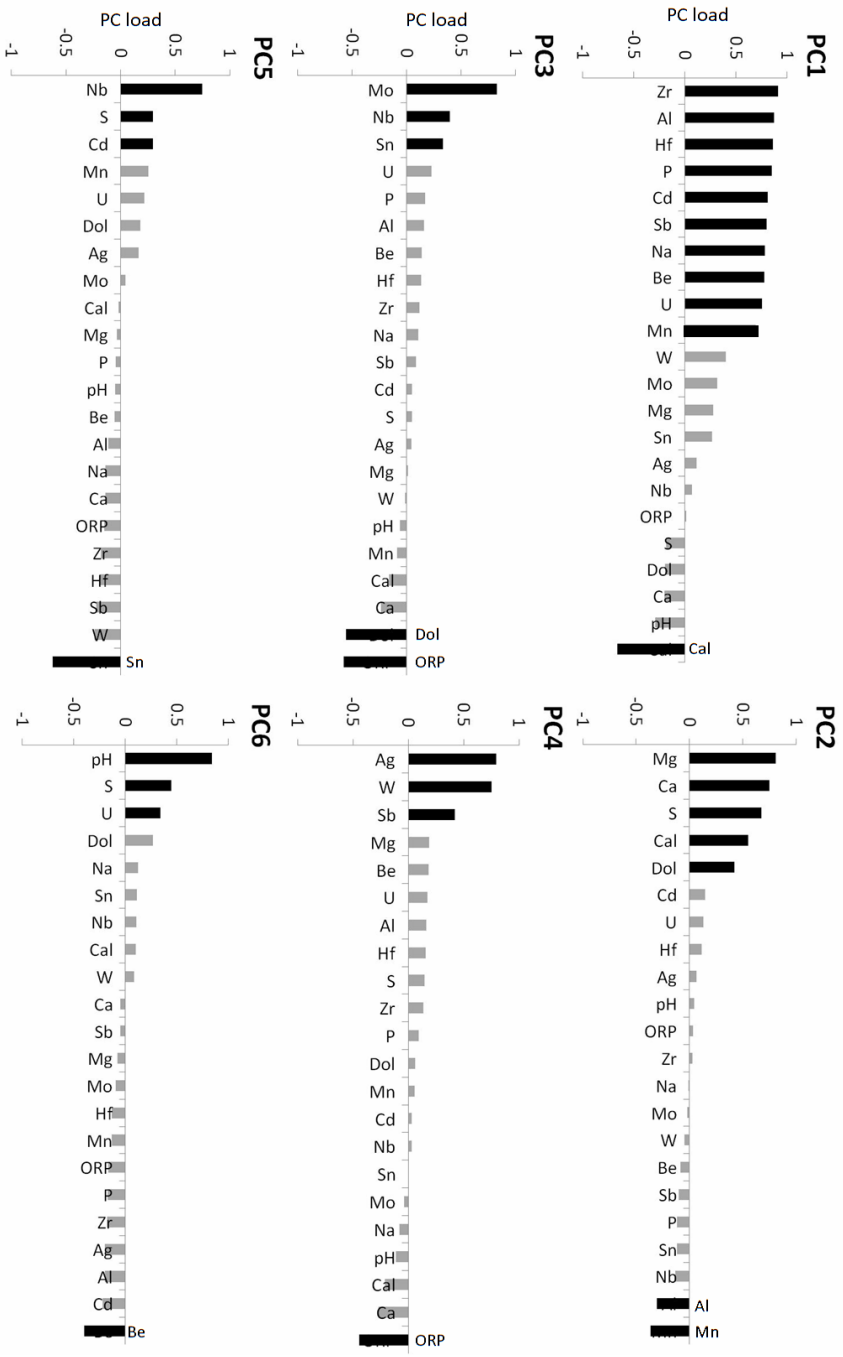

Principal component scores and monitoring of edge-related responses

Figure 20 displays the PC-scores calculated for the SENW line at the Bean ring. This line was selected because of its consistent media, and because it displays very strong rabbit-ear anomalies in total carbonate, which suggests a strong expression of edge-reactions. Indeed, all principal components display rabbit-ear anomalies. Residual-PC1, Carbonate-PC3 and ORPCal-PC4 have peak-responses with PC scores that increase drastically at the ring edge, whereas ORPDol-PC2, NbSn-PC5 and pH-PC6 have dip-responses with a decrease of PC scores at the ring edge. This emphasises the antithetic relationship between ring edge responses described in the analysis of linear trends.

One of the challenges posed by the analysis of linear trends is the correct differentiation of ring edge anomalies from other anomalies caused by, for example, accidental sampling of a different unit. For instance Ca-concentrations across BE-SENW display low Ca at 6 stations, 2 of which occur near the BE-SE ring edge resulting in a drop from 8.1 wt.% to approx. 4 wt.% (Figure 14). Carbonate-PC2 reflects all 6 sites of Ca depletion; however the responses are of highest amplitude for anomalies directly at the ring edge. The positive loading of Ca and Calcite suggest that the large Ca-depletions are caused by lower carbonate content. These sites coincide exactly with peaks in residual-PC1 and a low in pH-PC6. Changes in the ratio of soil-residual (largely siliciclastic) to carbonate components therefore resulted from dissolution of carbonates due to low pH, rather than compositional differences in the mineral soil.

FIGURE 20: Principal component (PC) scores across the SWNE transect at the Bean ring.

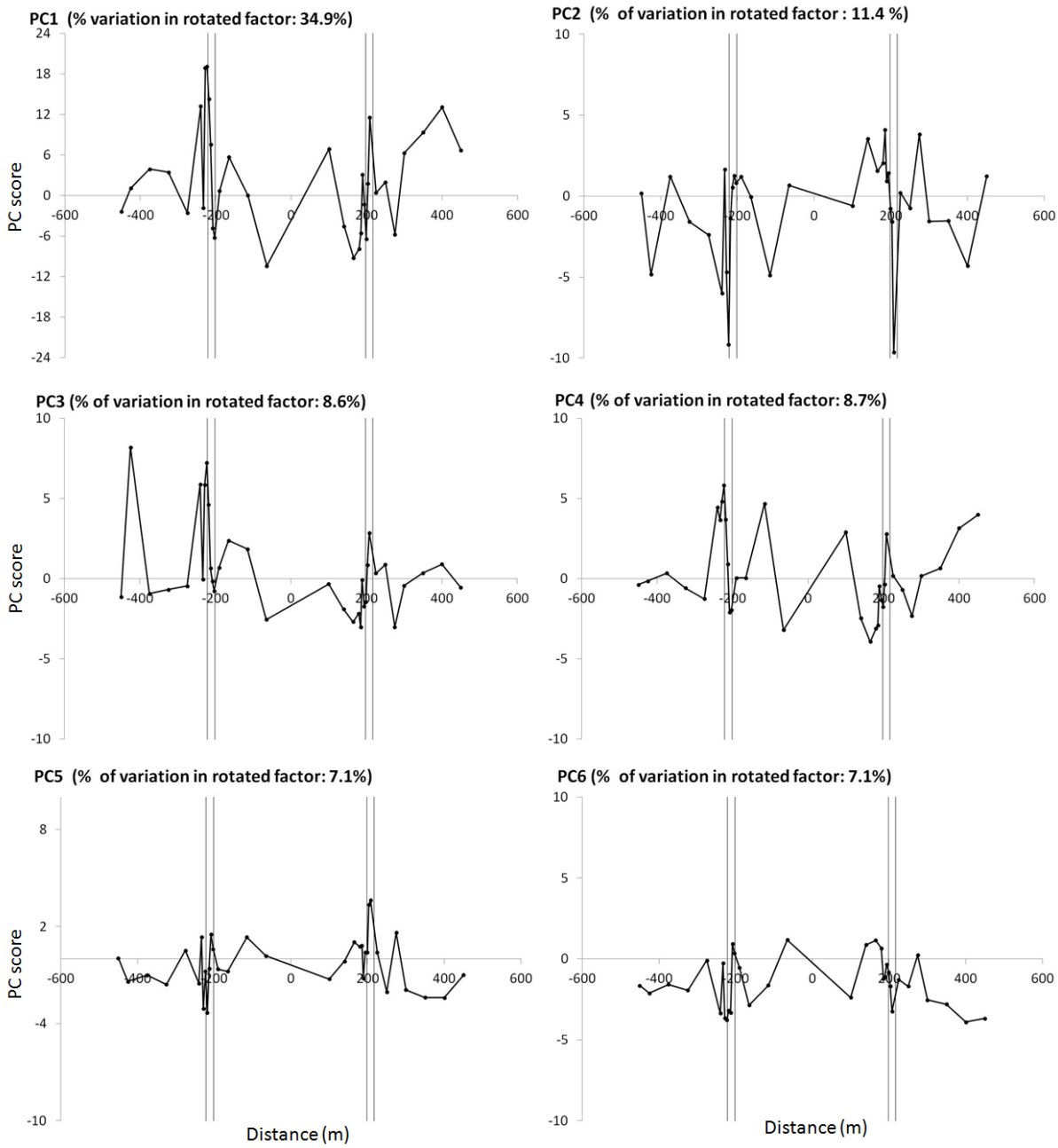

Discussion

1. Synthesis of geochemical responses at the ring edge

The results indicate that sharp geochemical changes occur close to ring edges. The linear trends across the forest ring show that each ring edge is characterized by several different reactions where redox, pH and carbonate parameters vary dramatically. On transects, these appear as rabbit-ear anomalies centered on each ring edge. It can therefore be assumed that among the 22 elements included in the PCA, those with the strongest PC loadings contribute most to the variability at the ring edges. The PCA confirms that the elements playing an important role along the BE-SWNE edges are Al, Mn, pH, ORP, S, Ca, Mg, Cal for major parameters, as well as Mo,Nb,Sn (in ORP,Dol-PC3) ; Ag,W,Sb (in ORP,Cal-PC4) and Nb,Sn in PC5 for trace metals.

FIGURE 21: Idealized responses within reduced clay in measured parameters at the ring edge.

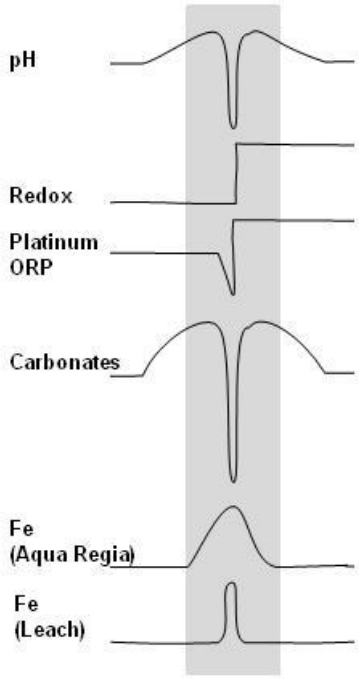

Among the increased variability in parameters at the ring edge, characteristic patterns stand out. In particular, a sharp, narrow dip in pH occurs on all ring edges and is typically only 1 to 2 sample stations across. The pH dip is centered within a trend of broad responses across the ring edge, including elevated carbonates in mineral soil across the ring edge. Thus while the ring edge is approximately 20m in width and the pH response is detected over one to two sampling sites (5 to 10 m), the overall impact of the edge-related geochemical processes seems to be more wide spread, and at least 150 m in width. Carbonate and pH responses in peat at the ring edge show almost completely the opposite trend as they do in the underlying clay. The peat is characterized by upward responses in pH, while the clay is characterized by downward dips. Carbonate enrichments in the peat occur either directly above depletions in the clay or are offset slightly, usually outward.

The PCA clearly indicates the opposite response within pH-PC6 and both PC`s negatively loaded with ORP, which are therefore preferentially indicating reduced conditions at the ring edges. PC3 and PC4 are associated with a removal of carbonate (negative loading of Dol and Cal) accompanied by reducing conditions (negative loading of ORP). As previously described, the variability of calcite caused by soil acidity is demonstrated in carbonate-PC2 and pH-PC6. PC3 and PC4 indicate that another mechanism, active under reduced conditions, is spatially associated to low Cal values. The transect data additionally shows that edges are characterized by increases in oxidation products, as exemplified by the peaks in Al, Fe and Mn that occur almost exactly at the same location as the ORP dips.

2. Proposed reactions at the ring edge

The existing model of forest ring formation is based on the reduced chimney theory (Hamilton and Hattori, 2008; Figure 2). In the model, the edge forms as the result of the outward transport of reduced species, their oxidation and subsequent carbonate dissolution. This model predicts low fO_2 in the ring and very strong redox gradients at edges, decreasing pH, depletion in carbonate, increased $pCO_{2(aq)}$ towards the edges and increased deposition of metal oxyhydroxides in soil.

All 6 studied ring edges with consistent sample media display responses in these parameters and support the proposed model. However, some observations are not explained by the model:

- **A coincidence of sharp ORP *lows* with the pH dips at the ring edges** - this contradicts the model, which stipulated that pH changes occur in response to sudden increases in ORP at ring edges.
- **The antithetic response in pH and carbonate concentrations between clay and peat.**

The occurrence of the sharp ORP lows is discussed at the end of this section. Figure 22 is a proposed model to account for all other observations, including the antithetic peat/clay responses in pH and carbonate. The following 5 stages are referenced on Figure 22.

Figure 22: Proposed model of redox and carbonate processes at the ring edge.

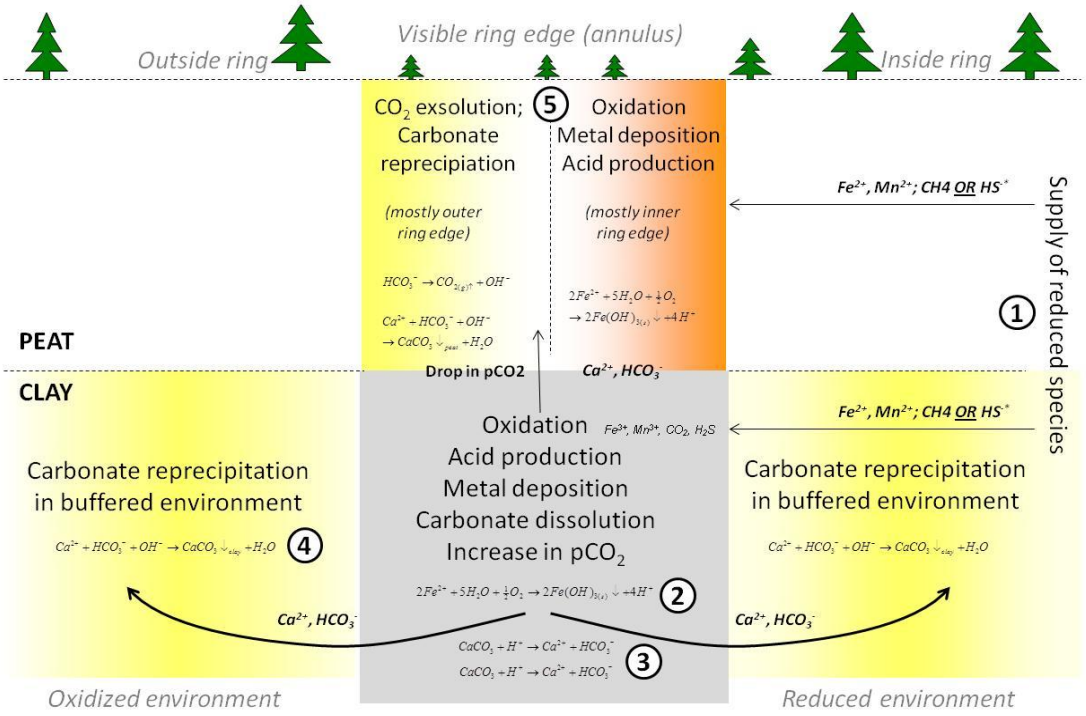

* Proposed transport mechanisms for species migration (lateral and vertical) :
Groundwater advection, Diffusion, Electrochemical transport (Cameron et al., 2004, Hamilton et al. 1998)

Stage 1: Migration of reduced species from inside of the ring into the annulus

The presence of CH_4 at the Bean Ring and H_2S at Thorn North maintains many species in reduced form, including metals such as Fe^{2+} and anions such as HS^-. There are several possible causes for the movement of reduced species outward toward the ring edge, including electrochemical transport (Hamilton and Hattori, 2008). Once the species reach the ring edges, they encounter oxidizing conditions. Therefore the migration could also be in response to activity gradients. Deposition of metals maintains continuously high activity gradients near the ring edges (reflected in ORP values) and promotes diffusion. At the Bean ring, groundwater advection is also a possible contributing transport mechanism since there are upward hydraulic gradients across the site as indicated by artesian conditions.

Stage 2: Oxidation of species and acid production in annulus

Oxidation of a number of species produces acid. At the Bean ring, the presence of CH_4 and ferrous Fe is known in groundwater near the center of the ring. At Thorn North, H_2S occurs in both shallow and deep (i.e. bedrock) groundwater. Once these species migrate to the ring edge they oxidize:

Bean Ring

$$CH_4 + 2O_2 \rightarrow CO_2 + 2H_2O$$

$$2Fe^{2+} + 5H_2O + \tfrac{1}{2}O_2 \rightarrow 2Fe(OH)_{3(s)} \downarrow + 4H^+$$

Thorn North

$$HS^- + 2O_2 \rightarrow SO_4^{2-} + H^+$$

Groundwater geochemical data at Thorn North indicates that HS^- oxidation is the predominant reaction forming SO_4^{2-} at Thorn North (Hamilton and Hattori, 2008). The products are soluble (SO_4^{2-}, H^+) and will therefore not leave direct evidence of the reaction in soils. Nor will there be accompanying metal oxidation reactions because most metals are insoluble in the presence of dissolved sulfide and therefore will not migrate outward toward the ring edge. At the Bean ring, the oxidation of CH_4 appears significant but the products of CO_2 will not leave direct evidence in soils. However, the elevated Fe concentrations in clay by aqua regia on both lines at the Bean Ring indicate that oxidation is occurring. The positive spikes in the ratio of Fe by weak leach vs. aqua regia that occur in the ring edge suggest active production of Fe(III)-O-OH which can be easily leached by a weak digestion. The presence of extremely localized low pH responses in the ring edge is more indirect evidence that oxidation is occurring. This low pH removes carbonate.

Stage 3: Acid dissolution of carbonate in mineral soils at the annulus

The formation of acid in the ring edge results in carbonate dissolution:

$$CaCO_3 + H^+ \rightarrow Ca^{2+} + HCO_3^-$$

The spatial coincidence between carbonate lows and pH lows in the ring edge suggest that the processes are related. Similar features have been noted over mineral deposits (Hall et al, 2005; Hamilton et al., 2004b) where carbonate is removed from an area of active oxidation over the deposit.

Stage 4: Lateral migration of DIC/Ca^{-} rich fluid in the clay; re-precipitation of carbonate

The dissolution of carbonate produces high Ca, DIC and pCO_2 in pore waters. The chemical gradient with surrounding areas favours the diffusion of species (Ca, HCO_3^-) inward and outward from the ring edge into areas. This lateral migration of carbonate-rich fluids is proposed to explain high contents of $CaCO_3$ in shallow soil flanking the pH lows in the annulus. Deposition of carbonate is the direct result of a more elevated pH in the surrounding environment :

$$Ca^{2+} + HCO_3^- + OH^- \rightarrow CaCO_3 \downarrow_{clay} + H_2O$$

The increased buffering capacity in the surrounding environment results in a greater availability of OH^-, as suggested by the occurrence of elevated areas of pH and carbonate around the negative pH anomalies.

Stage 5: Vertical migration of DIC/Ca rich fluid into the peat; re-deposition of carbonate

Dissolved species at the ring edge may also migrate upward from the mineral soil into the peat. Thus they migrate from a high pCO_2 in clay to low pCO_2 near the atmosphere, where CO_2 can be lost. This results in exsolution of CO_2 at the clay / peat interface and increased alkalinity (1). Interaction with the carbonate-species from the clay, results in carbonate redeposition (2):

$$(1) HCO_3^- \rightarrow CO_{2(g)} \uparrow + OH^- \text{ (as } pCO_2 \text{ drops)}$$

$$(2) Ca^{2+} + HCO_3^- + OH^- \rightarrow CaCO_3 \downarrow_{peat} + H_2O$$

This mechanism is proposed to explain the antipathy between the pH lows in the annulus in clay, and pH highs in the overlying peat and the elevated carbonate in peat in the ring edge. Carbonate contents in peat are otherwise low due to low pH in peat water.

Note that reduced species within the peat are also presumed to be migrating towards the ring edge and producing acidity, which could interfere with carbonate deposition. At least at BE-SWNE, the data seem to indicate that deposition of oxides occurs at the inner edge of the annulus, while deposition of carbonate occurs at the outer edge. The shift in the oxidation front in peat toward the inner ring edge is explained by generally higher oxidation state in the peat stratum than in the underlying clay causing a shift in the location of metal oxidation towards the source of reducing agents.

3. Discussion of model and potential involvement of microorganisms

The prevailing model for the formation of forest rings proposed by Hamilton and Hattori (2008) is supported by this study. However, we also observed a coincidence of sharp ORP lows with the pH dips at ring edges, which occurs together with the oxidation products. A similar paradox has been previously documented at the Thorn-North ring and above base metal sulfide deposits. At Thorn-North, anomalous methane in the vapour head-space of monitoring wells (up to 150 ppm against a background of zero) occurs in the same location as large increases in ORP and sulfate (SO_4^{2-}) concentration at ring edges (Hamilton and Hattori, 2008). Based on mass-balance calculations, the sulfate at a ring edge was interpreted to result from the oxidation of H_2S, which occurs across the whole ring but is particularly pronounced at the ring edges (Hamilton and Hattori, 2008). The origin of the H_2S is unknown but it does occur in bedrock beneath the ring at much higher concentrations than in the overlying overburden so it is reasonably to infer that it migrates up as a reduced species then outward. Biotic sulfur-oxidation dominates over abiotic oxidation where oxygen concentrations are low (Konhauser, 2007) and therefore an increase in the activity of anaerobic sulfur-oxidizing bacteria is likely at the ring edges. Peaks in trace concentrations of methane, coinciding with drops in O_2 in the headspace of monitoring wells, were also observed (Hamilton and Hattori, 2008). Methanogenesis is an exclusively anaerobic process, resulting from the reduction of CO_2 by autotrophic organisms. This occurs under highly reducing conditions, below the requirements of sulfate reduction. Therefore sulfate reduction is commonly coupled to methane oxidation into CO_2, through an electron shuttle process directly linking a methanotrophic Archea with a sulfate-reducing bacteria (Konhauser, 2007). Hamilton and Hattori (2008) however observed the co-existence of two terminal electron acceptors, CH_4 and H_2S, within groundwaters at the Thorn North ring edges. Organisms using SO_4^{2-} as electron acceptor can be heterotrophic, and occupy zones of high biomass formed by methanogenic bacteria (Southam and Saunders, 2005). In this case the sampling density of Hamilton and Hattori (2008) could not have been detailed enough to recognize the outward movement of biogenic CH_4 from a local zone of methane production, into a neighbouring zone where it becomes the organic carbon source for heterotrophic sulfate-reducing bacteria.

A more direct observation of this phenomenon was identified by Hamilton (2007) over the Cross Lake base metal sulfide deposit where ORP was determined using the same Pt-electrode slurry

method that was used in our study. At Cross Lake, the deposit is overlain by 30 m of glacial till, in which a reduced chimney has developed over the deposit. Hamilton (2007) showed symmetrical zones of highly reduced shallow soils at the same locations where oxidation reactions were occurring. These reduced zones were accompanied by pH lows over the chimney and high Fe-O-OH. The occurrences strongly correlate with elevated amounts of soil hydrocarbons, which are a proxy for bacterial biomass (Figure 23). Bacterial plate counts indicated an area of increased autotrophic sulfate-reducing bacteria in this area.

Another possible explanation for a low ORP signature coinciding with a presumed zone of oxidation, is that platinum ORP probes do not effectively measure the potential of soil slurry but respond better to some redox-active constituents of the slurry (Hamilton et al. 2004a). The prominent redox lows observed at Cross Lake in Timmins were attributed to the presence of bacterial biomass (Hamilton, 2007) in shallow soils. Some bacteria are known to colonize electrode surfaces (e.g. Parra and Lyn, 2009). Larger amounts of autotrophic organisms occupying the strong redox gradients in the areas may be colonizing the probe surfaces during the measurement, or perhaps the biomass itself has a more reduced response than soils with only background numbers of microorganisms.

FIGURE 23: The correlation between (1) Soil-gas-hydrocarbon (SGH) variability, as measured by their 2nd principal component of SGH compounds; (2) redox, as measured by the oxidation-reduction potential of soil slurries; and (3) sulfate-reducing bacteria in soils over mineralization (from Hall et al. 2005).

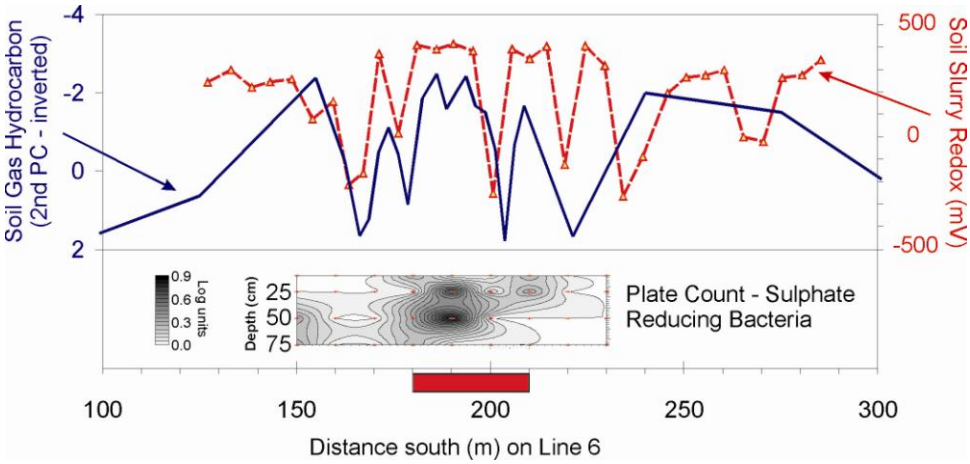

Summary and conclusions

Previous studies (Hamilton et al. 2004a; Hamilton and Hattori, 2008) supported the hypothesis that forest rings are centered on geological sources of reduced species and represent 'reduced chimneys' similar to those that form over mineral deposits (Cameron et al, 2004). Of the thousands of forest rings documented in northern Ontario, and the several dozen that have been examined closely by several researchers, two were chosen for a detailed study as part of this investigation. The Thorn-North ring has a significant accumulation of H_2S in groundwater in overburden with still larger concentrations in the underlying bedrock groundwater. The Bean ring is centered on an accumulation of methane in overburden, which does not persist in bedrock. Groundwaters from the 5 central wells in overburden of the Bean, all have vapour phase gas.

This study investigates the physical and chemical changes occurring at the edges of the Thorn North and Bean rings and interprets the results in light of the reduced chimney theory. From the start, a difficulty was recognized in that the products of the oxidation reactions (i.e. CO_2 at the Bean and SO_4^{2-} at Thorn North) are soluble and would not necessarily leave evidence of their reaction. In order to understand ring-edge process, I have therefore focused on proxy oxidation reactions such as metal oxidation and secondary carbonate processes related to the other product of these reactions – H^+.

Similar and profoundly symmetrical changes are occurring on the 3 full transects studied that had consistent sample media. The 4th line, TN-EW shows indications of similar responses but cannot be examined as a whole because 4 soil media were sampled on the same line: oxidized/reduced sand/clay.

Principal components analysis was carried out to help understand the controls on variability in the dataset. This showed that although variable residual (siliciclastic)/carbonate content) in the primary till explain much of the variance (PC1 and part of PC2), the other 4 PCs are related to ring edge responses. This exercise helped identify the precise locations of the major geochemical changes in the clay, which are characterized by a sudden negative pH response in the center of a wider pH high; and usually include a carbonate low corresponding with the pH low and wide carbonate highs roughly correlating with the pH highs. These support the hypothesis that carbonate is being

removed due to acid production at the ring edges and re-precipitated both inside and outside the ring where the pH is higher in the soil; mostly beyond the visible ring edge.

Comparing the data from mineral soil with that of overlying peat, it is apparent that fluids with elevated pCO_2 and Ca migrate upward from the zone of acidification. Degassing of CO_2 results in a pH rise and the deposition of secondary carbonate in the peat in measurable quantities. This process must be kinetic and ongoing to reverse the normal acidification processes due to humification of the peat. Metals also oxidize in the peat but the zone of oxidation, at least at the Bean ring, is inward from that in clay, presumably because of the naturally higher oxidation potential in the shallower peat.

Previous work over forest rings and other reduced chimneys suggests that microbiological processes are significant at redox boundaries over and adjacent to the features. My results support this, albeit with circumstantial evidence. The sudden and profound drops in ORP observed at approximately the same location as the ring-edge oxidation may be indicative of increased biomass in this area. Further studies should focus on these areas where the redox gradients are the greatest and therefore most likely to support autotrophic organisms.

Acknowledgements

First and foremost, I would like to thank my supervisors Dr. Stew Hamilton and Dr. Keiko Hattori for their continuously dedicated advice and constructive comments over the past years. My gratitude also goes to the Ontario Geological survey for providing full access to the vast dataset available on forest rings. The data selected for inclusion in this thesis, was collected by Stew Hamilton and his field assistants Devin Cranston and Boris Iotzov. Many thanks to the Ontario Geological Survey Geoscience Laboratories for their careful analyses. I am also thankful for the opportunity to have spent 3 field seasons working for the Ontario Geological Survey, which provided valuable financial support and field experience. Last but not least, thank you to my close friends and family.

References

Adams, P. (1998) Overview of Biogeochemical and Geochemical Exploration. Unpublished company report, Noranda Inc., 25 p.

Barnhart, C. (1995) An Improved gas-stripping column for deoxygenating water. Journal of the North American Benthological Society. V. 14, p. 347-350.

Brady, N.C. and Weil, R.R. (2002) The Nature and Properties of Soils, 13th Ed. Prentice Hall, New York, 960 p.

Brauneder, K. ; Hamilton, S.M. and Hattori, K.H. (2008) 28. Project Unit 07-025. 28. Project Unit 04-025. Detailed investigation of chemical and microbiological parameters over forest-ring edges in northern Ontario; *in* Summary of Fieldwork and Other Activities, Ontario Geological Survey Open File Report 6226, p.28-1 to 28-8.

Cameron, E.M. ; Hamilton, S.M. ; Leybourne, M.I. ; Hall, G.E.M. and McClenaghan, M.B (2004) Finding deeply buried deposits using geochemistry; Geochemistry: Exploration, Environment, Analysis, V. 4, p.7-32.

Chorover, J. ; Kretzschmar, R. ; Garcia-Pichel, F. and Sparks, D.L. (2007) Soil biogeochemical processes in the critical zone. Elements V. 3, 321-326.

Diatreme Explorations (1999) Corporate profile and property portfolio, August 17, 1999. Diatreme Explorations Inc., Queensland, 37 p.

Dreimanis, A. (1962) Quantitative gasometric determination of calcite and dolomite by using Chittick apparatus. Journal of Sedimentary Petrology V. 32, p. 520-529.

Dubois, J.-M. (1994) Mycological origin of rings in the coniferous forest of Anticosti Island in the Gulf of Saint Lawrence, Canada. Photo-Interpretation 1993–3, Juillet-Août. Éditions Eska, Paris. p. 209–210.

Dyke, A.S. (2004) An outline of the deglaciation of North America with emphasis on central and northern Canada, p. 373-424. *In* J. Ehlers and P.L. Gibbard, ed., Quaternary Glaciations-Extent and Chronology, Part II: North America. Developments in Quaternary Science, V. 2b. Elsevier, Amsterdam, 440 p.

Giroux, J.-F. ; Bergeron, Y. and Veillette J.J. (2001) Dynamics and morphology of giant circular patterns of low tree density in black spruce stands in northern Québec. Canadian Journal of Botany, V. 79, p. 420-428.

Hall, G.E.M. ; Vaive, J.E. ; Beer, R. and Hoashi, M.S. (1996) Selective leaches revisited, with emphasis on the amorphous Fe oxyhydroxide phase extraction; Journal of Geochemical Exploration V. 56, p. 59-78 (GSC Cont.# 21895)

Hall, G.E.M., McClenaghan, M.B. and Hamilton S.M. (2005) Selective extractions – secondary geochemical signatures in glaciated terrains; *in* Short Course Notes; Exploration Geochemistry Workshop; Canadian Institute of Mining and Metallurgy; Mining Rocks, Prospectors and Developers Convention 2005; Toronto, April 23.

Hamilton, S.M. ; Veillette, J.J. and Komararechka, R. (1999) A geological model to account for the formation and surprising circularity of forest rings of the James Bay basin. Poster presented at the 1999 Prospectors and Developers Association of Canada annual meeting, March 16, 1999. Toronto, Ontario.

Hamilton, S.M. and Cranston, D.R. (2000) Thick overburden geochemistry – methods and case studies; *in* Summary of Fieldwork and Other Activities, 2000, Ontario Geological Survey Open File Report 6032, p. 47-1 to 47-18.

Hamilton, S.M. ; Burt, A.K. ; Hattori, K.H. and Shirota, J. (2004a). The distribution and source of forest ring-related methane in northeastern Ontario; *in* Summary of Fieldwork and Other Activities, Ontario Geological Survey Open File Report 6145, p. 21-1 to 21-26.

Hamilton, S.M. ; Cameron, E.M. ; McClenaghan, M.B. and Hall, G. E. M. (2004b) Redox, pH and SP variation over mineralization in thick glacial overburden—Part I: Methodologies and field investigation at Marsh Zone gold property: Geochemistry: Exploration, Environment, Analysis, V. 4, p. 33–44.

Hamilton, S.M. ; Cameron, E.M. ; McClenaghan, M.B. and Hall, G.E.M. (2004c) Redox, pH and SP variation over mineralization in thick glacial overburden — Part II: Field investigations at the Cross Lake VMS property. Geochemistry: Exploration, Environment,Analysis, V. 4, p. 45–58.

Hamilton, S.M. and Hattori, K.H (2008) Spontaneous potential and redox responses over a forest ring. Geophysics, V. 37, p. B67 – B75.

Konhauser, K. (2007) Introduction to Geomicrobiology, 1st Ed. Blackwell Publishing, Oxford, 440 p.

Millar, W.N. (1973) Property report on Templeton Township property. Timmins Resident Geologist's Office, Templeton Township assessment file T-2253, 15 p.

Mollard, J. (1980) Landforms and surface materials of Canada: a stereoscopic atlas and glossary, 6th edition, Regina, Saskatchewan.

Parra, E. and Lin, L. (2009) Microbial fuel cell based on electrode-exoelectrogenic bacterial interface. Proceedings IEEE MEMS Conference, p. 31-34, Sorrento, 2009.

Paul, E.A. (2007) Soil Microbiology, Ecology and Biochemistry, 3rd Ed. Elsevier, New York, 535 p.

Paulen, R.C. and McClenaghan, M.B. (1998) Surficial geology, Manning Lake northeastern Ontario. Geological Survey of Canada Open File Report 3618, Scale 1:50,000.

Pinson, W.H.Jr. (1979) Origin of Circular Ring Features in the wetlands of Ontario. Lunar and Planetary Science X, p. 984-985.

Post, J.E. (1999) Manganese oxide minerals: Crystal structures and economic and environmental significance. Proceedings of the National Academy of Science, V. 96, p. 3447-3454.

Reed, L.E. (1980) Report on the investigation of two ring structures in the James Bay Lowlands. Unpublished company report, Selco Mining Corporation, 14 p.

Smith, S.L. and Burgess, M.M. (2002) A digital database of permafrost thickness in Canada. Geological Survey of Canada, Open File 4173. 1 CD-ROM.

SAS Institute Inc. (2012) Chapter 1: Principal Component Analysis. *In:* A Step-by-Step Approach to Using the SAS System for Factor Analysis and Structural Equation Modeling. SAS publishing, Cary, North Carolina. 608p. Retrieved from: *http://support.sas.com/publishing/pubcat/chaps/55129.pdf* (accessed 17 February 2012)

Southam, G. and Saunder, J.A. (2005) Geomicrobiology above ore deposits. Economic Geology, V. 100, p. 1067-1084.

Tan, K. (2010) Principles of Soil Chemistry, 4th Ed. CRC Press, Boca Raton, Florida, 362 p.

Usik, L. (1966) A report on circular features in organic terrain. Geological Survey of Canada, Dept. of Mines and Technical Surveys, Paper 66-2, Report of the Committee, Nov. 1965-April 1966.

Veillette, J. J. and Giroux, J.F. (1999) The enigmatic rings of the James Bay lowland : A probable geological origin. Geological Survey of Canada Open File Report 3708, 28.

Appendices

APPENDIX 1 (page 1/2): Field data for Bean sampling sites. The column A-type provides the degree of humidification of the organic horizon (a.k.a. A-horizon). These are very well / well / moderately / poorly humified peat (VWHP,WHP,MHP,PHP). The column C-type provides the medium sampled in the mineral horizon (a.k.a. C-horizon). These are clay or sand (snd.), and the grain size as observed in the field (fn.: fine, med.: medium, crs.: coarse). The oxidation degree as observed in the field ranges from unoxidized (unox.) to slightly (sl.), moderately (mod.), well and highly oxidized.

Sample	Transect	Location on transect	Ground surface (surveyed)	Peat thickness	A type	A saturation degree	A sample depth	C type	C sample depth	C oxidation degree
BE-20	SW-NE	-450	179	1.5	WHP		0.4	Clay	1.55	unox.
BE-21	SW-NE	-425	179	1.15	PHP		0.4	Clay	1.4	unox.
BE-22	SW-NE	-375	179	0.55	PHP		0.4	Clay	1.4	mod. ox.
BE-23	SW-NE	-325	179	0.7	WHP		0.45	Clay	1.6	mod. ox.
BE-24	SW-NE	-275	178	0.7	WHP		0.4	Clay	1	unox.
BE-25	SW-NE	-240	178	1.45	WHP		0.4	Clay	1.7	unox.
BE-26	SW-NE	-233	178	1.15	WHP		0.4	Clay	1.4	unox.
BE-27	SW-NE	-228	178	1.15	WHP		0.4	Clay	1.4	unox.
BE-28	SW-NE	-223	178	0.65	WHP		0.4	Clay	1.4	unox.
BE-29	SW-NE	-218	178	0.65	WHP		0.4	Clay	1.7	unox.
BE-30	SW-NE	-213	178	0.85	WHP		0.4	Clay	1.7	mod. ox.
BE-31	SW-NE	-208	178	0.85	WHP		0.4	Clay	1.7	unox.
BE-32	SW-NE	-203	178	1.05	WHP		0.4	Clay	1.4	unox.
BE-33	SW-NE	-190	177	0.75	WHP		0.4	Clay	1.4	unox.
BE-35	SW-NE	-115	177	1.15	WHP		0.4	Clay	1.25	unox.
BE-36	SW-NE	-65	177	0.85	MHP		0.4	Clay	1.4	sl. ox.
BE-19	SW-NE	-19.1	177	1.9	WHP		0.4	Clay	1.7	unox.
BE-18	SW-NE	50	176	2.15	WHP		0.4	Clay	2.1	unox.(?)
BE-17	SW-NE	100	176	0.7	WHP		0.4	Clay	1.1	mod. ox.
BE-16	SW-NE	140	175	0.8	WHP	Sat	0.4	Clay	1.85	mod. ox.
BE-15	SW-NE	165	175	0.6	WHP	Unsat	0.4	Clay	1.65	sl. ox.
BE-14	SW-NE	180	175	0.6	WHP		0.4	Clay	1.65	mod. ox.
BE-13	SW-NE	185	175	0.85	WHP		0.35	Clay	1.25	unox.(?)
BE-12	SW-NE	189	175	0.95	v.WHP		0.65	Clay	1.2	unox.(?)
BE-11	SW-NE	194	175	0.65	v.WHP		0.4	Clay	1.2	sl. ox.
BE-10	SW-NE	199	175	0.75	v.WHP		0.4	Clay	1.2	unox.(?)
BE-08	SW-NE	208	175	0.65	WHP		0.4	Clay	1.55	mod. ox.
BE-07	SW-NE	225	175	0.9	WHP		0.4	Clay	1.45	unox.(?)
BE-06	SW-NE	250	175	0.8	WHP		0.4	Clay	1.2	sl. ox.
BE-05	SW-NE	275	175	0.55	WHP		0.4	Clay	1.5	unox.(?)
BE-04	SW-NE	300	175	0.4	WHP		0.3	Clay	1.5	sl. ox.
BE-03	SW-NE	350	174	0.4	WHP		0.3	Clay	1.15	mod. ox.
BE-02	SW-NE	400	174	0.95	WHP		0.4	Clay	1	sl. ox.
BE-01	SW-NE	450	174	0.4	WHP		0.3	Clay	1.55	sl. ox.

APPENDIX 1 (page 2/2)

Sample	Transect	Location on transect	Ground surface (surveyed)	Peat thickness	A type	A saturation degree	A sample depth	C type	C sample depth	C oxidation degree
BE-58	SE-NW	-450	176	1.15	WHP	Sat	0.4	Clay	1.55	sl. ox.
BE-59	SE-NW	-400	176	1.05	WHP	Sat	0.4	Clay	1.1	unox.(?)
BE-60	SE-NW	-350	176	0.75	WHP	Mod.Sa	0.4	Clay	1.85	sl. ox.(?)
BE-61	SE-NW	-300	176	0.7	WHP	Sat	0.4	Clay	1.4	sl. ox.
BE-62	SE-NW	-250	176	0.65	WHP		0.4	Clay	1.6	sl. ox.
BE-67	SE-NW	-235	176	0.45	mod.WHP		0.4	Clay	1.2	sl. ox.
BE-68	SE-NW	-220	176	0.4	mod.WHP	Sat	0.2	Clay	1.55	sl. ox.
BE-69	SE-NW	-210	176	2	mod. WHP		0.4	Clay	2.1	unox.
BE-70	SE-NW	-205	176	2.15	WHP		0.4	Clay	2.15	unox.
BE-71	SE-NW	-200	176	1.85	WHP		0.4	Clay	1.85	unox.
BE-72	SE-NW	-195	176	1.7	WHP		0.4	Clay	1.85	unox.
BE-73	SE-NW	-190	176	1.4	WHP	Sat	0.4	Clay	1.85	unox.
BE-74	SE-NW	-185	176	2.65	WHP		0.4	Clay	2.8	unox.
BE-75	SE-NW	-180	176	3.8	WHP		0.4	Clay	4.05	unox.
BE-76	SE-NW	-175	176	3.3	WHP		0.4	Clay	3.45	unox.
BE-77	SE-NW	-170	176	3.15	WHP		0.4	Clay	3.3	unox.
BE-78	SE-NW	-150	176	3.45	WHP		0.4	Clay	3.3	unox.
BE-79	SE-NW	-100	176	1.25	WHP		0.4	Clay	1.4	unox.
BE-80	SE-NW	-50	176	3.45	WHP		0.4	Clay	3.45	unox.
BE-57	SE-NW	50	177	0.5	mod.WHP	Sat	0.4	Clay	1.65	sl. ox.
BE-56	SE-NW	100	177	0.3	mod.WHP	Sat	0.2	Clay	1.65	sl. ox.
BE-55	SE-NW	150	176	0.7	WHP		0.4	Clay	1.5	sl. ox.
BE-54	SE-NW	175	176	2.15	mod. WHP		0.4	Clay	2.3	unox.
BE-53	SE-NW	200	176	0.65	WHP	Sat	0.4	Clay	1.5	unox.
BE-52	SE-NW	215	176	0.5	WHP		0.4	Clay	1.05	mod. ox.
BE-51	SE-NW	221	176	0.5	WHP	Sat	0.4	Clay	1.45	mod. ox.
BE-50	SE-NW	225	176	0.5	WHP	Sat	0.4	Clay	1.75	sl. ox.
BE-49	SE-NW	230	176	0.5	WHP		0.4	Clay	1.5	sl. ox.
BE-48	SE-NW	235	176	0.5	WHP	Sat	0.4	Clay	1.75	mod. ox.
BE-47	SE-NW	240	177	0.5	WHP	Sat	0.35	Clay	1.55	sl. ox.
BE-46	SE-NW	245	177	0.5	WHP		0.3	Clay	1.6	mod. ox.
BE-44	SE-NW	255	177	0.65	WHP		0.4	Clay	1.85	mod. ox.
BE-43	SE-NW	260	177	0.4	WHP	Sat	0.3	Clay	1.7	mod. ox.
BE-42	SE-NW	272	177	0.4	WHP		0.3	Clay	1.25	sl. ox.
BE-41	SE-NW	300	177	0.55	WHP		0.4	Clay	1.4	sl. ox.
BE-40	SE-NW	350	177	3.85	mod. WHP		0.4	Clay	3.75	unox.
BE-39	SE-NW	399	177	4.52	mod. WHP		0.45	Clay	4.5	unox.
BE-38	SE-NW	469	177	2.25	WHP	Sat	0.4	Clay	2.6	unox.

APPENDIX 2 (page 1/2): Field data for the Thorn North sampling sites. The abbreviations used are as described in the legend of Appendix 1.

Sample	Transect	Location on transect	Ground surface (surveyed)	Water depth	Peat thickness	A type	A saturation degree	A sample depth	C type	C oxidation degree	C sample depth
TN-101	S-N	-500	305.09	0.075	1.4	WHP	sat	0.5	clay	unox.	1.55
TN-102	S-N	-450	304.97	0.075	1.45	WHP	sat	0.5	clay	unox.	1.55
TN-103	S-N	-425	305.05	0.15	1.55	WHP	sat	0.5	clay	unox.	1.65
TN-104	S-N	-400	305.15	0.075	1.65	MHP	sat	0.5	clay	unox.	1.8
TN-105	S-N	-378	305.17	0.075	1.55	MHP	sat	0.5	clay	unox.	1.8
TN-106	S-N	-353	305.1	0.125	1.5	MHP	sat	0.5	clay	unox.	2.15
TN-107	S-N	-338	305.05	0.125	1.5	MHP	sat	0.5	clay	unox.	2.15
TN-108	S-N	-328	305.1	0.125	1.5	MHP	sat	0.5	clay	unox.	2.15
TN-109	S-N	-323	305.12	0.125	1.45	WHP	sat	0.6	clay	unox.	2.15
TN-110	S-N	-318	305.14	0.125	1.6	WHP	sat	0.6	clay	unox.	
TN-111	S-N	-313	305.18	0.075	1.55	MHP	sat	0.8	clay	unox.	2.3
TN-112	S-N	-308	305.22	0.075	1.55	MHP	sat	0.8	clay	unox.	2.3
TN-113	S-N	-303	305.3	0.075	1.55	WHP	sat	0.8	clay	unox.	2.25
TN-114	S-N	-298	305.36	0.025	1.5	WHP	sat	0.75	clay	unox.	2.15
TN-115	S-N	-293	305.37	0.125	1.5	WHP	sat	0.6	clay	unox.	1.65
TN-116	S-N	-288	305.38	0.075	1.35	WHP	sat	0.6	clay	unox.	1.75
TN-117	S-N	-278	305.39	0.025	1.2	VWHP	sat	0.6	clay	unox.	2.05
TN-118	S-N	-265	305.48	0.075	1.05	WHP	sat	0.5	clay	unox.	2.1
TN-119	S-N	-250	305.6	0.075	1	WHP	sat	0.5	clay	unox.	2
TN-120	S-N	-225	305.78	0.075	1.35	WHP	sat	0.5	clay	unox.	2.15
TN-121	S-N	-175	305.96	0.075	1	VWHP	sat	0.5	clay	unox.	2.3
TN-122	S-N	-125	306.21	0.85	0.1	humus	unsat	0.025	no sample	no sample	
TN-123	S-N	-75	306.23	0.15	0.2	VWHP	sat	0.1	clay	unox.	2.15
TN-124	S-N	0	306.08	0.025	0.5	WHP	sat	0.3	clay	unox.	1.85
TN-125	S-N	50	305.95	0.25	0.4	WHP	sat	0.3	clay	unox.	1.7
TN-126	S-N	100	305.86	0.25	0.4	WHP	sat	0.3	clay	unox.	1.55
TN-127	S-N	118	305.82	0.125	0.5	WHP	sat	0.4	clay	unox.	1.8
TN-128	S-N	143	305.75	0.125	0.7	VWHP	sat	0.5	clay	unox.	1.85
TN-129	S-N	158	305.7	0.075	0.6	VWHP	sat	0.5	clay	unox.	1.45
TN-130	S-N	168	305.71	0.075	0.7	WHP	sat	0.5	clay	unox.	1.7
TN-131	S-N	173	305.73	0.175	0.75	WHP	sat	0.5	clay	unox.	1.55
TN-132	S-N	178	305.74	0.175	0.75	WHP	sat	0.6	clay	unox.	1.65
TN-133	S-N	183	305.76	0.175	0.75	WHP	sat	0.5	clay	unox.	1.7
TN-134	S-N	188	305.62	0.175	0.8	WHP	sat	0.5	clay	unox.	1.55
TN-135	S-N	194	305.5	0.175	0.9	WHP	sat	0.5	clay	unox.	1.55
TN-136	S-N	198	305.54	0.075	0.9	WHP	sat	0.5	clay	unox.	1.5
TN-137	S-N	203	305.58	0.125	0.85	WHP	sat	0.5	clay	unox.	1.4
TN-138	S-N	208	305.53	0.175	0.9	WHP	sat	0.5	clay	unox.	1.4
TN-139	S-N	218	305.44	0.125	0.9	WHP	sat	0.5	clay	unox.	1.25
TN-140	S-N	233	305.35	0.125	0.75	WHP	sat	0.5	clay	unox.	1.25
TN-141	S-N	258	305.24	0.125	0.85	WHP	sat	0.5	clay	unox.	1.35
TN-142	S-N	283	305.09	0.125	0.4	WHP	sat	0.35	clay	unox.	0.9
TN-143	S-N	300	304.97	0.075	0.15	WHP	sat	0.1	clay	mod. ox.	1.55
TN-144	S-N	350	304.62	0.075	0.65	WHP	sat	0.5	clay	sl. ox.	1.8
TN-145	S-N	400	304.45	0.075	0.6	WHP	sat	0.5	clay	mod. ox.	1.7

Appendix 2 (page 2/2)

Sample	Transect	Location on transect	Ground surface (surveyed)	Water depth	Peat thickness	A type	A saturation degree	A sample depth	C type	C oxidation degree	C sample depth
TN-146	W-E	-450	306.99	0.7	0.025	humus	unsat	0.025	snd, crs.	mod. ox.	2.05
TN-147	W-E	-400	307.17	0.7	0.075	humus	unsat	0.075	snd, crs.	well ox.	2.3
TN-148	W-E	-350	307.41	0.7	0.075	humus	unsat	0.075	snd, crs.	well ox.	1.85
TN-149	W-E	-300	307.78	0.8	0.075	humus	unsat	0.075	snd, crs.	well ox.	1.85
TN-150	W-E	-250	307.32	1	0.075	humus	unsat	0.075	snd, crs.	highly ox.	1.85
TN-151	W-E	-226	307.07	0.45	0.075	WHP	unsat	0.4	snd, med.	mod. ox.	2.05
TN-152	W-E	-201	306.77	0.125	1	WHP	sat	0.5	snd, fn. to med.	sl. ox.	2.05
TN-153	W-E	-186	306.62	0.125	1.6	WHP	sat	0.5	clay	unox.	2.4
TN-154	W-E	-176	306.68	0.125	1.55	WHP	sat	0.5	snd, fn. to med.	unox.	
TN-155	W-E	-171	306.71	0.125	1.55	WHP	sat	0.5	snd, fn. to med.	v. sl. ox.	
TN-156	W-E	-166	306.72	0.2	1.7	WHP	sat	0.7	snd, fn.	unox.	2.3
TN-157	W-E	-161	306.68	0.2	1.45	WHP	sat	0.5	clay	unox.	2.45
TN-158	W-E	-158	306.66	0.2	1.55	WHP	sat	0.5	clay	unox.	2.45
TN-159	W-E	-151	306.57	0.2	1.45	WHP	sat	0.5	clay	unox.	2.4
TN-160	W-E	-146	306.51	0.2	1.5	WHP	sat	0.5	clay	unox.	2.3
TN-161	W-E	-141	306.48	0.25	1.55	WHP	sat	0.5	clay	unox.	1.9
TN-162	W-E	-136	306.46	0.25	1.4	WHP	sat	0.5	clay	unox.	1.85
TN-163	W-E	-126	306.42	0.125	0.95	WHP	sat	0.5	clay	unox.	
TN-164	W-E	-111	306.37	0.125	0.7	WHP	sat	0.5	fn snd	sl. ox.	
TN-165	W-E	-86	306.29	0.125	0.3	WHP	sat	0.5	clay	unox.	1.5
TN-166	W-E	-60	306.22	0.075	0.5	WHP	sat	0.35	clay	unox.	1.55
TN-167	W-E	-25	306.14	0.075	0.5	WHP	sat	0.3	clay	unox.	1.85
TN-168	W-E	75	305.78	0.075	0.38	WHP	sat	0.25	clay	unox.	1.85
TN-169	W-E	125	305.73	0.025	0.25	MHP	sat	0.15	clay	unox.	1.85
TN-170	W-E	175	306.02	0.8	0.15	humus	unsat	0.1	clay	unox.	1.9
TN-171	W-E	225	306.61	1	0.025	humus	unsat	0.1	not sampled (c	not sampled	
TN-172	W-E	275	305.81	0.7	0.4	MHP	unsat	0.2	clay	unox.	1.85
TN-173	W-E	302	305.37	0.7	0.3	WHP	sat	0.15	clay	mod. ox.	1.85
TN-174	W-E	327	305.08	0.7	0.3	WHP	sat	0.2	clay	well ox.	1.85
TN-175	W-E	342	304.9	0.15	0.2	WHP	sat	0.3	clay	well ox.	1.85
TN-176	W-E	352	304.79	0.2	0.2	WHP	sat	0.15	clay	well ox.	2.3
TN-177	W-E	357	304.68	0.15	0.15	MHP	sat	0.1	clay	well ox.	2.1
TN-178	W-E	362	304.58	0.15	0.15	MHP	sat	0.1	clay	well ox.	1.85
TN-179	W-E	367	304.48	0.1	0.25	WHP	sat	0.15	not sampled (c	not sampled	
TN-180	W-E	372	304.37	0.125	0.2	WHP	sat	0.15	clay	well ox.	1.95
TN-181	W-E	377	304.3	0.125	0.38	WHP	sat	0.15	clay	well ox.	1.4
TN-182	W-E	382	304.4	0.125	0.5	WHP	sat	0.25	clay	well ox.	1.55
TN-183	W-E	385	304.46	0.075	0.6	WHP	sat	0.3	clay	well ox.	1.55
TN-184	W-E	392	304.47	0.125	0.3	WHP	sat	0.25	clay	well ox.	1.55
TN-185	W-E	402	304.43	0.2	0.5	WHP	unsat	0.4	clay	mod. ox.	1.9
TN-185.5	W-E	409	304.39	0.1		WHP	?		no sample	no sample	1.9
TN-186	W-E	417	304.33	0.1	0.5	VWHP	unsat	0.5	clay	sl. ox.	1.85
TN-187	W-E	442	304.14	0.3	0.5	VWHP	unsat	0.4	clay	mod. ox.	1.55
TN-188	W-E	467	303.96	0.5	0.4	VWHP	unsat	0.3	clay	well ox.	1.6
TN-189	W-E	500	303.73	0.075	0.05	WHP	sat	0.05	clay	well ox.	1.6
TN-190	W-E	550	303.49	0.3	0.02	humus	unsat	0.02	snd, fn.	well ox.	1.2
TN-191	W-E	600	303.35	0.5	0.02	humus	unsat	0.02	snd, fn.	well ox.	2

APPENDIX 3 (page 1/1): Correlation table of the 22 variables retained for the PCA of data from the Bean ring. These are: Cal, Dol, ORP, pH, Al, Mg, Mn, Na, P, S, Ag, Be, Ca, Cd, Hf, Mo, Nb, Sb, Sn, U, W, Zr. Variables displaying a correlation > 0.99 were excluded from the PCA analysis to reduce redundant variability. These were: Fe, K, Ti, V, Ba, Zn, Co, Cr, Cs, Cu, Ga, Li, Lu, Pb, Rb, Th, Tl, Y,REE.

	Cal	Dol	ORP3	pH1	Al_ES	Mg_ES	Mn_ES	Na_ES	P_ES	S_ES	Ag_MS
Cal	1	0.342	0.221	0.343	-0.803	0.179	-0.64	-0.454	-0.727	0.534	-0.203
Dol	0.342	1	0.094	0.253	-0.45	0.276	-0.274	-0.233	-0.293	0.394	-0.06
ORP3	0.221	0.094	1	0	-0.135	-0.014	0.029	-0.049	-0.212	-0.144	-0.244
pH1	0.343	0.253	0	1	-0.461	-0.097	-0.38	-0.129	-0.399	0.308	-0.185
Al_ES	-0.803	-0.45	-0.135	-0.461	1	0.057	0.724	0.662	0.891	-0.44	0.216
Mg_ES	0.179	0.276	-0.014	-0.097	0.057	1	-0.002	0.188	0.204	0.428	0.206
Mn_ES	-0.64	-0.274	0.029	-0.38	0.724	-0.002	1	0.431	0.613	-0.283	0.125
Na_ES	-0.454	-0.233	-0.049	-0.129	0.662	0.188	0.431	1	0.713	-0.177	0.115
P_ES	-0.727	-0.293	-0.212	-0.399	0.891	0.204	0.613	0.713	1	-0.356	0.208
S_ES	0.534	0.394	-0.144	0.308	-0.44	0.428	-0.283	-0.177	-0.356	1	0.009
Ag_MS	-0.203	-0.06	-0.244	-0.185	0.216	0.206	0.125	0.115	0.208	0.009	1
Be_MS	-0.657	-0.314	-0.118	-0.57	0.839	0.182	0.566	0.501	0.757	-0.332	0.215
Ca_ES	0.571	0.414	0.289	0.151	-0.466	0.436	-0.397	-0.166	-0.256	0.358	-0.157
Cd_MS	-0.453	-0.184	-0.04	-0.354	0.68	0.34	0.605	0.553	0.669	-0.078	0.312
Hf_MS	-0.568	-0.27	-0.122	-0.37	0.793	0.285	0.439	0.63	0.737	-0.152	0.202
Mo_MS	-0.387	-0.478	-0.313	-0.175	0.406	0.068	0.172	0.303	0.392	-0.093	0.103
Nb_MS	-0.213	-0.111	-0.243	0.017	0.058	-0.05	0.271	0.004	0.101	0.159	0.157
Sb_MS	-0.677	-0.298	-0.119	-0.283	0.844	0.198	0.507	0.613	0.725	-0.254	0.434
Sn_MS	-0.29	-0.283	-0.052	-0.046	0.381	0.079	0.205	0.288	0.297	-0.223	-0.043
U _MS	-0.461	-0.125	-0.259	-0.029	0.585	0.242	0.44	0.53	0.566	0.233	0.203
W _MS	-0.425	-0.136	-0.18	-0.153	0.497	0.24	0.359	0.25	0.383	0.034	0.466
Zr_MS	-0.647	-0.304	-0.074	-0.419	0.881	0.269	0.532	0.672	0.812	-0.241	0.195

	Be_MS	Ca_ES	Cd_MS	Hf_MS	Mo_MS	Nb_MS	Sb_MS	Sn_MS	U _MS	W _MS	Zr_MS
Cal	-0.657	0.571	-0.453	-0.568	-0.387	-0.213	-0.677	-0.29	-0.461	-0.425	-0.647
Dol	-0.314	0.414	-0.184	-0.27	-0.478	-0.111	-0.298	-0.283	-0.125	-0.136	-0.304
ORP3	-0.118	0.289	-0.04	-0.122	-0.313	-0.243	-0.119	-0.052	-0.259	-0.18	-0.074
pH1	-0.57	0.151	-0.354	-0.37	-0.175	0.017	-0.283	-0.046	-0.029	-0.153	-0.419
Al_ES	0.839	-0.466	0.68	0.793	0.406	0.058	0.844	0.381	0.585	0.497	0.881
Mg_ES	0.182	0.436	0.34	0.285	0.068	-0.05	0.198	0.079	0.242	0.24	0.269
Mn_ES	0.566	-0.397	0.605	0.439	0.172	0.271	0.507	0.205	0.44	0.359	0.532
Na_ES	0.501	-0.166	0.553	0.63	0.303	0.004	0.613	0.288	0.53	0.25	0.672
P_ES	0.757	-0.256	0.669	0.737	0.392	0.101	0.725	0.297	0.566	0.383	0.812
S_ES	-0.332	0.358	-0.078	-0.152	-0.093	0.159	-0.254	-0.223	0.233	0.034	-0.241
Ag_MS	0.215	-0.157	0.312	0.202	0.103	0.157	0.434	-0.043	0.203	0.466	0.195
Be_MS	1	-0.285	0.687	0.773	0.379	0.062	0.754	0.257	0.475	0.458	0.834
Ca_ES	-0.285	1	-0.126	-0.151	-0.268	-0.239	-0.317	-0.113	-0.208	-0.253	-0.215
Cd_MS	0.687	-0.126	1	0.693	0.3	0.212	0.589	0.065	0.624	0.198	0.728
Hf_MS	0.773	-0.151	0.693	1	0.373	-0.101	0.814	0.258	0.675	0.465	0.967
Mo_MS	0.379	-0.268	0.3	0.373	1	0.35	0.343	0.258	0.4	0.115	0.396
Nb_MS	0.062	-0.239	0.212	-0.101	0.35	1	-0.029	-0.11	0.257	-0.037	-0.074
Sb_MS	0.754	-0.317	0.589	0.814	0.343	-0.029	1	0.346	0.621	0.66	0.854
Sn_MS	0.257	-0.113	0.065	0.258	0.258	-0.11	0.346	1	0.122	0.273	0.289
U _MS	0.475	-0.208	0.624	0.675	0.4	0.257	0.621	0.122	1	0.39	0.657
W _MS	0.458	-0.253	0.198	0.465	0.115	-0.037	0.66	0.273	0.39	1	0.488
Zr_MS	0.834	-0.215	0.728	0.967	0.396	-0.074	0.854	0.289	0.657	0.488	1

APPENDIX 4 (page 1/2): Soil geochemical data for elements used in the PCA of the Bean ring. These are Na, P, S, Ag, Be, Cd, Hf, Mo, Nb, Sb, Sn, U, W, Zr. The PCA also includes the concentrations of calcite, dolomite, Ca, Mg, Al and Mn and the values of pH and ORP, which are presented in Appendix 8. Analytical methods referred to as MS (ICP-MS) and ES (ICP-OES), are described in the methodology.

Sample	Location	Transect	Cd	Na	P	S	Ag	Be	Hf	Mo	Nb	Sb	Sn	U	W	Zr
Lower detection limit >			*2*	*5*	*50*	*30*	*0.02*	*0.1*	*0.05*	*0.1*	*0.05*	*0.05*	*0.5*	*0.05*	*0.05*	*0.1*
Unit >			*ppm*	*ppm*	*ppm*	*ppm*	*ppm*	*ppm*	*ppm*	*ppm*	*ppm*	*ppm*	*ppm*	*ppm*	*ppm*	*ppm*
Method >			*ES*	*ES*	*ES*	*ES*	*MS*	*MS*	*MS*	*MS*	*MS*	*MS*	*MS*	*MS*	*MS*	*MS*
BE-58	-450	SE-NW	3	7	372	231	0.04	0.28	0.19	0.12	0.48	-0.05	0.8	0.453	0.07	7.39
BE-59	-400	SE-NW	5	8	451	456	0.03	0.54	0.28	0.52	0.46	-0.05	-0.5	0.551	0.08	11.79
BE-60	-350	SE-NW	6	13	556	256	0.04	0.68	0.47	0.23	0.41	0.09	0.61	0.831	0.15	16.61
BE-61	-300	SE-NW	5	9	437	399	0.14	0.48	0.33	0.32	0.53	0.08	-0.5	0.592	0.2	10.91
BE-62	-250	SE-NW	10	20	750	73	0.06	0.88	0.73	0.5	0.39	0.18	0.95	0.98	0.25	29.16
BE-67	-235	SE-NW	4	7	409	505	0.04	0.5	0.19	0.18	0.42	-0.05	-0.5	0.609	0.1	8.73
BE-68	-220	SE-NW	5	9	438	231	0.04	0.62	0.29	0.2	0.41	0.06	0.58	0.61	0.1	11.25
BE-69	-210	SE-NW	-2	-5	296	98	0.02	0.33	0.11	0.14	0.47	-0.05	-0.5	0.615	-0.05	3.66
BE-70	-205	SE-NW	6	9	430	731	0.15	0.56	0.37	0.28	0.51	0.08	-0.5	0.992	0.16	11.91
BE-71	-200	SE-NW	3	6	304	228	0.04	0.48	0.18	0.29	0.67	0.05	-0.5	0.566	0.1	5.84
BE-72	-195	SE-NW	5	8	383	283	0.04	0.52	0.41	0.14	0.38	0.06	-0.5	0.562	0.17	13.4
BE-73	-190	SE-NW	4	7	369	108	0.03	0.35	0.12	0.14	0.52	-0.05	-0.5	0.335	0.06	5.88
BE-74	-185	SE-NW	5	9	423	709	0.04	0.53	0.31	0.21	0.77	0.06	-0.5	0.635	0.09	10.88
BE-75	-180	SE-NW	6	10	463	738	0.04	0.58	0.3	0.22	0.56	0.06	-0.5	0.754	0.09	12.22
BE-76	-175	SE-NW	7	13	577	674	0.06	0.55	0.48	0.29	0.56	0.08	0.92	1.073	0.14	17.36
BE-77	-170	SE-NW	8	13	581	557	0.05	0.83	0.49	0.34	0.58	0.12	0.53	1.045	0.13	19.02
BE-78	-150	SE-NW	7	14	579	529	0.07	0.81	0.48	0.94	1.32	0.09	0.51	1.022	0.1	17.56
BE-79	-100	SE-NW	5	10	406	902	0.05	0.65	0.29	0.31	0.58	0.08	-0.5	0.773	0.42	11.05
BE-80	-50	SE-NW	6	10	417	885	0.05	0.45	0.36	0.28	0.48	0.07	1.32	0.855	0.31	11.18
BE-57	50	SE-NW	7	12	554	117	0.04	0.76	0.43	0.22	0.6	0.11	0.51	0.61	0.19	16.02
BE-56	100	SE-NW	5	9	458	393	0.04	0.36	0.21	0.18	0.53	0.06	1.26	0.566	0.13	8.96
BE-55	150	SE-NW	6	10	453	283	0.02	0.49	0.15	0.2	0.35	0.06	2.9	0.479	0.22	6.98
BE-54	175	SE-NW	4	9	468	419	0.14	0.29	0.3	0.22	0.62	0.09	0.92	0.584	0.17	10.1
BE-53	200	SE-NW	4	7	641	298	0.02	0.43	0.18	0.22	0.56	-0.05	-0.5	0.506	0.06	7.42
BE-52	215	SE-NW	5	9	459	353	0.03	0.45	0.17	0.21	0.54	0.05	2.33	0.523	0.1	7.71
BE-51	221	SE-NW	5	10	466	439	0.03	0.52	0.27	0.26	0.41	0.05	-0.5	0.616	0.1	10.3
BE-50	225	SE-NW	6	10	594	337	0.03	0.48	0.33	0.29	0.49	0.06	0.79	0.667	0.06	12.82
BE-49	230	SE-NW	5	9	458	347	0.04	0.47	0.32	0.29	0.4	0.07	-0.5	0.731	0.08	12.56
BE-48	235	SE-NW	7	14	582	157	0.04	0.81	0.46	0.33	0.43	0.12	1.03	0.809	0.16	19.32
BE-46	245	SE-NW	6	11	483	388	0.05	0.64	0.55	0.28	0.4	0.12	0.68	0.795	0.33	20.56
BE-47	245	SE-NW	7	13	547	248	0.04	0.61	0.29	0.25	0.68	0.08	-0.5	0.649	0.08	12.27
BE-45	250	SE-NW	7	13	545	238	0.13	0.95	0.47	0.3	0.53	0.16	0.61	0.656	0.24	17.74
BE-44	255	SE-NW	8	16	682	156	0.04	0.68	0.49	0.32	0.44	0.14	0.77	0.843	0.19	20.34
BE-43	260	SE-NW	5	9	472	450	0.03	0.52	0.34	0.24	0.37	0.06	-0.5	0.673	0.11	12.13
BE-42	272	SE-NW	3	-5	262	251	0.02	0.3	0.13	0.15	0.3	-0.05	0.58	0.391	-0.05	2.95
BE-41	300	SE-NW	5	7	379	284	0.04	0.34	0.27	0.18	0.39	-0.05	-0.5	0.492	0.08	9.55
BE-40	350	SE-NW	7	12	585	315	0.06	0.7	0.57	0.29	0.6	0.09	0.67	1.033	0.12	18.09
BE-39	399	SE-NW	7	14	620	580	0.07	0.8	0.58	0.37	0.72	0.1	0.59	0.973	0.15	20.06
BE-38	469	SE-NW	5	9	428	1015	0.04	0.44	0.36	0.25	0.6	0.06	-0.5	0.77	0.12	11.2

Appendix 4 (page 2/2)

Sample	Location	Transect	Cd	Na	P	S	Ag	Be	Hf	Mo	Nb	Sb	Sn	U	W	Zr
Lower detection limit >			*2*	*5*	*50*	*30*	*0.02*	*0.1*	*0.05*	*0.1*	*0.05*	*0.05*	*0.5*	*0.05*	*0.05*	*0.1*
Unit >			*ppm*	*ppm*	*ppm*	*ppm*	*ppm*	*ppm*	*ppm*	*ppm*	*ppm*	*ppm*	*ppm*	*ppm*	*ppm*	*ppm*
Method >			*ES*	*ES*	*ES*	*ES*	*MS*	*MS*	*MS*	*MS*	*MS*	*MS*	*MS*	*MS*	*MS*	*MS*
BE-20	-450	SW-NE	6	10	470	256	0.04	0.64	0.41	0.13	0.46	0.07	-0.5	0.546	0.11	13.95
BE-21	-425	SW-NE	6	10	518	85	0.05	0.62	0.3	1.15	0.6	0.08	1.48	0.645	0.1	12.6
BE-22	-375	SW-NE	7	13	557	365	0.05	0.8	0.5	0.21	0.4	0.1	0.57	0.674	0.12	17.84
BE-23	-325	SW-NE	7	13	541	179	0.03	0.84	0.41	0.23	0.35	0.09	0.64	0.686	0.14	16.48
BE-24	-275	SW-NE	6	11	613	110	0.03	0.68	0.23	0.19	0.47	-0.05	-0.5	0.6	0.12	10
BE-25	-240	SW-NE	8	16	640	92	0.07	1.05	0.56	0.46	0.54	0.11	1.68	0.774	0.2	21.45
BE-26	-233	SW-NE	6	11	511	376	0.13	0.68	0.19	0.17	0.54	0.08	-0.5	0.602	0.22	9.45
BE-27	-228	SW-NE	10	19	724	76	0.06	1.01	0.74	0.53	0.33	0.18	1.02	0.902	0.24	25.99
BE-28	-223	SW-NE	10	20	684	91	0.06	1.08	0.58	0.47	0.66	0.18	1.02	0.895	0.22	24.88
BE-29	-218	SW-NE	9	16	685	153	0.06	1.1	0.68	0.5	0.43	0.14	2.13	0.714	0.2	24.45
BE-30	-213	SW-NE	8	13	603	317	0.04	0.89	0.52	0.33	0.45	0.1	0.61	0.734	0.13	18.92
BE-31	-208	SW-NE	6	9	425	374	0.04	0.53	0.33	0.31	0.64	-0.05	0.52	0.589	0.07	11.65
BE-32	-203	SW-NE	5	8	450	337	0.02	0.62	0.35	0.25	0.44	-0.05	-0.5	0.504	0.09	10.28
BE-33	-190	SW-NE	6	11	492	368	0.03	0.8	0.35	0.32	0.38	0.09	0.84	0.643	0.09	14.8
BE-34	-165	SW-NE	7	13	562	324	0.04	0.97	0.49	0.48	0.47	0.08	0.52	0.64	0.12	17.41
BE-35	-115	SW-NE	5	11	556	109	0.17	0.61	0.27	0.3	0.6	0.08	-0.5	0.514	0.21	10.76
BE-36	-65	SW-NE	4	8	422	385	0.03	0.38	0.23	0.16	0.44	-0.05	-0.5	0.498	0.09	8.29
BE-17	100	SW-NE	7	14	580	209	0.13	0.76	0.44	0.26	0.35	0.14	0.6	0.668	0.21	16.75
BE-16	140	SW-NE	6	9	449	395	0.03	0.48	0.33	0.27	0.49	-0.05	1.1	0.634	0.08	12.34
BE-15	165	SW-NE	4	8	391	419	0.03	0.43	0.25	0.25	0.48	-0.05	-0.5	0.5	-0.05	9.48
BE-14	180	SW-NE	5	8	390	438	0.03	0.48	0.2	0.3	0.46	-0.05	-0.5	0.574	0.1	9.46
BE-13	185	SW-NE	6	9	493	494	0.03	0.46	0.3	0.28	0.42	-0.05	-0.5	0.536	0.06	11.8
BE-12	189	SW-NE	7	11	515	341	0.04	0.78	0.51	0.3	0.46	0.08	0.91	0.641	0.14	17.85
BE-11	194	SW-NE	6	11	465	406	0.03	0.73	0.34	0.28	0.47	0.08	-0.5	0.608	0.11	14.21
BE-10	199	SW-NE	6	10	479	219	0.04	0.62	0.25	0.25	0.56	-0.05	-0.5	0.45	0.13	10.6
BE-09	203	SW-NE	6	13	587	199	0.05	0.8	0.24	0.28	1.06	0.06	-0.5	0.737	0.12	11.29
BE-08	208	SW-NE	8	21	578	114	0.06	0.81	0.26	0.26	0.96	0.08	0.84	0.747	0.22	12.82
BE-07	225	SW-NE	6	11	508	346	0.05	0.69	0.44	0.27	0.57	0.06	0.57	0.591	0.12	15.92
BE-06	250	SW-NE	6	12	505	285	0.04	0.85	0.42	0.32	0.5	0.08	1.9	0.585	0.12	16.1
BE-05	275	SW-NE	6	10	442	498	0.04	0.74	0.26	0.18	0.56	-0.05	-0.5	0.574	0.07	10.77
BE-04	300	SW-NE	7	14	548	180	0.04	0.74	0.52	0.19	0.45	0.11	0.8	0.652	0.17	21.6
BE-03	350	SW-NE	8	16	596	195	0.05	0.9	0.58	0.29	0.31	0.11	0.77	0.811	0.15	22.71
BE-02	400	SW-NE	8	16	644	82	0.06	1.12	0.62	0.26	0.36	0.14	0.78	0.721	0.24	22.39
BE-01	450	SW-NE	8	13	552	315	0.14	0.96	0.46	0.23	0.45	0.13	0.64	0.589	0.24	19.38

APPENDIX 5 (page 1/1): Results of the PCA on the Bean ring. The number of variables is 22. Included are the % of total variation within each principal component (PC), the PC loadings and the communalities for each variable. A communality is the percent of variance in an observed variable that is accounted for by the retained components.

	PC 1	PC 2	PC 3	PC 4	PC 5	PC 6	Total
% variation in PC	34.917	11.379	8.574	8.692	7.08	7.138	77.78

	PC 1	PC 2	PC 3	PC 4	PC 5	PC 6	Communalities (%)
Cal	-0.659	0.55	-0.163	-0.213	-0.018	0.101	81.973
Dol	-0.196	0.42	-0.558	0.062	0.182	0.267	63.383
ORP	0.012	0.031	-0.578	-0.44	-0.151	-0.166	57.973
pH	-0.289	0.043	-0.06	-0.113	-0.047	0.841	81.08
Al_ES	0.874	-0.305	0.16	0.162	-0.114	-0.198	96.125
Mg_ES	0.275	0.809	0.01	0.187	-0.033	-0.073	77.193
Mn_ES	0.694	-0.366	-0.087	0.057	0.253	-0.131	70.814
Na_ES	0.781	-0.009	0.106	-0.081	-0.137	0.124	66.168
P_ES	0.852	-0.118	0.173	0.094	-0.042	-0.169	80.97
S_ES	-0.18	0.674	0.048	0.145	0.299	0.444	79.701
Ag_MS	0.115	0.063	0.045	0.795	0.163	-0.196	71.576
Be_MS	0.775	-0.086	0.141	0.184	-0.057	-0.396	82.169
Ca_ES	-0.198	0.75	-0.236	-0.269	-0.139	-0.048	75.139
Cd_MS	0.812	0.146	0.05	0.031	0.296	-0.219	82.056
Hf_MS	0.863	0.112	0.135	0.156	-0.191	-0.129	85.228
Mo_MS	0.317	-0.019	0.831	-0.038	0.044	-0.09	80.301
Nb_MS	0.07	-0.135	0.398	0.029	0.749	0.11	75.536
Sb_MS	0.799	-0.104	0.088	0.421	-0.223	-0.05	88.561
Sn_MS	0.269	-0.12	0.335	0.003	-0.622	0.111	59.79
U _MS	0.753	0.129	0.228	0.174	0.22	0.343	83.186
W _MS	0.404	-0.048	-0.013	0.751	-0.238	0.085	79.354
Zr_MS	0.912	0.028	0.116	0.137	-0.182	-0.176	92.889

APPENDIX 6 (page 1/2): Raw soil geochemical data at Thorn North.

Sample	Transect	Location	%_Cal	%_Dol	Ttl_CO3	pH(3min)	ORP(5min)	Al	Ca	Fe	Mg	Mn	Ti
Lower detection limit >			*NA*	*NA*	*NA*	*NA*	*NA*	*30*	*15*	*5*	*20*	*1*	*3*
Unit >			*Weight %*	*Weight %*	*Weight %*	*NA*	*mV*	*ppm*	*ppm*	*ppm*	*ppm*	*ppm*	*ppm*
Method >			*Chittick*	*Chittick*	*Chittick*	*pH probe*	*ORP probe*	*ES*	*ES*	*ES*	*ES*	*ES*	*ES*
TN-101	S-N	-500	21.22	8.98	30.19	7.13	-47	22996	53463	35083	31277	607	1186
TN-102	S-N	-450	20.86	8.98	29.84	7.85	-75	24148	53574	36287	32700	624	1230
TN-103	S-N	-425	20.08	10.57	30.65	8.14	-77	22982	53398	35551	30644	635	1185
TN-104	S-N	-400	22.24	7.27	29.51	8.09	-74	24855	53515	37610	31524	617	1257
TN-105	S-N	-378	18.59	9.32	27.91	8.05	-88	23434	53547	34601	29631	567	1163
TN-106	S-N	-353	18.98	11.36	30.34	8.67	-116	22193	53452	33591	27936	558	1115
TN-107	S-N	-338	15.91	11.14	27.04	8.27	-113	23959	55112	36043	30003	580	1194
TN-108	S-N	-328	20.78	8.18	28.96	8.33	-90	24141	54989	36080	30383	582	1172
TN-109	S-N	-323	20.6	6.82	27.41	8.85	-105	26098	55083	38501	31608	577	1262
TN-110	S-N	-318	22.05	8.98	31.02	8.89	-107	26180	55107	38172	32992	620	1287
TN-111	S-N	-313	18.48	9.09	27.57	8.66	-91	25214	55132	37220	30720	600	1196
TN-112	S-N	-308	21.26	7.87	29.14	8.94	-51	24897	54996	38000	31648	625	1256
TN-113	S-N	-303	18.83	10.76	29.6	8.12	-74	24164	55086	37051	33057	615	1215
TN-114	S-N	-298	19.78	9.23	29.02	8.6	-68	23228	55199	35291	31251	586	1194
TN-115	S-N	-293	21.69	7.48	29.17	8.85	-29	24253	55078	35922	30550	588	1204
TN-116	S-N	-288	22.14	8.04	30.19	9.02	-79	23042	55083	34654	30729	567	1156
TN-117	S-N	-278	19.95	9.63	29.58	9.07	-68	24567	54991	36599	30774	596	1227
TN-118	S-N	-265	23.82	10.41	34.22	8.16	29	13996	55118	21998	22982	379	834
TN-119	S-N	-250	21.03	6.31	27.34	8.48	72	26299	55083	37827	29383	603	1281
TN-120	S-N	-225	22.11	8.81	30.92	9.01	174	20584	55016	29416	29869	476	1055
TN-121	S-N	-175	22.66	14.32	36.97	9.13	94	20995	55205	29480	34014	519	1111
TN-123	S-N	-75	18.56	10.03	28.59	8.83	56	23148	55035	33982	29517	566	1166
TN-124	S-N	0	20.24	9.54	29.79	9.1	36	26239	55120	38943	31584	627	1294
TN-125	S-N	50	21.09	12.04	33.13	8.5	33	23327	55120	35628	28569	596	1161
TN-126	S-N	100	20.82	12.73	33.55	8.65	69	19431	54992	30203	31562	522	1053
TN-127	S-N	118	25.5	8.65	34.16	8.67	-62	18356	55179	27950	29127	519	992
TN-128	S-N	143	23.01	11.49	34.5	8.77	-16	19757	54989	29887	27121	528	1030
TN-129	S-N	158	21.47	12.69	34.16	8.81	-65	16707	54988	26299	22994	444	874
TN-130	S-N	168	21.1	10.2	31.3	9.09	-35	18214	55142	27288	23322	454	987
TN-131	S-N	173	20.74	10.54	31.27	8.71	-17	17539	55313	26169	23194	436	992
TN-132	S-N	178	21.91	7.93	29.84	7.68	-55	21025	55163	30065	29787	527	1077
TN-133	S-N	183	23.31	8.38	31.69	8.58	-48	17332	55140	25936	22695	449	926
TN-134	S-N	188	22.13	8.38	30.51	8.67	-44	19517	55202	29675	23971	468	1025
TN-135	S-N	194	23.3	8.72	32.02	8.97	-2	16719	55144	25712	22923	451	934
TN-136	S-N	198	22.04	10.54	32.57	8.83	-37	17302	55262	27313	23717	461	924
TN-137	S-N	203	20.65	9.86	30.5	8.92	32	16013	55170	24960	21362	423	880
TN-138	S-N	208	17.63	12.88	30.51	8.38	-48	17400	55161	26114	23570	440	942
TN-139	S-N	218	19.53	12.43	31.96	8.74	-54	19967	55252	29692	26443	523	1027
TN-140	S-N	233	19.62	10.28	29.9	8.83	-33	21515	55192	32061	25663	531	1111
TN-141	S-N	258	21.78	9.44	31.22	8.69	21	19819	55151	29787	25897	499	1034
TN-142	S-N	283	21.26	7.73	29	8.64	-49	24157	55140	34838	26056	503	1148
TN-143	S-N	300	19.9	9.2	29.11	8.84	-5	23604	55164	33866	27142	554	1166
TN-144	S-N	350	21.21	9.09	30.3	8.65	2	24192	55144	34605	27086	527	1172
TN-145	S-N	400	28.61	13.75	42.36	8.61	-18	12027	55392	16976	28902	326	726

APPENDIX 6 (page 2/2):

Sample	Transect	Location	%_Cal	%_Dol	Ttl_CO3	pH(3min)	ORP(5min)	Al	Ca	Fe	Mg	Mn	Ti
Lower detection limit >			*NA*	*NA*	*NA*	*NA*	*NA*	*30*	*15*	*5*	*20*	*1*	*3*
Unit >			*Weight %*	*Weight %*	*Weight %*	*NA*	*mV*	*ppm*	*ppm*	*ppm*	*ppm*	*ppm*	*ppm*
Method >			*Chittick*	*Chittick*	*Chittick*	*pH probe*	*ORP probe*	*ES*	*ES*	*ES*	*ES*	*ES*	*ES*
TN-146	W-E	-450	6.3	2.61	8.91	7.89	188	3716	6629	7269	2261	117	357
TN-147	W-E	-400	5.72	2.27	7.99	7.84	234	2254	4250	4318	1325	54	199
TN-148	W-E	-350	10.06	9.09	19.15	8.62	242	2640	6512	5778	1881	71	261
TN-149	W-E	-300	15.44	5.23	20.67	8.01	259	4737	16920	10738	3466	124	482
TN-150	W-E	-250	11.75	2.84	14.59	8.08	264	4305	11894	14984	2771	113	544
TN-151	W-E	-226	9.06	3.39	12.45	8.43	119	2981	7641	6436	1868	75	329
TN-152	W-E	-201	8.45	3.84	12.29	8.26	141	2158	6250	4257	1602	44	230
TN-153	W-E	-186	23.24	9.57	32.82	8.68	-34	17533	55140	24911	24124	427	957
TN-154	W-E	-176	11.14	4.47	15.61	8.22	153	2210	7901	5053	2053	56	302
TN-155	W-E	-171	9.9	5.94	15.84	8.31	205	2251	6074	4140	1901	54	296
TN-156	W-E	-166	9.76	5	14.76	8.31	217	2927	10023	6165	2685	77	422
TN-157	W-E	-166	10.42	4.7	15.12	8.31	-22	20397	54961	28378	25224	455	1042
TN-158	W-E	-161	19.4	9.97	29.37	8.89	1	18095	54930	27155	23478	440	977
TN-159	W-E	-158	21.61	9.24	30.85	9.01	12	18339	54875	28110	26902	488	988
TN-160	W-E	-151	21.65	11.04	32.69	9.12	29	19158	54888	28550	27970	484	1042
TN-161	W-E	-141	21.11	7.21	28.31	8.54	-77	20584	55009	32060	24879	544	1044
TN-162	W-E	-136	18.3	12.39	30.69	8.71	-82	21106	54902	30388	26259	462	1058
TN-163	W-E	-126	20.29	9.8	30.09	8.65	-85	19662	55166	29511	24720	490	1018
TN-164	W-E	-111	9.21	4.38	13.59	8.61	44	2202	5121	4137	1685	49	267
TN-165	W-E	-86	20.08	11.13	31.21	8.66	-66	22456	54976	31827	26587	481	1076
TN-166	W-E	-60	20.65	8.66	29.31	8.42	-32	24694	54940	33408	27133	525	1168
TN-167	W-E	-25	21.48	8.43	29.91	8.74	-51	24145	55034	33664	26443	538	1189
TN-168	W-E	75	23.06	9.89	32.96	7.29	-48	20571	54875	29706	28376	510	1090
TN-169	W-E	125	13.88	4.83	18.72	7.78	385	4253	13046	8977	4116	91	413
TN-170	W-E	175	20.9	8.21	29.11	8.78	65	19022	54935	29372	23255	476	975
TN-172	W-E	275	18.89	8.77	27.65	8.16	69	19581	54914	29205	22581	462	1025
TN-173	W-E	302	14.88	9.22	24.09	8.12	85	18352	54874	25989	17604	452	947
TN-174	W-E	327	15.7	6.3	22	8.43	63	23787	54898	34006	21050	509	1149
TN-175	W-E	342	16.61	7.08	23.69	8.17	89	22017	54891	31636	20474	507	1090
TN-176	W-E	352	16.66	8.77	25.42	7.9	57	20550	54915	28510	20359	431	1018
TN-177	W-E	357	16.82	7.64	24.46	8.05	63	25570	54964	34846	23760	614	1179
TN-178	W-E	362	18.26	6.97	25.23	8.24	102	22147	54872	31496	22276	522	1075
TN-180	W-E	372	14.27	8.52	22.79	7.78	42	27262	54929	36956	24954	640	1258
TN-181	W-E	377	13.74	12.8	26.54	7.7	42	18126	54740	24586	18202	426	898
TN-182	W-E	382	19.15	7.49	26.64	7.78	68	19726	54800	28844	26195	534	963
TN-183	W-E	385	21.85	6.31	28.16	8.06	67	21069	54747	31267	22630	523	987
TN-184	W-E	392	18.01	8.11	26.12	8.32	45	20871	54911	30917	23134	592	1010
TN-185	W-E	402	16.18	6.87	23.05	8.11	375	23553	54863	33385	22511	509	1058
TN-186	W-E	417	16.16	7.32	23.48	8.14	109	17083	54889	29050	21115	573	291
TN-187	W-E	442	19.95	6.76	26.71	7.93	342	22717	54737	32170	21629	567	1056
TN-188	W-E	467	3.53	5.52	9.05	7.73	116	30229	23440	42570	18725	809	1311
TN-189	W-E	500	19.83	6.87	26.7			22226	54835	31232	22402	542	1055
TN-190	W-E	550	0.15	2.02	2.17	7.19	254	2886	1158	4865	1356	76	248
TN-191	W-E	600	6.43	3.81	10.24	7.93	132	2868	9246	5771	2005	81	247

APPENDIX 7 (page1/2): Raw peat geochemical data at Thorn North.

Sample	Transect	Location	%_Cal	%_Dol	Ttl_CO3	ORP(3min)	pH(5min)	Al	Ca	Fe	Mg	Mn	Ti
Lower detection limit >			*NA*	*NA*	*NA*	*NA*	*NA*	*30*	*15*	*5*	*20*	*1*	*3*
		Unit >	*Weight %*	*Weight %*	*Weight %*	*mV*	*NA*	*ppm*	*ppm*	*ppm*	*ppm*	*ppm*	*ppm*
		Method >	*Chittick*	*Chittick*	*Chittick*	*ORP probe*	*pH probe*	*ES*	*ES*	*ES*	*ES*	*ES*	*ES*
TN-101	**S-N**	-500	1.1	2.05	3.15	109	6.4	1664	36621	4279	1255	250	28
TN-102	**S-N**	-450	0.74	2.16	2.9	156	5.7	1623	32270	2364	1063	83	28
TN-103	**S-N**	-425	0.65	1.59	2.24	227	5.69	2244	32402	2991	1150	179	35
TN-104	**S-N**	-400	0.65	1.59	2.24	249	5.74	1445	31270	3353	1009	100	24
TN-105	**S-N**	-378	0	2.61	2.62	244	5.63	1343	29980	3300	1055	155	21
TN-106	**S-N**	-353	1.48	4.31	5.78	280	5.55	1515	28771	2986	1143	173	27
TN-107	**S-N**	-338	0.63	1.92	2.56	263	5.53	1346	29112	3281	1121	70	25
TN-108	**S-N**	-328	0.92	0.68	1.6	269	5.75	1396	34055	4042	1300	118	23
TN-109	**S-N**	-323	0.57	3.27	3.85	227	5.86	1672	31582	3423	1276	373	29
TN-110	**S-N**	-318	0.65	1.36	2.01	223	5.75	1343	32252	4665	1282	238	27
TN-111	**S-N**	-313	0.63	1.81	2.44	253	5.9	1717	34776	4291	1321	179	30
TN-112	**S-N**	-308	0.8	0.56	1.37	171	6.68	984	37726	4604	1401	110	19
TN-113	**S-N**	-303	0.17	1.47	1.64	198	6.34	1644	40349	4693	1598	124	29
TN-114	**S-N**	-298	0.92	0.68	1.59	221	6.05	1271	35780	4075	1347	66	22
TN-115	**S-N**	-293	0.38	2.26	2.64	255	6.01	2132	45748	3913	1486	122	39
TN-116	**S-N**	-288	0.63	1.93	2.56	248	6.02	1218	37864	2535	1402	192	22
TN-117	**S-N**	-278	0.75	1.81	2.56	241	5.91	1605	41272	4075	1428	221	33
TN-118	**S-N**	-265	1.14	0.9	2.05	214	6.52	1459	41397	3512	1653	178	28
TN-119	**S-N**	-250	0.85	2.5	3.35	283	5.41	958	35001	2108	1097	53	16
TN-120	**S-N**	-225	1.15	0.91	2.06	264	5.97	1223	53742	2151	1509	214	22
TN-121	**S-N**	-175	1.1	2.05	3.15	222	6.09	4324	77974	5459	2104	150	53
TN-123	**S-N**	-75	1.06	2.95	4.02	196	5.49	4968	30909	4156	1583	125	57
TN-124	**S-N**	0	0.89	1.36	2.26	227	5.57	6296	26181	9537	1210	110	72
TN-125	**S-N**	50	0.96	2.5	3.46	167	6.21	3294	24089	15165	1145	726	57
TN-126	**S-N**	100	1.25	1.36	2.61	233	6.05	5603	22735	20973	1268	852	71
TN-127	**S-N**	118	0.83	2.95	3.78	79	6.53	4703	16716	13962	820	502	69
TN-128	**S-N**	143	0.75	1.93	2.68	138	6.38	7494	23290	15424	933	520	58
TN-129	**S-N**	158	1.15	0.91	2.06	143	6.29	4617	24594	12654	998	579	49
TN-130	**S-N**	168	1.08	2.5	3.58	130	6.82	4306	29689	12356	1025	423	38
TN-131	**S-N**	173	2.13	0.23	2.35	153	6.2	5542	22223	15635	935	533	61
TN-132	**S-N**	178	0.86	2.05	2.91	228	6.03	5393	21106	14591	959	540	54
TN-133	**S-N**	183	0.63	1.93	2.56	193	5.95	3233	27645	11859	1236	613	42
TN-134	**S-N**	188	0.76	1.7	2.46	254	5.75	3129	30360	12548	1232	1236	34
TN-135	**S-N**	194	0.75	1.93	2.68	213	6.13	3530	26456	14052	1143	962	37
TN-136	**S-N**	198	1.77	0.11	1.89	202	6.31	3901	31641	14837	1169	1365	46
TN-137	**S-N**	203	0.88	1.95	2.83	193	6.24	3328	26976	19345	1138	1751	41
TN-138	**S-N**	208	0.33	6.53	6.85	205	6.34	4076	30756	8740	1217	372	50
TN-139	**S-N**	218	1.14	7.23	8.36	231	6.12	3227	26462	10502	1131	903	40
TN-140	**S-N**	233	2.1	1.37	3.47	211	6.48	3678	37525	8814	1283	582	53
TN-141	**S-N**	258	0.75	2.06	2.81	220	6.55	3279	32704	9041	1088	531	43
TN-142	**S-N**	283	0.15	2.06	2.21	201	6.48	5178	32775	13835	1464	438	85
TN-143	**S-N**	300	0.51	2.06	2.57	132	6.29	4879	27880	11614	1115	494	57
TN-144	**S-N**	350	0.76	1.95	2.7	146	6.14	4986	33580	7685	1458	711	72
TN-145	**S-N**	400	0.89	1.6	2.49	199	6.43	6554	37672	7146	1610	698	95
TN-122	**S-N**	-125				454	3.05	1783	3377	2259	474	44	36

APPENDIX 7 (page2/2):

Sample	Transect	Location	%_Cal	%_Dol	Ttl_CO3	ORP(3min)	pH(5min)	Al	Ca	Fe	Mg	Mn	Ti
Lower detection limit >			*NA*	*NA*	*NA*	*NA*	*NA*	*30*	*15*	*5*	*20*	*1*	*3*
		Unit >	*Weight % Chittick*	*Weight % Chittick*	*Weight % Chittick*	*mV ORP probe*	*NA pH probe*	*ppm ES*	*ppm ES*	*ppm ES*	*ppm ES*	*ppm ES*	*ppm ES*
		Method >											
TN-146	**W-E**	-450	1.11	2.06	3.17	444	2.63	1828	2424	2085	450	34	33
TN-147	**W-E**	-400	1.15	1.14	2.29	440	3.08	1894	4806	1723	493	44	32
TN-148	**W-E**	-350	0.24	17.06	17.3	382	4.23	1899	5291	3113	613	1091	65
TN-149	**W-E**	-300	1.35	2.06	3.41	426	3.21	1571	5493	2345	282	551	38
TN-150	**W-E**	-250	0.39	2.06	2.45	431	3.32	1872	3371	6604	276	295	53
TN-151.5	**W-E**	-226	0.76	1.95	2.7	262	6.98	5223	59058	3977	2013	1479	34
TN-152.5	**W-E**	-201	0.88	1.82	2.7	311	6.72	1231	58931	2806	1812	394	16
TN-153.5	**W-E**	-186	1.12	1.82	2.94	323	6.4	998	57586	1042	1788	763	13
TN-154.5	**W-E**	-176	0.29	4.57	4.85	304	6.32	972	57091	878	1966	978	14
TN-155.5	**W-E**	-171	0.32	3.65	3.98	306	6.36	1087	57010	1342	1903	594	15
TN-156.5	**W-E**	-166	0.92	0.91	1.83	332	6.43	1011	47381	2003	1818	186	19
TN-157.5	**W-E**	-161	0.51	1.94	2.46	335	6.41	749	37431	876	1824	222	12
TN-158.5	**W-E**	-158	1.27	3.88	5.15	361	6.1	1122	54744	1359	2069	20	17
TN-159.5	**W-E**	-151	1.32	2.74	4.06	318	6.38	1072	52136	1173	2011	199	17
TN-160.5	**W-E**	-146	0.65	1.72	2.37	273	6.47	1230	53136	1377	1991	81	17
TN-161.5	**W-E**	-141	0.13	2.52	2.66	332	6.21	1117	45477	1423	1852	54	17
TN-162.5	**W-E**	-136	0.15	2.06	2.22	283	6.2	1031	48877	1224	2007	38	14
TN-163.5	**W-E**	-126	0.35	6.07	6.41	317	6.06	1537	54338	3007	2062	44	24
TN-164.5	**W-E**	-111	0.63	2.06	2.69	309	6.01	3095	32427	3557	1351	98	68
TN-165.5	**W-E**	-86	0.53	1.72	2.24	288	6.05	3439	43783	3404	1977	211	41
TN-166	**W-E**	-60	0.89	1.6	2.49	229	6.64	6292	38578	7433	1657	248	70
TN-167	**W-E**	-25	0.64	1.83	2.47	271	6.29	5854	29801	16756	1398	114	75
TN-168	**W-E**	75	0.86	2.28	3.14	266	6.01	2355	43558	8119	1900	325	29
TN-169	**W-E**	125	0.75	2.06	2.8	287	6.58	3037	28618	16811	1475	531	42
TN-170	**W-E**	175	0.84	2.63	3.47	408	3.14	1727	2740	1262	343	24	24
TN-171	**W-E**	225	0.88	1.83	2.7	448	2.65	2357	2229	3202	198	22	66
TN-172	**W-E**	275	0.64	1.83	2.47	386	4.59	2563	48068	2243	1700	26	41
TN-173	**W-E**	302	1.61	1.37	2.98	398	3.59	6842	7514	5138	533	32	82
TN-174	**W-E**	327	0.53	1.48	2.02	209	6.12	5053	36190	7169	1437	730	70
TN-175	**W-E**	342	1.11	2.06	3.16	239	5.98	8222	29897	7271	1429	296	95
TN-176	**W-E**	352	0.88	1.83	2.7	167	6.51	3650	15018	6782	860	394	66
TN-177	**W-E**	357	0.75	1.94	2.69	146	6.51	6300	19606	6099	1105	288	71
TN-178	**W-E**	362	0.86	2.28	3.14	220	5.67	7004	18459	5381	914	215	79
TN-179	**W-E**	367	0.84	2.63	3.47	195	5.64	8711	16555	7197	968	170	110
TN-180	**W-E**	372	1.34	2.17	3.51	265	5.75	4461	19332	13846	1254	396	89
TN-181	**W-E**	377	0.89	1.6	2.49	217	6.08	6455	25599	12140	1416	683	94
TN-182	**W-E**	382	0.62	2.28	2.9	209	6.19	3488	24261	8145	1386	1963	47
TN-183	**W-E**	385	1.38	1.14	2.52	227	6.2	6588	23726	9091	1313	421	96
TN-184	**W-E**	392	0.63	2.06	2.68	264	6.16	4583	33454	7948	1535	592	68
TN-185	**W-E**	402	0.97	2.51	3.48	270	6.21	2033	44937	8457	1538	631	28
TN-185.5	**W-E**	409	1	1.71	2.71	273	6.13	8217	14608	3356	926	31	105
TN-186	**W-E**	417	1.11	2.06	3.16	294	6.06	1090	44361	4091	1656	242	16
TN-187	**W-E**	442	1.11	2.06	3.16	318	5.37	4901	27285	2841	1377	21	120
TN-188	**W-E**	467	0.83	2.97	3.8	272	5.57	4146	13291	6252	1141	93	102
TN-189	**W-E**	500	0.72	2.85	3.57	230	5.93	7596	17161	10767	1775	326	135
TN-190	**W-E**	550	1.19	2.84	4.04	264	4.86	10277	3705	5300	1060	72	112

APPENDIX 8 (page 1/2): Raw soil geochemical data at Bean.

Sample	Location	Transect	%_Cal	%_Dol	Ttl_CO3	pH (3min)	ORP (5min)	Al	Ca	Fe	Mg	Mn	Ti
		Lower detection limit >	*NA*	*NA*	*NA*	*NA*	*NA*	*30*	*15*	*5*	*20*	*1*	*3*
		Unit >	*Weight %*	*Weight %*	*Weight %*	*NA*	*mV*	*ppm*	*ppm*	*ppm*	*ppm*	*ppm*	*ppm*
		Method >	*Chittick*	*Chittick*	*Chittick*	*pH probe*	*ORP probe*	*ES*	*ES*	*ES*	*ES*	*ES*	*ES*
BE-20	-450	SW-NE	23.39	16.15	39.54	7.56	-41.6	8791	81530	15080	24603	282	616
BE-21	-425	SW-NE	16.48	-0.01	4.25	7.63	-61.4	11329	70673	16358	21915	193	666
BE-22	-375	SW-NE	22.48	16.99	39.47	7.77	124	12071	81530	20775	31896	425	797
BE-23	-325	SW-NE	19.71	13.78	33.5	7.78	139	12799	81491	21318	21874	427	793
BE-24	-275	SW-NE	17.94	15.09	33.03	8.26	-60	10412	79731	18130	18002	336	678
BE-25	-240	SW-NE	10.69	10.36	21.05	7.66	-145	17561	57659	28904	22496	420	1078
BE-26	-233	SW-NE	22.79	17.9	40.69	7.76	-177	9051	81477	14923	32302	293	584
BE-27	-228	SW-NE	15.48	6.17	21.65	7.82	-100.8	21590	72790	35038	23329	591	1339
BE-28	-223	SW-NE	8.42	7.34	15.77	7.45	-95	23386	41069	37450	19644	509	1322
BE-29	-218	SW-NE	17.31	14.8	32.11	7.75	-102	16791	81542	28399	29572	410	1048
BE-30	-213	SW-NE	20.64	16.95	37.59	7.93	73	13015	81568	21587	31651	489	888
BE-31	-208	SW-NE	28.51	14.91	43.43	8.22	-7.7	7501	81610	12731	24994	325	621
BE-32	-203	SW-NE	27.75	16.27	44.02	7.91	-109	6860	81602	12734	22101	252	522
BE-33	-190	SW-NE	23.61	16.61	40.21	7.82	-103	9849	81589	16615	31313	408	648
BE-34	-165	SW-NE	20.64	6.18	26.82	7.76	85	11591	81469	19580	32378	386	797
BE-35	-115	SW-NE	12.54	13.22	25.76	7.83	-99	10386	57840	17359	20070	284	664
BE-36	-65	SW-NE	30.32	14.01	44.33	8.01	62	6182	81558	11399	19796	225	439
BE-17	100	SW-NE	21.05	12.77	33.82	8.05	157	13744	83379	22832	26113	506	874
BE-16	140	SW-NE	24.9	19.43	44.33	8.15	155	6178	83444	11284	36428	246	465
BE-15	165	SW-NE	25.68	17.74	43.42	8.17	120	5586	83425	10437	22288	221	427
BE-14	180	SW-NE	29.13	14.23	43.37	8.01	148	6127	83352	11408	25815	257	454
BE-13	185	SW-NE	30.27	20.79	51.06	7.37	184.6	6714	83540	12050	33363	247	485
BE-12	189	SW-NE	23.57	13.37	36.94	8.05	145	10962	83414	18571	28482	320	705
BE-11	194	SW-NE	23.13	18.47	41.59	8.09	136	8761	83340	15391	26691	337	576
BE-10	199	SW-NE	21.81	16.09	37.89	7.64	45	8317	83303	15100	21114	296	513
BE-09	203	SW-NE	16.92	14.16	31.08	7.64	117	11548	83287	18704	25867	512	630
BE-08	208	SW-NE	9.43	9.4	18.83	7.55	74.5	17603	53367	29189	17005	1626	925
BE-07	225	SW-NE	21.07	16.77	37.83	7.47	-44	10115	83298	17444	25086	374	664
BE-06	250	SW-NE	23.11	13.14	36.25	7.61	95	10885	83300	18337	23101	351	701
BE-05	275	SW-NE	30.58	21.3	51.88	7.83	141	7274	83332	12010	32354	284	489
BE-04	300	SW-NE	17.77	11.96	29.73	7.71	192	13952	83388	23129	24471	474	859
BE-03	350	SW-NE	18.21	12.75	30.96	7.71	178	15522	83296	26232	23079	476	959
BE-02	400	SW-NE	10.58	13.68	24.26	7.71	180	16389	69194	27330	24748	631	955
BE-01	450	SW-NE	22.8	16.59	39.39	7.53	142	12287	83430	21197	32885	430	767

APPENDIX 8 (page 2/2):

Sample	Location	Transect	%_Cal	%_Dol	Ttl_CO3	pH (3min)	ORP (5min)	Al	Ca	Fe	Mg	Mn	Ti
		Lower detection limit >	*NA*	*NA*	*NA*	*NA*	*NA*	*30*	*15*	*5*	*20*	*1*	*3*
		Unit >	*Weight %*	*Weight %*	*Weight %*	*NA*	*mV*	*ppm*	*ppm*	*ppm*	*ppm*	*ppm*	*ppm*
		Method >	*Chittick*	*Chittick*	*Chittick*	*pH probe*	*ORP probe*	*ES*	*ES*	*ES*	*ES*	*ES*	*ES*
BE-58	-450	SE-NW	27.61	1.81	29.42	8.63	87	5449	82584	8859	18301	154	403
BE-59	-400	SE-NW	27.02	18.69	45.71	8.55	-59	6274	82568	11444	31548	241	425
BE-60	-350	SE-NW	21.65	14.16	35.81	7.88	91	11860	82559	19915	24376	417	773
BE-61	-300	SE-NW	26.99	16.54	43.53	7.99	48	6666	82574	11592	30672	236	453
BE-62	-250	SE-NW	12.58	10.36	22.94	8.09	101	22947	61993	36882	22700	787	1434
BE-67	-235	SE-NW	29.31	21.24	50.55	8.14	140	5725	82536	9855	23796	172	433
BE-68	-220	SE-NW	23.73	19.2	42.94	8.3	92	7401	82528	13075	24622	288	522
BE-69	-210	SE-NW	27.79	15.36	43.15	8.71	111	3051	65481	5608	8538	83	277
BE-70	-205	SE-NW	25.15	16.38	41.53	8.15	-42	8149	82502	14433	27474	273	586
BE-71	-200	SE-NW	21.24	16.72	37.96	8.14	69	4452	67220	7317	17320	110	342
BE-72	-195	SE-NW	23.59	14.685	38.28	8.5	58	5870	78393	10449	21202	174	426
BE-73	-190	SE-NW	23.2	17.84	41.04	8.4	49	4348	71857	7281	18544	116	338
BE-74	-185	SE-NW	28.42	17.15	45.57	8.71	29	6430	78371	11388	28971	241	501
BE-75	-180	SE-NW	24.61	18.07	42.67	8.6	-59	7934	78577	14467	25742	306	593
BE-76	-175	SE-NW	21.59	21.06	42.65	8.71	-28	11446	78433	19377	28524	369	813
BE-77	-170	SE-NW	19.28	17.12	36.4	8.51	-42	12026	78394	20342	29344	418	873
BE-78	-150	SE-NW	16.27	13.07	29.34	8.45	-15	11816	78268	20910	23313	473	821
BE-79	-100	SE-NW	25.53	19.6	45.13	8.58	-32	6877	78538	12428	27543	257	506
BE-80	-50	SE-NW	27.31	16.45	43.75	8.61	-25	7011	78436	12047	32600	273	510
BE-57	50	SE-NW	16.61	14.71	31.32	8.7	86	12220	82947	19861	24904	282	780
BE-56	100	SE-NW	25.38	16.49	41.87	8.55	95	7606	82661	12856	25176	274	517
BE-55	150	SE-NW	24.045	16.6	40.64	8.44	78	9102	82526	14615	29937	299	542
BE-54	175	SE-NW	26.69	16.14	42.84	8.68	-24	6423	82667	10714	32352	226	486
BE-53	200	SE-NW	24.79	19.43	44.22	8.41	-48	6680	82551	11834	20586	217	512
BE-52	215	SE-NW	24.76	17.28	42.04	8.64	91	7886	82517	13697	22947	294	520
BE-51	221	SE-NW	26.3	17.06	43.36	8.42	102	7961	82500	13372	33805	266	514
BE-50	225	SE-NW	24.11	15.93	40.03	8.64	106	8520	82578	14885	26620	300	582
BE-49	230	SE-NW	27.4	16.04	43.45	8.63	109	7839	82578	14078	24174	301	525
BE-48	235	SE-NW	20.17	11.41	31.58	8.06	100	13870	82499	23118	23792	471	889
BE-46	245	SE-NW	20.035	16.755	36.785	8.15	76	9581	82705	15270	32971	311	597
BE-47	245	SE-NW	24.34	16.04	40.38	7.92	93	12005	81620	20308	31244	448	798
BE-45	250	SE-NW	22.45	21.69	44.14	8.02	87	12197	81508	21127	27174	319	852
BE-44	255	SE-NW	3.84	23.84	27.68	8.01	34	15768	81699	26053	26806	593	1020
BE-43	260	SE-NW	27.83	17.17	45	8.98	92	7655	81505	12483	32648	230	512
BE-42	272	SE-NW	24.08	22.14	46.22	8.65	104	2163	81476	5149	11794	143	216
BE-41	300	SE-NW	25.03	22.14	47.17	8.46	76	6076	81569	11563	22079	245	482
BE-40	350	SE-NW	17.24	16.49	33.73	8	-61	11941	81483	20578	29806	431	861
BE-39	399	SE-NW	17.14	18.98	36.12	8.34	-113	12098	81541	20712	34120	478	874
BE-38	469	SE-NW	26.53	14.46	40.99	7.98	-9.3	6595	81508	11913	22828	223	482

APPENDIX 9 (page 1/2): Raw peat geochemical data at Bean.

Sample	Transect	Location	%_Cal	%_Dol	Ttl_CO3	pH(3min)	ORP(5min)	Al	Ca	Fe	Mg	Mn	Ti
		Lower detection limit >	*NA*	*NA*	*NA*	*NA*	*NA*	*30*	*15*	*5*	*20*	*1*	*3*
		Unit >	*Weight %*	*Weight %*	*Weight %*	*NA*	*mV*	*ppm*	*ppm*	*ppm*	*ppm*	*ppm*	*ppm*
		Method >	*Chittick*	*Chittick*	*Chittick*	*pH probe*	*ORP probe*	*ES*	*ES*	*ES*	*ES*	*ES*	*ES*
BE-58	SE-NW	-450	0.61	2.37	2.97	5.86	162	13925	33509	12978	3484	261	282
BE-59	SE-NW	-400	0.61	2.37	2.97	5.95	186	4769	37198	4243	2995	426	85
BE-60	SE-NW	-350	0.73	4.96	5.69	5.97	205	5367	33934	6240	2555	266	91
BE-61	SE-NW	-300	1.78	2.48	4.26	5.99	218	3735	38641	4092	2651	285	41
BE-62	SE-NW	-250	0.61	2.37	2.97	5.5	236	10242	38120	22254	3485	2017	163
BE-67	SE-NW	-235	0.58	3.03	3.61	5.6	222	9485	36297	12446	3773	553	177
BE-68	SE-NW	-220	0.46	0.22	0.69	5.36	91	7619	31741	11493	2920	735	140
BE-69	SE-NW	-210	0.88	1.35	2.23	5.82	185	9425	32972	9415	2917	360	175
BE-70	SE-NW	-205	0.83	2.7	3.52	6.08	231	4779	37005	3931	2677	185	66
BE-71	SE-NW	-200	2.6	5.41	8	5.45	195	4671	39569	4279	2850	602	58
BE-72	SE-NW	-195	1	1.35	2.35	5.5	186	3287	43170	6512	2905	435	35
BE-73	SE-NW	-190	1.24	4.05	5.29	5.19	180	3101	31985	2825	2398	277	33
BE-74	SE-NW	-185	0.6	2.47	3.07	5.3	207	3840	34017	3399	2497	161	48
BE-75	SE-NW	-180	1.71	4.05	5.76	5.33	211	4328	36159	3470	2631	495	50
BE-76	SE-NW	-175	0.89	1.12	2.02	5.86	216	5395	34926	2250	2632	153	93
BE-77	SE-NW	-170	0.14	2.25	2.39	6.55	218	4196	33806	4362	2663	659	65
BE-78	SE-NW	-150	0.34	3.15	3.49	6.52	220	2810	32978	2176	2482	151	37
BE-79	SE-NW	-100	0.36	2.7	3.06	6.86	218	2847	37214	3666	2891	250	48
BE-80	SE-NW	-50	0.87	1.8	2.67	5.86	187	2396	32708	5128	2504	467	38
BE-57	SE-NW	50				5.85	219	1335	43073	887	2894	682	27
BE-56	SE-NW	100	0.89	1.24	2.13	5.7	237	6023	39951	5996	2768	23	136
BE-55	SE-NW	150	0.83	2.7	3.53	5.83	109	6607	45179	7265	3012	266	124
BE-54	SE-NW	175	0.36	2.59	2.95	5.36	180	3228	37568	3884	2464	198	48
BE-53	SE-NW	200	-0.01	9.01	8.64		187	3289	52471	4335	5029	362	45
BE-52	SE-NW	215	0.84	5.42	6.26		206	8272	60164	9071	3991	63	153
BE-51	SE-NW	221	1.41	0.23	1.63		199	7010	54976	7097	4037	18	119
BE-50	SE-NW	225	0.88	1.35	2.24		266	6216	46651	5769	3741	47	108
BE-49	SE-NW	230	0.4	13.07	13.46		332	7969	34447	8140	3113	95	162
BE-48	SE-NW	235	0.58	2.93	3.51	5.81	304	4154	35193	4870	2721	43	92
BE-47	SE-NW	240	0.26	4.96	5.22	6.32	269	6280	35372	5621	2905	111	147
BE-46	SE-NW	245	0.53	1.46	1.99	5.9	270	4990	30665	4827	2532	21	100
BE-45	SE-NW	250	0.48	2.59	3.07	5.81	130	11617	28643	12243	4274	389	339
BE-44	SE-NW	255	0.37	2.48	2.85	5.99	253	8931	34983	7967	3625	333	205
BE-43	SE-NW	260	0.79	3.6	4.4	6.04	330	8671	39184	9681	3760	164	207
BE-42	SE-NW	272	0.88	1.46	2.34	5.81	244	17539	26214	16494	4485	68	324
BE-41	SE-NW	300	1.72	3.83	5.55	5.88	298	4614	50650	6039	3536	80	105
BE-40	SE-NW	350	1.11	1.58	2.69	5.7	196	2938	37922	3418	2442	234	58
BE-39	SE-NW	399	1.72	3.83	5.55	5.97	240	3001	37240	3262	2976	293	49
BE-38	SE-NW	469	0.87	1.8	2.67	6.12	248	2354	32684	4748	2617	158	53

APPENDIX 9 (page 2/2):

Sample	Transect	Location	%_Cal	%_Dol	Ttl_CO3	pH(3min)	ORP(5min)	Al	Ca	Fe	Mg	Mn	Ti
		Lower detection limit >	*NA*	*NA*	*NA*	*NA*	*NA*	*30*	*15*	*5*	*20*	*1*	*3*
		Unit >	*Weight %*	*Weight %*	*Weight %*	*NA*	*mV*	*ppm*	*ppm*	*ppm*	*ppm*	*ppm*	*ppm*
		Method >	*Chittick*	*Chittick*	*Chittick*	*pH probe*	*ORP probe*	*ES*	*ES*	*ES*	*ES*	*ES*	*ES*
BE-20	SW-NE	-450	0.85	2.26	3.11	6.51	13	5006	38366	21509	2903	671	74
BE-21	SW-NE	-425	0.77	4.07	4.84	6.88	33	3013	39413	10445	2716	2302	43
BE-22	SW-NE	-375	3.02	6.78	9.8	6.61	193	3142	43803	3945	3318	48	64
BE-23	SW-NE	-325	0.61	2.26	2.87	5.51	299	5778	35405	5145	2873	15	123
BE-24	SW-NE	-275	0.72	2.49	3.21	6.68	54	11355	37585	13505	3920	932	244
BE-25	SW-NE	-240	1.51	9.04	10.55	7	42	5110	43672	5932	3222	591	85
BE-26	SW-NE	-233	1.01	1.36	2.36	6.89	68	3163	39903	5102	2703	295	55
BE-27	SW-NE	-228	0.82	2.94	3.76	6.7	68	5760	40131	10091	3272	500	118
BE-28	SW-NE	-223	0.87	1.81	2.68	6.74	41	7447	35237	9418	3089	433	179
BE-29	SW-NE	-218	0.95	2.6	3.55	6.74	94	8774	38994	8939	3484	462	201
BE-30	SW-NE	-213	0.38	2.26	2.64	6.66	45	7212	38449	8109	2920	397	132
BE-31	SW-NE	-208	0.88	1.57	2.45	6.68	84	4120	40260	10191	2851	1551	61
BE-32	SW-NE	-203	1.06	2.7	3.77	6.64	156	7792	38430	8927	3097	504	181
BE-33	SW-NE	-190	1.04	3.15	4.2	6.54	113	7080	35269	8352	3063	912	133
BE-34	SW-NE	-165	1.21	2.03	3.24	6.5	115	4530	37734	5692	3100	416	93
BE-35	SW-NE	-115	1.11	1.58	2.69	6.11	198	3535	39296	7320	2593	401	68
BE-36	SW-NE	-65	0.83	2.7	3.53	6.84	211	10021	47980	10318	4193	100	184
BE-19	SW-NE	-19.1	1	1.46	2.46	6.05	208	2397	34482	2814	2506	113	48
BE-18	SW-NE	50	0.85	2.14	2.99	6.13		5758	40381	11348	2991	525	88
BE-17	SW-NE	100	0.59	2.7	3.29	5.83	188	18936	32793	16024	4877	244	333
BE-16	SW-NE	140	0.54	3.82	4.37	6.08	238	4973	38741	7790	3315	1350	60
BE-15	SW-NE	165	0.76	1.46	2.22	5.91	273	5068	47409	4596	3188	25	52
BE-14	SW-NE	180	1.52	2.92	4.44	5.85	225	9446	52047	10045	3646	292	137
BE-13	SW-NE	185	0.37	2.47	2.84	5.77	203	6153	42551	10380	2313	250	85
BE-12	SW-NE	189	0.51	1.91	2.42	6.07	150	9949	42861	6166	3242	272	159
BE-11	SW-NE	194	1.23	1.57	2.8	5.76	193	6518	36697	7372	2876	566	101
BE-10	SW-NE	199	0.49	2.36	2.85	5.77	167	8958	36319	6691	3040	322	143
BE-09	SW-NE	203	3.5	6.29	9.79	5.87	138	8036	35602	8028	3028	713	128
BE-08	SW-NE	208	-0.01	2.92	2.8	6.14	149	5197	31562	6539	2746	422	92
BE-07	SW-NE	225	0.82	2.92	3.74	5.93	161	3777	42286	6120	3384	499	69
BE-06	SW-NE	250	0.51	1.91	2.42	5.86	204	3083	39394	3912	2736	397	69
BE-05	SW-NE	275	1.22	1.68	2.91	5.87	236	7622	28064	7116	2643	365	207
BE-04	SW-NE	300	2.12	2.69	4.82	5.69	273	10952	33884	11026	3828	1743	222
BE-03	SW-NE	350	1.31	2.47	3.78	5.3	210	27805	19320	32474	8035	285	703
BE-02	SW-NE	400	1.26	3.71	4.96	6.16	174	10506	53740	10783	4660	504	224
BE-01	SW-NE	450				6.09	155	5581	43370	6552	4120	250	104